GMM Estimation with Brownian Kernels Applied to Income Inequality Measurement

JIN SEO CHO*

School of Economics, Yonsei University, Seoul 03722, Korea
Email: jinseocho@yonsei.ac.kr

PETER C. B. PHILLIPS

Yale University, University of Auckland & Singapore Management University
Email: peter.phillips@yale.edu

April 2025

Abstract

In GMM estimation, it is well known that if the moment dimension grows with the sample size, the asymptotics of GMM differ from the standard finite dimensional case. The present work examines the asymptotic properties of infinite dimensional GMM estimation when the weight matrix is formed by inverting Brownian motion or Brownian bridge covariance kernels. These kernels arise in econometric work such as minimum Cramér-von Mises distance estimation when testing distributional specification. The properties of GMM estimation are studied under different environments where the moment conditions converge to a smooth Gaussian or non-differentiable Gaussian process. Conditions are also developed for testing the validity of the moment conditions by means of a suitably constructed J-statistic. In case these conditions are invalid we propose another test called the U-test. As an empirical application of these infinite dimensional GMM procedures the evolution of cohort labor income inequality indices is studied using the Continuous Work History Sample database. The findings show that labor income inequality indices are maximized at early career years, implying that economic policies to reduce income inequality should be more effective when designed for workers at an early stage in their career cycles.

Key Words: Infinite dimensional GMM estimation; Brownian motion kernel; Brownian bridge kernel; Gaussian process; Infinite dimensional MCMD estimation; Labor income inequality.

Subject Classification: C13, C18, C32, C55, D31, O15, P36.

*: Corresponding author.

1 Introduction

The generalized method of moments (GMM) approach to estimation and inference has been adapted to several nonstandard environments. A particular extension that has proved to be important theoretically and empirically useful involves the application of GMM when the number of moment conditions is allowed to pass to infinity with the sample size. An example of such high dimensional GMM occurs with the use of minimum Cramér-von Mises distance (MCMD) estimation, which is useful in estimating unknown parameters in a model's distribution and can be extended to test distributional specification. Early work by Pollard (1980) and later Cho et al. (2018) showed how to develop limit theory for MCMD estimation in GMM form with a particular weight matrix. The latter paper applied MCMD to test the Pareto distributional form for income data in Korea, an approach that is commonly used in estimating top income shares (see Piketty, 2003; Piketty and Saez, 2003; Atkinson et al., 2011, among others). In another context, Angrist and Keueger (1991) estimated the monetary return to education in the labor market using two-stage least squares on U.S. census data with a large number of instruments.

The large sample properties of high dimensional GMM with many moment conditions rely on the asymptotic behavior of the GMM components and these are case-dependent. For example, when persistently correlated moment conditions are employed in GMM estimation, large sample analysis differs from that when the moment conditions are weakly correlated as assumed by Carrasco (2012). Therefore, GMM using the moment conditions for MCMD is very different from that formed by weakly correlated moment conditions because the moment conditions for MCMD converge to a Brownian bridge (BB) process.

Different weight matrices in GMM may also produce different limit properties. But when the matrix dimension grows, inversion inevitably becomes imprecise as the smallest eigenvalue of the matrix approaches zero. Indeed, the limiting inverse may not exist and computation becomes case-dependent and difficult even when the limit exists. For example, the BB process for MCMD estimation allows GMM to be computed using the inverse of the BB covariance matrix, but it is unknown how the inverse matrix affects GMM asymptotically, irrespective of the existence of the limit inverse. Likewise, if the moment conditions form a unit-root process (another persistently correlated process) that converges to Brownian motion (BM) upon standarization, the size of the moment conditions grows and an asymptotically optimal GMM is obtained by inverting the BM covariance matrix. Nonetheless, its influence on GMM limit behavior is presently unknown in the literature. The reason is that the limit of the inverse of the BM covariance matrix does not exist in any standard form of the type that assumes a finite number of moment conditions. These restrictions effectively diminish the scope of GMM applications in the literature to reliance on stationary moment

conditions. Challenges of the type just described associated with high dimensional matrix inversions relate to the so-called ill-posedness problem associated with the inversion of operators in functional analysis, a problem that is typically resolved by various forms of regularization.

A primary goal of the present paper is to tackle directly and without regularization the challenges of high dimensional GMM that are associated with BM and BB covariance matrices, which are in turn induced by persistently correlated moment conditions. Direct inversion of BM and BB covariance matrices and the manner of doing so is quite new and opens up a wide range of potential applications. To mention a few of them here: (i) For empirical processes that converge to a BB process, as for the Kolmogorov-Smirnov (KS) test, it is necessary to invert the BB covariance matrix when testing a distributional hypothesis within the GMM framework; (ii) BM and BB processes are widely assumed in finance for series such as stock prices, interest rates, and option prices among others (e.g., Andersen and Piterbarg, 2010; Hirsa and Neftci, 2014). If the sample paths of these processes are employed as a series of moment conditions for GMM estimation it becomes necessary to invert BM or BB covariance matrices; (iii) More generally, the use of covariance matrices based on BM and BB processes and kernels is common because of convenience of form and ease of analysis, yet they are rarely applied in empirical work because of the difficulties induced by ill-posedness problems in inversion.

To meet these needs the main aim of the present study is to provide a unified framework for delivering the asymptotic properties of GMM when BM or BB covariance matrix inversions are involved in a wide range of different circumstances where moment conditions are persistently correlated in a manner that yields a continuous sample path. In particular, our approach allows the moment dimension to grow infinitely large and makes explicit the variate space and inner product framework that provides the mechanism for embodying the GMM limit theory. We call these GMM techniques BM-GMM and BB-GMM.

The asymptotic properties of BM- and BB-GMMs depend intimately on two key components – the weight matrix and the moment conditions – both of which become infinite dimensional in the limit. We briefly explain here how our theory is developed using these elements. First, the properties of the weight matrix in BM- and BB-GMMs inevitably affect the limit properties of the estimation procedure, just as they do in the finite dimensional case. The BM and BB covariance matrices become infinite dimensional as the moment size grows, and they are often called the BM-kernel and BB-kernel, in accord with their use as kernels for integral operators. If the moment index is adjusted to fit to the unit interval, the BM and BB covariance matrices can be positioned on the unit square. Further, as the moment size increases, the corresponding BM and BB covariance matrices converge to continuous functions. Hence, when they are both suitably standardized, the product of a BM (or BB) covariance matrix and a vector (whose standardized

form has a continuous function limit on the unit interval) converges to a double integral formed with the BM (or BB) kernel and the limiting continuous function of the standardized vector. We can also represent this limit using an inner product between two continuous functions such that the first is the integral transform of the limiting continuous function using the BM (or BB) kernel, and the second is the limiting continuous function. For our GMM analysis, the GMM distance is constructed using the inverted BM (or BB) covariance matrix as the weight matrix instead of the BM (or BB) covariance matrix itself. This inversion affects GMM estimation by ensuring that the GMM distance converges to an inner product between the derivatives or differentials defined by the limit process of the moment conditions. Heuristically, the quadratic form product that uses the 'inverted' BM covariance matrix in finite sample formulations yields asymptotically an inner product between the 'dis-integrated' processes. To the best of our knowledge, this approach and the associated mathematical development is quite new; and in formulating the GMM distance it delivers directly the requisite mathematics implied in the prior literature that the inverse BM-kernel operator is a second-order differential kernel operator (e.g., Carrasco et al., 2007). This linkage is established in the paper using generalized function analysis.[1]

Second, infinite dimensional moment conditions also affect the limit properties of GMM. As mentioned above, there may be two types of infinite dimensional moment conditions: persistently correlated moment conditions and weakly correlated moment conditions. We distinguish these by their sample path characteristics. If the sample path is continuous, we say that the moment conditions are persistently correlated. Otherwise, we call them weakly correlated moment conditions. For the current study, we assume persistently correlated moment conditions and leave the case of weakly correlated moment conditions for future research. This approach is convenient because the large sample analysis of GMM based on the two types of moment conditions are distinct and better treated in separate work. Further, continuous BM and BB kernels are incompatible with weakly correlated moment conditions, although we do not necessarily require that the moment conditions themselves converge to BM or BB processes. Instead, our framework requires that the moment conditions converge to a twice continuously differentiable Gaussian process or an Itô process for which BM and BB processes are just special cases. Using this wide class of infinite dimensional moment conditions, we have a unified framework for investigating the large sample properties of GMM.

In two studies that relate to the present work, Carrasco and Florens (2000) and Amengual et al. (2020) considered infinite dimensional GMM estimation by using Tikhonov regularization methods. Specifically, these authors obtained the limit of an infinite dimensional weight matrix by combining its spectrum with asymptotically negligible bias in a manner analogous to ridge regression so that the methodology is applica-

[1] In this respect the analysis relates to the derivation of least absolute deviation (LAD) asymptotics given in Phillips (1991).

ble even when the weight matrix is not bounded in the limit. Picard (1910) provided necessary and sufficient conditions for the existence of a bounded inverted kernel function. But many popular kernel functions for empirical applications do not satisfy those conditions. In consequence, it is generally believed that it is necessary to apply regularization techniques to enable analysis of inverse kernels in such cases. Indeed, Carrasco and Florens (2000) used regularized kernel inversion to obtain the limit distribution of the estimators defined in terms of the inverse kernel, and Amengual et al. (2020) applied that approach in testing distributional assumptions by GMM (see also Kirsch, 1996; Carrasco et al., 2007). Neither BM-GMM nor BB-GMM kernels satisfy Picard's conditions, so the option of using regularized kernel inversion is available in the present study. But our approach is instead to develop explicit derivations of the inverse BM-kernel and inverse BB-kernel, enabling us to develop and analyze GMM asymptotics without having to resort to the use of regularized kernel inversions.

In addition, the current study addresses overidentification testing. We provide regularity conditions under which the Sargan J-test statistic (Sargan, 1958; Hansen, 1982) can be validly used for testing overidentification in the high-dimensional moment case. In case the regularity conditions for the J-test do not hold, we revisit the T-test approach taken in Donald et al. (2003) and provide a new test for the present setting called the U-test, showing how the two different testing methods supplement each other according to the context.

High dimensional BM- and BB-GMM methods can be applied in many areas where large datasets are available to test relevant economic hypotheses. We demonstrate their use in labor economics, focusing on BB-GMM estimation to measure top labor income shares over time. Among others, Piketty (2003), Piketty and Saez (2003), and Atkinson et al. (2011) have estimated top income shares in many countries over time using income data. A key assumption in their approach is that income observations in the right tail of the distribution closely follow the form of a Pareto tail. In our approach BB-GMM estimation is conducted under the Pareto tail hypothesis by employing the Continuous Work History Sample (CWHS) database, which collects labor income data from individuals born in the U.S. between 1960 and 1962. We test the Pareto tail distributional condition using the U-test. Unless the Pareto tail hypothesis is rejected, we estimate the top income shares using the BB-GMM approach.

A further goal of our empirical study is to examine the evolution of income inequality within the same cohort. Previous research has examined income inequality over time using country-level data, which may not adequately capture structural factors involved in the evolution. Instead, we compute income inequality indices using observations from the same cohort in the CWHS database over time, enabling us to identify a standard pattern in income inequality evolution. By constructing several cohorts from the database, we

derive policy implications to reduce income inequality.

The plan of the present study is as follows. Section 2 develops limit theory in our high dimensional setting for GMM estimation and the tests for overidentification. A particular focus in this discussion is the large sample behavior of BB-GMM estimation when it is applied to MCMD estimation, which is subsequently treated as a running example in the rest of the paper. Section 3 reports the results of a simulation study that employs this running example and corroborates the large sample behavior established in Section 2. Section 4 examines the CWHS database and measures various labor income inequality indices, focusing on data classified by gender, education, race, and birth year. Conclusions are drawn in Section 5. All the main results of the paper are proved in the Online Supplement, together with some additional technical results and empirical evidence.

For ease of reference we introduce some notation. For an arbitrary function $f(\cdot)$ and $j = 1, 2, \ldots$, we use $(d^j/d^j x)f(\bar{x})$ for $(d^j/dx^j)f(x)|_{x=\bar{x}}$. Integral operators are shown in boldface, and $(a(\cdot), b(\cdot))$ is the L^2 inner product of $a(\cdot)$ and $b(\cdot)$, so that $(a(\cdot), b(\cdot)) := \int a(u)b(u)du$. If $A(\cdot) \in \mathbb{R}^a$ and $B(\cdot) \in \mathbb{R}^b$, then $[A(\cdot), B(\cdot)]$ denotes the Gramian matrix of $A(\cdot)$ and $B(\cdot)$, viz., the matrix of inner products between the elements of $A(\cdot)$ and $B(\cdot)$, so that $[A(\cdot), B(\cdot)]$ is an $a \times b$ matrix with (i, j)-th element $(A_i(\cdot), B_j(\cdot))$. Finally, for i and $j = 1, 2, \ldots, n$, we let $i_n := \frac{i}{n}$ and $j_n := \frac{j}{n}$. Other notation in the paper is standard.

2 Estimation and Inference for BM-GMM and BB-GMM

This section develops a large sample theory for BM-GMM and BB-GMM estimation and inference. Section 2.1 describes the modeling environment for BM-GMM and BB-GMM together with two running examples. The large sample theory is discussed in Section 2.2. Section 2.3 extends the large sample theory to testing for overidentification, and Section 2.4 applies BB-GMM and BM-GMM to the running examples.

2.1 Environments of BM- and BB-GMMs

To fix ideas the standard framework for finite dimensional GMM involves extremum estimation with an objective function to be minimized that has the form

$$\bar{q}_n(\cdot) := \bar{G}_n(\cdot)'\widehat{\Sigma}_n^{-1}\bar{G}_n(\cdot) \quad \text{with} \quad q_n(\cdot) := n\bar{q}_n(\cdot)$$

for which there is assumed to be a unique vector $\theta_* \in \Theta$ satisfying the moment condition $\mathbb{E}[\bar{G}_n(\theta_*)] = 0$. Here Θ is a convex and compact parameter space that is a subset of $\mathbb{R}^d$ ($d \in \mathbb{N}$) and the sample moment vector $\bar{G}_n(\cdot)$ is defined by a sequence of strictly stationary and ergodic random variables $\{W_t \in \mathbb{R}^r : t =$

$1, 2, \ldots, n\}$ defined on a complete probability space and continuously differentiable on Θ with probability (prob.) 1. Here, $\widehat{\Sigma}_n \in \mathbb{R}^{s\times s}$ is a symmetric, positive definite matrix for large enough n. Let $\widehat{\theta}_n$ denote the GMM estimator obtained as $\widehat{\theta}_n := \arg\min_{\theta\in\Theta} \bar{q}_n(\theta)$. The dimension of the moment conditions is the dimension, s, of $G_n(\cdot) := n\bar{G}_n(\cdot)$.

Typically in GMM limit theory the number of moment conditions s is invariant to the sample size, although this is not always the case in practical work as in many problems the underlying theory provides a large number of possible moment conditions. Hansen (1982) and Bates and White (1985) among many others explored the asymptotic behavior of the GMM estimator in fixed dimensional settings. Specifically, if the GMM estimator is approximated as

$$\sqrt{n}(\widehat{\theta}_n - \theta_*) = -\left[\nabla_\theta \bar{G}_n(\theta_*)\widehat{\Sigma}_n^{-1}\nabla_\theta' \bar{G}_n(\theta_*)\right]^{-1}\left[\nabla_\theta \bar{G}_n(\theta_*)\widehat{\Sigma}_n^{-1}\widetilde{G}_n(\theta_*)\right] + o_{\mathbb{P}}(1) \tag{1}$$

by way of Taylor expansion, where $\widetilde{G}_n(\theta_*) := \sqrt{n}\bar{G}_n(\theta_*)$, the limit distribution of the GMM estimator is obtained by deriving the limit behavior of the components on the right side of (1). If $\nabla_\theta \bar{G}_n(\theta_*)$ and $\widehat{\Sigma}_n$ converge to H_* and Σ with prob. converging to 1, and $\widetilde{G}_n(\theta_*) \overset{\text{A}}{\sim} \mathcal{N}(0, \Sigma_*)$, then $\sqrt{n}(\widehat{\theta}_n - \theta_*)$ is asymptotically normal.

The current study differs from the standard GMM framework as the number of moment conditions s is allowed to increase with $n \to \infty$. For this purpose we let $s = s_n$ be the dimension of the moment conditions with consequent implications for the weight matrices in GMM estimation. Our particular focus in estimating θ when $\widehat{\Sigma}_n$ has the following possible $\ddot{\Sigma}_n$ or $\widetilde{\Sigma}_n$. Here the (i, j)-th element of $\ddot{\Sigma}_n$ is $\min(i_n, j_n)$ and the dimension of $\ddot{\Sigma}_n$ is n, which corresponds to the finite sample analog of a Brownian motion kernel. We refer to the GMM driven by $\ddot{\Sigma}_n$ as Brownian motion GMM (BM-GMM) and we denote the corresponding estimator as $\ddot{\theta}_n$. Similarly, $\widetilde{\Sigma}_n$ is a sample analog of the Brownian bridge kernel, and the (i, j)-th element is $\min(i_n, j_n)(1 - \max(i_n, j_n))$. The dimension of $\widetilde{\Sigma}_n$ is $n - 1$, as inclusion of the n-th row and n-th column would make $\widetilde{\Sigma}_n$ singular. So $\widetilde{\Sigma}_n$ is defined by the first $(n - 1)$ rows and columns by letting $i, j = 1, 2, \ldots, n - 1$. We call the estimator based on $\widetilde{\Sigma}_n$ the Brownian bridge GMM (BB-GMM) and it is denoted $\widetilde{\theta}_n$. A primary goal of the paper is to derive the limit properties of BM-GMM and BB-GMM.

Example 1: MCMD Estimation Bontemps and Meddahi (2012) test distributional assumptions by GMM methods using the moment conditions implied by the assumption. Use of BM- and BB-GMMs is more related to MCMD estimation. In that connection, Pollard (1980) and Cho et al. (2018) examined estimating an unknown parameter θ_* in the distribution function, $F(\cdot, \theta_*)$, of a variable x_t by minimizing the Cramér-von Mises distance. Specifically, it was assumed that grouped data $\{[c_{j-1}, c_j), \#\{x_t \in$

$[c_{j-1}, c_j)\} : j = 1, 2, \ldots, s; t = 1, \ldots, n\}$ are available on x_t and θ_* is estimated by minimizing the objective function $\bar{q}_n^{(s)}(\theta) := \sum_{j=1}^{s}\{\widehat{p}_{n,j} - F(c_j, \theta)\}^2$ with respect to θ, where for each $j = 1, 2, \ldots, s$, $\widehat{p}_{n,j} := n^{-1}\sum_{t=1}^{n}\mathbb{I}(x_t \in [c_0, c_j])$, and $\{x_t : t = 1, 2, \ldots, n\}$ is a sequence of independent identically distributed (IID) random variables. In this formulation the quantity $\widehat{p}_{n,j}$, giving the proportion of the data in interval j, is treated as the dependent variable, and $F(c_j, \cdot)$ serves as a nonlinear model for $\widehat{p}_{n,j}$. When $F(\cdot, \theta_*)$ correctly matches the distribution of x_t, the MCMD estimator of θ_* is consistent, and its distribution is asymptotically normal. In particular, if the MCMD estimator is used to construct the Kolmogorov-Smirnov (KS) statistic to test a distributional hypothesis with an unknown parameter, the null limit distribution is a functional of a linearly transformed Brownian bridge.

MCMD estimation of this type can be formulated in GMM format. For each $j = 1, 2, \ldots, s$, the parameter θ_* satisfies the moment condition $\mathbb{E}[\widehat{p}_{n,j} - F(c_j, \theta_*)] = 0$. Let $\widehat{\theta}_n^{(s)}$ be the GMM extremum estimator satisfying

$$\widehat{\theta}_n^{(s)} := \arg\min_{\theta\in\Theta}(\widehat{P}_n^{(s)} - F^{(s)}(\theta))' W^{(s)} (\widehat{P}_n^{(s)} - F^{(s)}(\theta)),$$

where $\widehat{P}_n^{(s)} := [\widehat{p}_{n,1}, \ldots, \widehat{p}_{n,s}]'$, $F^{(s)}(\theta) := [F(c_1, \theta), \ldots, F(c_s, \theta)]'$, and $W^{(s)}$ is an $s \times s$ positive definite matrix that converges to a positive definite matrix as n tends to infinity. The MCMD estimator is therefore a GMM estimator with a structure of generalized least squares. The GMM estimator $\widehat{\theta}_n^{(s)}$ is consistent for θ_* and asymptotically normal under the standard framework that applies when the number of groups s is fixed. The MCMD estimator is then the special case where the weight matrix is $W^{(s)} = I_s$. As another case, if the data is grouped and the group dimension is $s_n = n - 1$ with $W^{(s_n)} = \widetilde{\Sigma}_n^{-1}$, then MCMD falls within the framework of BB-GMM. Section 2.4 demonstrates that $\sqrt{n}(\widehat{P}_n^{(s)} - F^{(s)}(\theta_*))$ weakly converges to a Brownian bridge process $\mathcal{B}^0(\cdot)$ if the distribution of x_t is continuous, which motivates $\widetilde{\Sigma}_n^{-1}$ as the weight matrix for GMM. Accordingly, we now refer to MCMD estimation driven by $W^{(s_n)} = \widetilde{\Sigma}_n^{-1}$ as infinite dimensional MCMD estimation. □

Example 2: Regression Using Integrated Series Consider two independent, integrated time series u_t and $x_t \in \mathbb{R}^k$ where $\Delta u_t = O_{\mathbb{P}}(1)$ and $\Delta x_t = O_{\mathbb{P}}(1)$ are strictly stationary with $\mathbb{E}[\Delta u_t] = 0$ and $\mathbb{E}[\Delta x_t] = 0$. Further suppose that y_t is generated such that for some unknown $\beta_* \in \mathbb{R}^k$, $y_t = x_t'\beta_* + u_t$. Without loss of generality, let $y_0 = 0$ and $x_0 = 0$. This data generating process (DGP) differs from the cointegrating systems in Phillips and Durlauf (1986) and Engle and Granger (1987), where a stationary series is assumed for u_t in generating y_t and the cointegrating vector β_* is being estimated. In the present case u_t is nonstationary and the vector β_* in the generating mechanism is to be estimated, even though the DGP is analogous to the spurious regression considered in Phillips (1986).

Ordinary least squares (OLS) does not deliver a consistent estimate of β_*. In fact, since x_t and u_t are both integrated processes, the OLS estimate $\bar{\beta}_n$ is inconsistent with the following limit behavior (Phillips and Durlauf, 1986)

$$\bar{\beta}_n = \beta_* + \left(\frac{1}{n^2} \sum_{t=1}^{n} x_t x_t' \right)^{-1} \frac{1}{n^2} \sum_{t=1}^{n} x_t u_t \Rightarrow \beta_* + \left(\int_0^1 \mathcal{B}_x(v) \mathcal{B}_x(v)' dv \right)^{-1} \int_0^1 \mathcal{B}_x \mathcal{B}_u(v) dv, \quad (2)$$

where $\mathcal{B}_x(\cdot) := \Omega_x^{1/2} \mathcal{W}_x(\cdot)$ and $\mathcal{B}_u(\cdot) = \sigma_u \mathcal{W}_u(\cdot)$ are Brownian motions driven by partial sums of the innovations Δx_t and Δu_t. Here, $\mathcal{W}_x(\cdot)$ and $\mathcal{W}_u(\cdot)$ are independent Wiener processes, Ω_x is the nonsingular long run variance matrix of Δx_t and σ_u^2 is the long run variance of Δu_t. The limit theory (2) depends on the joint weak convergence $\left(n^{-1/2} \sum_{t=1}^{\lfloor (\cdot) n \rfloor} x_t, n^{-1/2} \sum_{t=1}^{\lfloor (\cdot) n \rfloor} u_t \right) \Rightarrow (\mathcal{B}_x(\cdot), \mathcal{B}_u(\cdot))$ under some mild regularity conditions (e.g., Phillips and Durlauf (1986), White (2001, ch. 7)), where $\lfloor a \rfloor$) denotes the integer part of a.

By contrast, BM-GMM estimates β_* consistently. Since $\mathbb{E}[u_t] = 0$ for each t, let $\widehat{\beta}_n$ be the infinite dimensional GMM estimator obtained by extremum estimation as

$$\widehat{\beta}_n := \arg\min_{\beta} n \bar{q}_n(\beta), \quad \text{where} \quad \bar{q}_n(\beta) := \bar{G}_n(\beta)' \ddot{\Sigma}_n^{-1} \bar{G}_n(\beta) \quad \text{with} \quad \bar{G}_n(\beta) := n^{-1} (y - X\beta),$$

where $y := (y_1, \ldots, y_n)'$ and $X := (x_1, \ldots, x_n)'$, so that $\widehat{\beta}_n = (X' \ddot{\Sigma}_n^{-1} X)^{-1} X' \ddot{\Sigma}_n^{-1} y$. We demonstrate below that this infinite dimensional GMM estimator is consistent and asymptotically normal with $\sqrt{n}$ convergence rate. □

In addition to the above infinite dimension GMM estimations there are other examples where the moment dimension is determined by the sample size n. Grenander (1981) developed a theory of abstract inference in function space that deals with parameters in models involving various stochastic processes and studied best linear unbiased estimation in that context. The abstract space setting relates to the approach taken in the current study where our focus involves inverse BM and BB kernels. Carrasco and Florens (2000) also worked with a model that falls into the infinite dimensional GMM framework. They noted the important limitation that the limiting form of the usual weight matrix (in this setting $\ddot{\Sigma}_n^{-1}$ and $\widetilde{\Sigma}_n^{-1}$) does not necessarily exist as a bounded linear operator, because the associated covariance operator does not satisfy Picard's (1910) conditions for the existence of a linear inverse operator in the limit. Their approach instead uses Tikhonov's regularization, as in ridge regression, so that the inverse operator can be represented in terms of an approximate spectral decomposition of the covariance operator. This involves bias that vanishes asymptotically (see also Kirsch, 1996). Amengual et al. (2020) applied this method to test distributional assumptions by GMM. Our MCMD approach, in contrast to these methods, focuses directly on the underlying kernel and works explicitly with its inverse in a manner that enables the limit behavior of BB-GMM to be

obtained without applying Tikhonov regularization.

Several other high-dimensional studies relate to the present work. Shi (2016) examines estimating a nonlinear structural model similar to that of the present paper but with an approach that maximizes a constrained empirical likelihood and selects only informative moment conditions. Donald and Newey (2001), Bai and Ng (2010) and Belloni et al. (2012) also examine estimating linear structural parameters using high-dimensional moment conditions in environments that differ from the current study, supposing different dimension sizes for the moments compared to the current study. Donald and Newey (2001) assume $s_n^2 = o(n)$ and select the set of instruments to produce an asymptotically efficient GMM estimator based on mean squared error. Bai and Ng (2010) let $s_n = o(n)$ and estimate the parameter by exploiting a factor structure in the data. Belloni et al. (2012) select informative instrumental variables by means of Lasso and Post-Lasso regressions to estimate the unknown parameter by two-stage least squares estimation for $\log(s_n) = o(n^{1/2})$.

2.2 Limit Properties of BM- and BB-GMMs

The limit distribution of the BM- and BB-GMM estimators are obtained by deriving the limit behaviors of the components on the right side of (1), viz., $(\bar{G}_n(\theta_*), \nabla_\theta \bar{G}_n(\theta_*), \widehat{\Sigma}_n)$. For the limit distribution, it is convenient to translate them using functional representation. We first transform $\bar{G}_n(\theta_*)$ into a càdlàg function defined on $[0,1]$. For each θ, we let $\bar{G}_{n,j}(\theta)$ be the j-th row element of $\bar{G}_n(\theta) \in \mathbb{R}^{s_n}$ and define

$$g_n(u,\theta) := \begin{cases} \bar{G}_{n,j}(\theta), & \text{if } u \in [(j-1)/n, j/n),\ j = 1, 2, \ldots, s_n; \text{ and} \\ 0, & \text{if } u \in [s_n/n, 1]. \end{cases}$$

Note that $\bar{G}_n(\theta)$ has s_n rows, and the above function $g_n(\cdot,\theta)$ is defined by translating $\bar{G}_n(\theta)$ into a function defined on the unit interval, which represents the space of the standardized index.

This standardization makes the weak limit analysis of $\bar{G}_n(\theta_*)$ straightforward. As s_n grows to infinity, it is appropriate to apply the functional central limit theorem (FCLT). Many applications of FCLT methods have appeared in the econometric literature since, in one context, the work of Phillips (1987) on limit theory in unit root time series regression using partial sums, and in another, Cho and White (2011) on limit theory for generalized runs tests. Here we suppose that $\widetilde{g}_n(\cdot,\theta_*) := \sqrt{n} g_n(\cdot,\theta_*)$ weakly converges to a Gaussian stochastic process $\mathcal{G}(\cdot)$ say, such that for a continuous function $\omega(\cdot,\cdot)$ defined on $[0,1]^2$, $\mathbb{E}[\mathcal{G}(u_1)\mathcal{G}(u_2)] = \omega(u_1,u_2)$. From this weak convergence, the uniform law of large numbers (ULLN) follows for $g_n(\cdot,\theta_*)$ so that $\sup_{u\in[0,1]} |g_n(u,\theta_*)| \to 0$ with prob. converging to 1.

We focus on two types of Gaussian processes in this work. We suppose that $\mathcal{G}(\cdot)$ is either a Gaussian

process in $\mathcal{C}^{(2)}([0,1])$ with prob. 1, or an Itô process satisfying a stochastic differential equation so that for some $\mu : [0,1] \times \Omega \mapsto \mathbb{R}$ and $\sigma : [0,1] \times \Omega \mapsto \mathbb{R}$, $d\mathcal{G}(u) = \mu(u, \mathcal{G}(u))du + \sigma(u, \mathcal{G}(u))d\bar{\mathcal{B}}(u)$, where $\bar{\mathcal{B}}(\cdot)$ is a Brownian motion. As discussed below, BM-GMM and BB-GMM estimators have different asymptotic behavior depending on the path properties of $\mathcal{G}(\cdot)$. If $\mathcal{G}(\cdot)$ is differentiable with prob. 1, $\omega(\cdot,\cdot)$ is also differentiable on $[0,1]^2$, and $\mathcal{G}'(\cdot)$ becomes another Gaussian process. This further implies that $\mathcal{G}''(\cdot)$ is also a Gaussian process. On the other hand, if $\mathcal{G}(\cdot)$ is an Itô process, $\omega(\cdot,\cdot)$ is not differentiable. There are many such Gaussian examples, including Brownian motion and Brownian bridge processes. To simplify notation from now on, we suppress θ_* in $\widetilde{g}_n(\cdot, \theta_*)$, writing $\widetilde{g}_n(\cdot) \equiv \widetilde{g}_n(\cdot, \theta_*)$; and we let $\mu(u)$ and $\sigma(u)$ denote $\mu(u, \mathcal{G}(u))$ and $\sigma(u, \mathcal{G}(u))$, respectively.

We next rewrite $\nabla_\theta \bar{G}_n(\theta_*)$ as a set of functions defined on the unit interval that uniformly converges to a continuous function on the same interval. For $j = 1, 2, \ldots, s_n$ and $j = 1, 2, \ldots, d$, first let $H_n^{(j,i)}$ be the j-th row and i-th column element of $\nabla'_\theta \bar{G}_n(\theta_*) \in \mathbb{R}^{s_n \times d}$, and then for each $i = 1, 2, \ldots, d$ further let

$$H_{n,i}(u) := \begin{cases} H_n^{(j,i)}, & \text{if } u \in [(j-1)/n, j/n),\ j = 1, 2, \ldots, s_n; \text{ and} \\ 0, & \text{if } u \in [s_n/n, 1], \end{cases}$$

and $H_n(\cdot) := [H_{n,1}(\cdot), H_{n,2}(\cdot), \ldots, H_{n,d}(\cdot)]'$. As for $g_n(\cdot)$, $H_{n,i}(\cdot)$ has a jump at each increment of j/n, where $j = 1, 2, \ldots, s_n$. Here, we suppose that the ULLN holds for this stochastic function, so that as n tends to infinity for each j and for a continuous function $H_j(\cdot)$, $\sup_{u \in [0,1]} |H_{n,j}(u) - H_j(u)| \to 0$ with prob. converging to 1. We also let $H(\cdot) := [H_1(\cdot), H_2(\cdot), \ldots, H_d(\cdot)]'$.

As a final functional reformulation, we translate $\widehat{\Sigma}_n$ as a two-dimensional càdlàg function defined on $[0,1]^2$ by defining

$$\widehat{\sigma}_n(u_1, u_2) := \begin{cases} \widehat{\Sigma}_n^{(j,i)}, & \text{if } u_1 \in [(j-1)/n, j/n),\ u_2 \in [(i-1)/n, i/n), \text{ and } j, i = 1, 2, \ldots, s_n; \text{ and} \\ 0, & \text{if } u_1 \in [s_n/n, 1] \text{ and } u_2 \in [s_n/n, 1], \end{cases}$$

where $\widehat{\Sigma}_n^{(j,i)}$ is the j-th row and i-th column element of $\widehat{\Sigma}_n$. For the case of $\ddot{\Sigma}_n$, $\widehat{\Sigma}_n^{(j,i)} = \min[j_n, i_n]$, and we let $\ddot{\sigma}_n(\cdot, \circ)$ denote $\widehat{\sigma}_n(\cdot, \circ)$, which converges to $\ddot{\sigma}(\cdot, \circ) := \min[\cdot, \circ]$ uniformly on $[0,1] \times [0,1]$. For the case of $\widetilde{\Sigma}_n$, $\widehat{\Sigma}_n^{(j,i)} = \min[j_n, i_n](1 - \max[j_n, i_n])$, and we let $\widetilde{\sigma}_n(\cdot, \circ)$ denote $\widehat{\sigma}_n(\cdot, \circ)$, which converges to $\widetilde{\sigma}(\cdot, \circ) := \min[\cdot, \circ](1 - \max[\cdot, \circ])$ uniformly on $[0,1] \times [0,1]$.

The functional representations discussed above make it convenient to represent the associated statistics by an integral transform. For example, if we let $B_n := [b_n(\frac{1}{n}), \ldots, b_n(\frac{s_n}{n})]'$ and $C_n := [c_n(\frac{1}{n}), \ldots, c_n(\frac{s_n}{n})]'$,

where $b_n(\cdot) := b(\lfloor n(\cdot)\rfloor/n)$ and $c_n(\cdot) := c(\lfloor n(\cdot)\rfloor/n)$ with $b(\cdot)$ and $c(\cdot)$ being continuous on $[0,1]$,

$$B_n'\widehat{\Sigma}_n C_n = \sum_{j=1}^{s_n}\sum_{i=1}^{s_n} b_n(j_n)\, c_n(i_n)\, \widehat{\Sigma}_n^{(j,i)} = n^2 \int_0^1 \int_0^1 b_n(u_1)\widehat{\sigma}_n(u_1,u_2)c_n(u_2)du_1du_2.$$

Here, $\lfloor\cdot\rfloor$ denotes the smallest integer greater than the given argument. If we further let $\widehat{\mathbf{\Sigma}}_n$ be an integral operator with kernel $n^2\widehat{\sigma}_n(\cdot,\circ)$, viz., $\widehat{\mathbf{\Sigma}}_n b_n(\circ) = n^2\int_0^1 b_n(u_1)\widehat{\sigma}_n(u_1,\circ)du_1$, we also have $B_n'\widehat{\Sigma}_n C_n = (\widehat{\mathbf{\Sigma}}_n b_n(\cdot), c_n(\cdot))$. Likewise, the inner product representation for the integral transform of the quadratic product can apply to a quadratic product with the weight matrix $\widehat{\Sigma}_n^{-1}$. For an integral operator $\widehat{\mathbf{\Xi}}_n$ with a kernel $\widehat{\xi}_n(\cdot,\circ)$, we suppose that

$$\bar{q}_n(\theta_*) = \bar{G}_n(\theta_*)'\widehat{\Sigma}_n^{-1}\bar{G}_n(\theta_*) = \int_0^1\int_0^1 g_n(u_1)\widehat{\xi}_n(u_1,u_2)g_n(u_2)du_1du_2 = (\widehat{\mathbf{\Xi}}_n g_n(\cdot), g_n(\cdot)).$$

Note that $\widehat{\xi}_n(\cdot,\circ)$ corresponds to the kernel of $\widehat{\mathbf{\Sigma}}_n$, viz., $n^2\widehat{\sigma}_n(\cdot,\circ)$. Likewise, it follows that

$$\nabla_\theta\bar{G}_n(\theta_*)\widehat{\Sigma}_n^{-1}\nabla_\theta'\bar{G}_n(\theta_*) = [\widehat{\mathbf{\Xi}}_n H_n(\cdot), H_n(\cdot)] \quad \text{and} \quad \nabla_\theta\bar{G}_n(\theta_*)\widehat{\Sigma}_n^{-1}\widetilde{G}_n(\theta_*) = [\widehat{\mathbf{\Xi}}_n H_n(\cdot), \widetilde{g}_n(\cdot)]$$

by analogy. Here, $[\widehat{\mathbf{\Xi}}_n H_n(\cdot), H_n(\cdot)]$ denotes the Gramian matrix constructed by $\widehat{\mathbf{\Xi}}_n H_n(\cdot)$ and $H_n(\cdot)$, viz., its j-th row and i-column element is $(\widehat{\mathbf{\Xi}}_n H_{n,j}(\cdot),\ H_{n,i}(\cdot))$. The same interpretation also applies to $[\widehat{\mathbf{\Xi}}_n H_n(\cdot), \widetilde{g}_n(\cdot)]$. Note that these inner products involving the integral transforms are employed to handle the large dimension of the moment conditions tending to infinity. From now, we specifically let $\widetilde{\mathbf{\Xi}}_n$ and $\ddot{\mathbf{\Xi}}_n$ be the integral operators associated with $\widehat{\Sigma}_n^{-1}$ and $\ddot{\Sigma}_n^{-1}$, respectively, and their limit operators are also denoted as $\widetilde{\mathbf{\Xi}}$ and $\ddot{\mathbf{\Xi}}$, respectively.

The inverse kernel $\widehat{\xi}_n(\cdot,\circ)$ exhibits various asymptotic properties, and the asymptotic behavior of $\widehat{\mathbf{\Xi}}_n$ critically depends on them. Before examining the asymptotic properties of BM-GMM and BB-GMM, we first examine the asymptotic behavior of $\widetilde{\xi}_n(\cdot,\cdot)$ and $\ddot{\xi}_n(\cdot,\circ)$. The inverse kernel property is substantially different from being continuous. We first focus on $\widetilde{\xi}_n(\cdot,\circ)$ denoting the kernel function of $\widetilde{\mathbf{\Xi}}_n$, which we provide in Section A.5. The following lemma delivers the limit behavior of $(\widetilde{\mathbf{\Xi}}_n b_n(\cdot), c_n(\cdot))$:

Lemma 1. *Given that $b(\cdot)$ and $c(\cdot)$ are such that $b(0) = c(0) = b(1) = c(1) = 0$,*

(i) (i.a) if $b(\cdot) \in \mathcal{C}^{(2)}([0,1])$, $\widetilde{\mathbf{\Xi}}_n b_n(\cdot) = -b''(\cdot) + o(1)$;
(i.b) if it further holds that $c(\cdot) \in \mathcal{C}^{(1)}([0,1])$, $(\widetilde{\mathbf{\Xi}}_n b_n(\cdot), c_n(\cdot)) = (b'(\cdot), c'(\cdot)) + o(1)$;
(ii) if $b(\cdot)$ and $c(\cdot)$ are continuous functions with finite second variations, $n^{-1}(\widetilde{\mathbf{\Xi}}_n b_n(\cdot), c_n(\cdot)) = (db(\cdot), dc(\cdot)) + o(1)$, where $db(\cdot)$ and $dc(\cdot)$ denote the differentials of $b(\cdot)$ and $c(\cdot)$, respectively. □

Remarks 1. (i) Lemma 1 shows that the limit properties and convergence rate of $(\widehat{\mathbf{\Xi}}_n b_n(\cdot), c_n(\cdot))$ both depend on the functions attached to the operator.

(ii) Lemma 1 (i.a) shows that the kernel function of $\widetilde{\mathbf{\Xi}}$ is given by $-\delta''(\cdot - \circ)$, viz., the negative second-order derivative of the Dirac delta generalized function. Under the condition of Lemma 1 (i.a), we

show that $n\widetilde{\Sigma}_n^{-1}B_n \to -b''(\cdot)$ which can be written as $-\int_0^1 \delta''(u-\cdot)b(u)du$.

(iii) Lemma 1 (i.b) follows by the integration by parts. That is, $c(1)b'(1)-c(0)b'(0) = \int_0^1 d\{c(u)b'(u)\} = \int_0^1 c'(u)b'(u)du + \int_0^1 c(u)b''(u)du$. Note that $(b'(\cdot), c'(\cdot)) = -(c(\cdot), b''(\cdot))$, as $c(0) = c(1) = 0$ implies that relation.

(iv) By the bounded second variation condition, $\int_0^1 (db(u))^2 < \infty$ and $\int_0^1 (dc(u))^2 < \infty$. The sample path generated by the Brownian bridge process satisfies the conditions in Lemma 1 (ii). For example, if we let $\mathcal{B}^0(\cdot)$ be the Brownian bridge process and $b(\cdot) = c(\cdot) = \mathcal{B}^0(\cdot)$, Lemma 1 (ii) implies that $n^{-1}(\widehat{\Xi}_n b_n(\cdot), c_n(\cdot)) \Rightarrow \int_0^1 (d\mathcal{B}^0(u))^2$, which is identical to 1 by noting that $d\mathcal{B}^0(u) = -(1-u)^{-1}\mathcal{B}^0(u)du + d\mathcal{W}(u)$, so that $(d\mathcal{B}^0(u))^2 = du$. If $b(\cdot)$ and $c(\cdot)$ are continuously differentiable, it simply follows that $(db(\cdot), dc(\cdot)) = 0$.

(v) The boundary conditions at zero and unity are needed for the desired results. For example, suppose $b(0) \neq 0$ and $b(1) \neq 0$ such that for some $b_0 \neq 0$ and $b_1 \neq 0$, $n^2 b_n(0) = b_0 + o(1)$ and $n^2 b_n(1) = b_1 + o(1)$. It then follows that $\ddot{\Xi}_n b_n(\cdot) = g(\cdot) + o(1)$ such that $g(0) = b_0 - b''(0)$, $g(1) = b_1 - b''(1)$, and for $x \in (0,1)$, $g(x) = -b''(x)$ under the conditions in Lemma 1 (i.a). Note that the non-zero boundary conditions modify the limit. □

We next examine $\ddot{\Sigma}_n^{-1}$ by letting $\ddot{\xi}_n(\cdot, \circ)$ denote the kernel function of $\ddot{\Xi}_n$, which is given in Section A.5. The following lemma reveals the asymptotic properties of $(\ddot{\Xi}_n b_n(\cdot), c_n(\cdot))$:

Lemma 2. *Given that $b(\cdot)$ and $c(\cdot)$ are such that $b(0) = c(0) = 0$,*

(i) (i.a) if $b(\cdot) \in \mathcal{C}^{(2)}([0,1])$ and $b'(1) = 0$, $\ddot{\Xi}_n b_n(\cdot) = -b''(\cdot) + o(1)$;
(i.b) if it further holds that $c(\cdot) \in \mathcal{C}^{(1)}([0,1])$, $(\ddot{\Xi}_n b_n(\cdot), c_n(\cdot)) = (b'(\cdot), c'(\cdot)) + o(1)$;

(ii) if $b(\cdot)$ and $c(\cdot)$ are continuous functions with finite second variations, $n^{-1}(\ddot{\Xi}_n b_n(\cdot), c_n(\cdot)) = (db(\cdot), dc(\cdot)) + o(1)$. □

Remarks 2. (i) Lemma 2 derives the results of Lemma 1 under different conditions for $c_n(\cdot)$ and $b_n(\cdot)$.

(ii) The result in Lemma 2 (i.a) is consistent with the standard result on the inverse BM-kernel, which is a kernel for second-order differentiation (e.g., Carrasco et al., 2007). Lemma 2 (i.b) elaborates Lemma 2 (i.a) and obtains the inner product between the derivatives using the inverse BM-kernel.

(iii) The sample path generated by the Brownian motion satisfies the conditions in Lemma 2 (ii). If we let $\mathcal{B}(\cdot)$ be the Brownian motion and $b(\cdot) = c(\cdot) = \mathcal{B}(\cdot)$, we obtain that $n^{-1}(\ddot{\Xi}_n b_n(\cdot), c_n(\cdot)) \Rightarrow \int_0^1 (d\mathcal{B}(u))^2 = \int_0^1 du = 1$.

(iv) Lemma 2 (ii) provides an intuitive interpretation of the BM- and BB-kernels. The BM-kernel is the covariance kernel of an integrated process, so that if we use the integral transform operator using its inverse kernel, it should deliver anti-integrated processes, viz., differentials. Therefore, the quadratic transform using $\ddot{\Sigma}_n^{-1}$ should converge to the inner product between the differentials of $b(\cdot)$ and $c(\cdot)$, viz., $(db(\cdot), dc(\cdot))$. This interpretation also applies to the BB-kernel, and Lemmas 1 (ii) and 2 (ii) provide conditions for the desired result. Furthermore, if $b_n(\cdot)$ and $c_n(\cdot)$ converge to differentiable functions, the quadratic transform converges to the inner product between the derivatives of $b(\cdot)$ and $c(\cdot)$, viz., $(b'(\cdot), c'(\cdot))$. Lemmas 1 (i.b) and 1 (i.b) provides the conditions for this result.

(v) As for Lemma 1, the boundary condition at zero is needed for the desired results. For example, if $b(0) \neq 0$ such that for some $b_0 \neq 0$, $n^2 b_n(0) = b_0 + o(1)$, then it follows that $\ddot{\Xi}_n b_n(\cdot) = f(\cdot) + o(1)$ such that $f(0) = b_0 - b''(0)$ and for $x \in (0,1]$, $f(x) = -b''(x)$ under the conditions in Lemma 2 (i.a). Hence, a non-zero boundary condition modifies the limit result. □

The properties of $\widetilde{\Sigma}_n^{-1}$ and $\ddot{\Sigma}_n^{-1}$ established in Lemmas 1 and 2 facilitate the derivation of the limit behavior of the BM-GMM and BB-GMM estimators for which the following assumptions are employed.

Assumption 1. *(i)* $(\Omega, \mathcal{F}, \mathbb{P})$ *is a complete probability space on which the strictly stationary and ergodic sequence* $\{W_t \in \mathbb{R}^p : t = 1, 2, \ldots, n\}$ *is defined;*

(ii) for each $n \in \mathbb{N}$ *and* $t = 1, 2, \ldots, s_n$, $\bar{g}_{n,t} : \mathbb{R}^{p \cdot t} \times \Theta \mapsto \mathbb{R}$ *(*$s_n = n$ *or* $n - 1$*) defines the* t*-th row component of the moment condition* $\bar{G}_n(\cdot)$ *such that for each* t *and* n *and* $\theta \in \Theta$, $\bar{g}_{n,t}(\cdot, \theta)$ *is a measurable function, and for each* $\omega \in \Omega_0 \in \mathcal{F}$, $\bar{g}_{n,t}(W^t(\omega), \cdot) \in \mathcal{C}^{(2)}(\Theta)$ *and* $\mathbb{P}(\omega \in \Omega_0) = 1$*, where* $W^t := (W_1, W_2, \ldots, W_t)$*;*

(iii) there is a unique $\theta_* \in \text{int}(\Theta)$ *such that* $\mathbb{E}[\bar{g}_{n,t}(\theta_*)] = 0$*, and* θ_* *is invariant to* t *and* n*, where* $\Theta \subset \mathbb{R}^d$ $(d \in \mathbb{N})$ *is compact and convex, and* $\bar{g}_{n,t}(\cdot) := \bar{g}_{n,t}(W^t, \cdot)$. □

Assumption 2. $\widetilde{g}_n(\cdot) \Rightarrow \mathcal{G}(\cdot)$*, where* $\mathcal{G}(\cdot)$ *is a Gaussian stochastic process defined on* $[0, 1]$ *with a continuous covariance kernel* $\omega(\cdot, \circ) : [0, 1]^2 \mapsto \mathbb{R}$ *such that* $\mathcal{G}(0) = 0$ *with prob. 1 and*

(i) $\mathcal{G}(\cdot) \in \mathcal{C}^{(2)}([0, 1])$ *with prob. 1; or*

(ii) $\mathcal{G}(\cdot)$ *is an Itô process satisfying the following stochastic differential equation: for some* $\mu : [0, 1] \times \Omega \mapsto \mathbb{R}$ *and* $\sigma : [0, 1] \times \Omega \mapsto \mathbb{R}$, $d\mathcal{G}(u) = \mu(u)du + \sigma(u)d\bar{\mathcal{B}}(u)$ *such that*

(ii.a) $\mu(\cdot, \omega)$ *and* $\sigma(\cdot, \omega)$ *are continuous for each* $\omega \in \Omega$*;*

(ii.b) for each $i = 1, 2, \ldots, n$, $\sigma(i_n)$ *is stationary, ergodic, adapted mixingale of size* -1 *such that for a continuous function* $\Psi_1 : [0, 1] \mapsto \mathbb{R}^+$ *and a continuous and symmetric function* $\Psi_2 : [0, 1]^2 \mapsto \mathbb{R}$*,*

$$\text{cov}\left[\left(\Delta\widetilde{g}_n\left(i_n\right)\right)^2, \left(\Delta\widetilde{g}_n\left(j_n\right)\right)^2\right] = \begin{cases} n^{-2}\Psi_1(i_n) + o(n^{-2}), & \text{if } i = j; \\ n^{-3}\Psi_2(i_n, j_n) + o(n^{-3}), & \text{if } i \neq j \end{cases}$$

uniformly in n*, where for each* $i = 1, 2, \ldots, n$, $\Delta\widetilde{g}_n\left(i_n\right) := \widetilde{g}_n\left(i_n\right) - \widetilde{g}_n\left((i-1)/n\right)$*;*

(ii.c) $\mathbb{E}[\sigma^2(\cdot)]$ *is finite uniformly on* $[0, 1]$. □

For the following assumption, we let $\odot$ denote the Hadamard product between two matrices.

Assumption 3. *For* $j = 1, 2, \ldots, d$*, there is* $H_j(\cdot) \in L^2([0, 1])$ *such that* $H_n(\cdot) \to H(\cdot)$ *uniformly on* $[0, 1]$ *in prob., where* $H(\cdot) \in \mathcal{C}^{(2)}([0, 1])$*, and for continuous* $C_1(\cdot) : [0, 1] \mapsto \mathbb{R}^d$ *and* $C_j(\cdot) : [0, 1] \mapsto \mathbb{R}^{d \times d}$ *(*$j = 2, 3, 4$*),*

$$\sqrt{n}\Delta H_n(\cdot) = n^{-1/2}C_1(\cdot) + C_2(\cdot)\Delta\widetilde{h}_n(\cdot) + n^{-1/2}C_3(\cdot)(\widetilde{h}_n(\cdot) \odot \Delta\widetilde{h}_n(\cdot)) + n^{-1}C_4(\cdot)\widetilde{h}_n(\cdot) + O_{\mathbb{P}}(n^{-3/2})$$

such that $\widetilde{h}_n(\cdot) \Rightarrow \mathcal{H}(\cdot)$*, where* $\mathcal{H}(\cdot)$ *is a Gaussian stochastic process defined on* $[0, 1]$ *and*

(i) $\mathcal{H}(\cdot) \in \mathcal{C}^{(2)}([0, 1])$ *with prob. 1; or*

(ii) $\mathcal{H}(\cdot)$ *is an Itô process satisfying the following stochastic differential equation: for some* $\nu : [0, 1] \times \Omega \mapsto \mathbb{R}^d$ *and* $\tau : [0, 1] \times \Omega \mapsto \mathbb{R}^{d \times d}$, $d\mathcal{H}(u) = \nu(u)du + \tau(u)d\widetilde{\mathcal{B}}(u)$ *such that*

(ii.a) $\nu(\cdot, \omega)$ *and* $\tau(\cdot, \omega)$ *are continuous for each* $\omega \in \Omega$*;*

(ii.b) $\mathbb{E}[\text{tr}(\tau(\cdot)\tau(\cdot)')]$ *is finite uniformly on* $[0, 1]$*;*

(ii.c) for each $i = 1, 2, \ldots, n$, $\sigma(i_n)\tau(i_n)$ *is a stationary, ergodic, adapted mixingale of size* -1 *such that for a continuous function* $\Gamma_1 : [0, 1] \mapsto \mathbb{R}^{d \times d}$ *and a continuous and symmetric function*

$\Gamma_2 : [0,1]^2 \mapsto \mathbb{R}^{d\times d}$,

$$\operatorname{cov}\left[\Delta\widetilde{g}_n(i_n)\,\Delta\widetilde{h}_n(i_n), \Delta\widetilde{g}_n(j_n)\,\Delta\widetilde{h}_n(j_n)\right] = \begin{cases} n^{-2}\Gamma_1(i_n) + o(n^{-2}), & \text{if } i = j; \\ n^{-3}\Gamma_2(i_n, j_n) + o(n^{-3}), & \text{if } i \neq j \end{cases}$$

uniformly in n, where for each $i = 1, 2, \ldots, n$, $\Delta\widetilde{h}_n(i_n) := \widetilde{h}_n(i_n) - \widetilde{h}_n((i-1)/n)$; and

(ii.d) for some Φ, $d\mathcal{B}(\cdot) = \Phi d\mathcal{W}(\cdot)$, where $\mathcal{B}(\cdot) := [\bar{\mathcal{B}}(\cdot), \widetilde{\mathcal{B}}(\cdot)]'$ and $\mathcal{W}(\cdot) := [\bar{\mathcal{W}}(\cdot), \widetilde{\mathcal{W}}(\cdot)]'$ such that $\bar{\mathcal{W}}(\cdot)$ and $\widetilde{\mathcal{W}}(\cdot)$ are two independent Wiener processes, and for each $u \in [0,1]$, $\bar{\mathcal{W}}(u) \in \mathbb{R}$ and $\widetilde{\mathcal{W}}(u) \in \mathbb{R}^d$. □

For the following assumption, let Φ be partitioned as follows:

$$\Phi = \begin{bmatrix} \phi_{11} & \phi_{12} \\ \phi_{21} & \Phi_{22} \end{bmatrix},$$

where $\phi_{11} \in \mathbb{R}$, $\Phi_{22} \in \mathbb{R}^{d\times d}$, so that $\phi_{12} \in \mathbb{R}^{1\times d}$ and $\phi_{21} \in \mathbb{R}^{d\times 1}$. Also, let $\Phi_2 := (\phi_{21}, \Phi_{22})$ and $\phi_1 := (\phi_{11}, \phi_{12})$.

Assumption 4. *(i) $A_d := [C_1(\cdot), C_1(\cdot)]$ is positive definite; or*
(ii) $A_u := [C_1(\cdot), C_1(\cdot)] + [C_2(\cdot)\tau(\cdot)\Phi_2, C_2(\cdot)\tau(\cdot)\Phi_2]$ is positive definite. □

Remarks 3.
(i) Assumption 1 (i) extends the notion of the moment conditions to be defined by W^t instead of W_t. We introduce this notion to tackle nonstationary moment conditions.
(ii) The conditions stated in Assumption 2 (i and ii) imply different convergence rates for the variation of $\widetilde{g}_n(\cdot)$, viz., $\Delta\widetilde{g}_n(\cdot)$. Assumption 2 (i) supposes that $\Delta\widetilde{g}_n(\cdot) = O_{\mathbb{P}}(n^{-1})$, whereas Assumption 2 (ii) supposes that $\Delta\widetilde{g}_n(\cdot) = O_{\mathbb{P}}(n^{-1/2})$. Specifically, we can derive that $n\Delta\widetilde{g}_n(\cdot) = \mathcal{G}'(\cdot) + o_{\mathbb{P}}(1)$ and $n(\Delta\widetilde{g}_n(\cdot))^2 = \sigma^2(\cdot) + o_{\mathbb{P}}(1)$ under Assumptions 2 (i and ii), respectively.
(iii) As we detail below, the asymptotic distribution of the BM- or BB-GMM estimator is determined by applying central limit theory (CLT) to the sequence $\{(\Delta\widetilde{g}_n(i_n))^2\}$. Infinite dimensional MCMD estimation belongs to this case and Assumption 2 (ii.b) is imposed to handle this case. More specifically it provides the condition required to deliver the asymptotic variance of $\sum_{i=1}^{s_n}(\Delta\widetilde{g}_n(i_n))^2$.
(iv) Assumption 3 imposes continuity conditions on $\mu(\cdot)$, $\sigma(\cdot)$, $H(\cdot)$, $C_1(\cdot)$, $C_2(\cdot)$, $C_3(\cdot)$, and $C_4(\cdot)$ to ensure finite integrals of these functions, continuous functions being integrable on a compact set.
(v) The approximation $\sqrt{n}\Delta H_n(\cdot)$ given in Assumption 3 produces different asymptotic behavior under Assumptions 3 (i and ii). Under Assumption 3 (i), $C_2(\cdot)\Delta\widetilde{h}_n(\cdot) = O_{\mathbb{P}}(n^{-1})$, $n^{-1/2}C_3(\cdot)(\widetilde{h}_n(\cdot) \odot \Delta\widetilde{h}_n(\cdot)) = O_{\mathbb{P}}(n^{-3/2})$, and $n^{-1}C_4(\cdot)\widetilde{h}_n(\cdot) = O_{\mathbb{P}}(n^{-1})$. Therefore, $n\Delta H_n(\cdot) = C_1(\cdot) + o_{\mathbb{P}}(1)$. We also note that $n\Delta H_n(\cdot) = H'(\cdot) + o_{\mathbb{P}}(1)$ by differentiation, which implies that $H'(\cdot) = C_1(\cdot)$. Further, Assumption 3 (ii) implies that $C_2(\cdot)\Delta\widetilde{h}_n(\cdot) = O_{\mathbb{P}}(n^{-1/2})$, $n^{-1/2}C_3(\cdot)(\widetilde{h}_n(\cdot) \odot \Delta\widetilde{h}_n(\cdot)) = O_{\mathbb{P}}(n^{-1})$, and $n^{-1}C_4(\cdot)\widetilde{h}_n(\cdot) = O_{\mathbb{P}}(n^{-1})$. Therefore, $n\Delta H_n(\cdot) = C_1(\cdot) + C_2(\cdot)\sqrt{n}\Delta\widetilde{h}_n(\cdot) + o_{\mathbb{P}}(1)$. These different asymptotic behaviors affect the limit distribution of the BM- and BM-GMM estimator in a different way. □

We now examine the limit properties of BM- and BB-GMMs. For notational simplicity, we first let $\bar{A}_n := [\widehat{\boldsymbol{\Xi}}_n H_n(\cdot), H_n(\cdot)]$ and $D_n := [\widehat{\boldsymbol{\Xi}}_n H_n(\cdot), \widetilde{g}_n(\cdot)]$ and give their limit behavior in the following lemma:

Lemma 3. *Given that Assumption 1 holds for $\widehat{\Sigma}_n = \ddot{\Sigma}_n$ or for $\widehat{\Sigma}_n = \widetilde{\Sigma}_n$ with $\mathcal{G}(1) = 0$ and $H(1) = 0$,*

(i) if Assumptions 2 (i), 3 (i) and 4 (i) hold such that $H'(1) = 0$ or $\mathcal{G}'(1) = 0$ for the BM-GMM estimator,

(i.a) $q_n(\theta_*) \Rightarrow \mathcal{Q}_d := (\mathcal{G}'(\cdot), \mathcal{G}'(\cdot))$;

(i.b) $\bar{A}_n \to A_d$ with prob. converging to 1;

(i.c) $D_n \Rightarrow \mathcal{D}_d := [C_1(\cdot), \mathcal{G}'(\cdot)]$;

(ii) if Assumptions 2 (ii), 3 (i), and 4 (ii) hold,

(ii.a) $n^{-1} q_n(\theta_*) \to q_u := \varphi_q(\sigma(\cdot), \sigma(\cdot))$ with prob. converging to 1, where $\varphi_q := (\phi_{11}^2 + \phi_{12}\phi_{12}')$;

(ii.b) $\bar{A}_n \to A_u$ with prob. converging to 1;

(ii.c) $D_n - n^{1/2} \sum_{i=1}^{s_n} C_2(i_n) \Delta\widetilde{g}_n(i_n) \Delta\widetilde{h}_n(i_n) \Rightarrow \mathcal{D}_u := [C_1(\cdot), d\mathcal{G}(\cdot)] + [C_3(\cdot)(\mathcal{H}(\cdot) \odot \tau(\cdot)\Phi_2\phi_1'), \sigma(\cdot)]$;

(ii.d) if it further holds that $[C_2(\cdot)\tau(\cdot)\Phi_2\phi_1', \sigma(\cdot)] = 0$ with prob. 1 and Γ is positive definite, $D_n \Rightarrow \mathcal{D}_w := \mathcal{Z} + \mathcal{D}_u$, where $\mathcal{Z} \sim \mathcal{N}(0, \Gamma)$ and $\Gamma := \int_0^1 \Gamma_1(u) C_2(u) C_2(u)' du + \int_0^1 \int_0^1 \Gamma_2(u, v) C_2(u) C_2(v)' du dv$. □

Remarks 4.

(i) Lemma 3 (i) corresponds to the results in Lemmas 1 (ii) and 2 (ii). It also follows that $\mathcal{Q}_d = -(\mathcal{G}''(\cdot), \mathcal{G}(\cdot))$, $A_d = -[H''(\cdot), H(\cdot)]$, and $\mathcal{D}_d = -[H''(\cdot), \mathcal{G}(\cdot)]$ by Lemma 1 (i) and 2 (i).

(ii) The process $\mathcal{G}'(\cdot)$ in Lemma 3 (i) is a continuous Gaussian process because the derivative of a Gaussian process is Gaussian, here with covariance kernel $\dot{\omega}(u_1, u_2) := (\partial^2 / \partial u_1 \partial u_2)\omega(u_1, u_2)$.

(iii) The variable $\mathcal{D}_d$ is normally distributed. That is, $\mathcal{D}_d \sim \mathcal{N}(0, B_d)$, where $B_d := [\dot{\mathbf{\Omega}} C_1(\cdot), C_1(\cdot)] = \int_0^1 \int_0^1 C_1(u_1) \dot{\omega}(u_1, u_2) C_1(u_2)' du_1 du_2$ by letting $\dot{\mathbf{\Omega}}$ be the integral transform operator with the kernel function $\dot{\omega}(\cdot, \circ)$.

(iv) By Lemma 3 (ii.c) the BM-GMM and BB-GMM are asymptotically biased, unless the probability limit of $\sum_{i=1}^{s_n} \Delta\widetilde{g}_n(i_n) \Delta\widetilde{h}_n(i_n) C_2(i_n)$ is zero. Here, $\sum_{i=1}^{s_n} \Delta\widetilde{g}_n(i_n) \Delta\widetilde{h}_n(i_n) C_2(i_n) \to \int_0^1 \sigma(u)\tau(u) C_2(u) du$ with prob. converging to 1, so that if the final entity is zero, we can apply the CLT to obtain the limit distribution of $n^{1/2} \sum_{i=1}^{s_n} \Delta\widetilde{g}_n(i_n) \Delta\widetilde{h}_n(i_n) C_2(i_n)$, giving the normal random variable $\mathcal{Z}$ in Lemma 3 (ii.d). Assumption 3 (ii.c) provides regularity conditions for the CLT.

(v) The limit distribution of the infinite dimensional MCMD estimator is obtained by applying Lemma 3 (ii.d). For this application, the functions corresponding to $C_1(\cdot)$, $C_2(\cdot)$, and $C_3(\cdot)$ are found from the model assumption. Further, $\sigma(\cdot) \equiv 1$, $C_1'(\cdot) = C_3(\cdot)$, so that it holds that $\mathcal{D}_u = 0$ by integration by parts. Hence, if $\int_0^1 C_2(u) du = 0$, $\Gamma_1(\cdot) = c_1$, and $\Gamma_2(\cdot, \circ) = c_2$ for some constants c_1 and c_2, then $\Gamma = c_1 [C_2(\cdot), C_2(\cdot)]$ because $\int_0^1 \int_0^1 \Gamma_2(u, v) C_2(u) C_2(v)' du dv = c_2 \int_0^1 C_2(u) du \int_0^1 C_2(v)' dv = 0$. We demonstrate these properties in Section 2.4. □

In the next step we derive the limit distributions of the BM-GMM and BB-GMM using Lemma 3. The limit distributions are obtained by noting that $\sqrt{n}(\widehat{\theta}_n - \theta_*) = -\bar{A}_n^{-1} D_n + o_{\mathbb{P}}(1)$. The asymptotics are given in the following result.

Theorem 1. *Let Assumption 1 hold for $\widehat{\Sigma}_n = \ddot{\Sigma}_n$ or for $\widehat{\Sigma}_n = \widetilde{\Sigma}_n$ with $\mathcal{G}(1) = 0$ and $H(1) = 0$,*

(i) if Assumptions 2 (i), 3 (i), and 4 (i) hold such that $H'(1) = 0$ or $\mathcal{G}'(1) = 0$ for the BM-GMM estimator, $\sqrt{n}(\widehat{\theta}_n - \theta_*) \Rightarrow -A_d^{-1} \mathcal{D}_d$;

(ii) if Assumptions 2 (ii), 3 (ii), and 4 (ii) hold such that $[C_2(\cdot)\tau(\cdot)\Phi_2\phi_1', \sigma(\cdot)] = 0$ with prob. 1, $\sqrt{n}(\widehat{\theta}_n - \theta_*) \Rightarrow -A_u^{-1} \mathcal{D}_w$. □

Theorem 1 also implies that BM-GMM and BB-GMMs are consistent for the parameter θ_*.

2.3 Testing Overidentification Using BM-GMM and BB-GMM

For testing overidentification using BM-GMM and BB-GMM we consider the following hypotheses: for every t,

$$\mathcal{H}_0 : \text{ for some } \theta_* \in \Theta, \ \ \mathbb{E}[\bar{g}_{n,t}(\theta_*)] = 0 \ \text{ versus } \ \mathcal{H}_1 : \text{ for each } \theta \in \Theta, \mathbb{E}[\bar{g}_{n,t}(\theta)] \neq 0.$$

Note that $\mathcal{H}_0$ is one of the regularity conditions given in Assumption 1. We consider two types of tests.

First, we follow Sargan (1958) and Hansen (1982) with their motivation for an overidentification test defined as $J_n := q_n(\widehat{\theta}_n)$. In standard cases, the J-test follows a chi-squared null distribution asymptotically under $\mathcal{H}_0$ and is unbounded under $\mathcal{H}_1$. But this null limit distribution is modified if the number of moment conditions tends to infinity. Second, we examine the following standardized J-test:

$$U_n := \frac{J_n - n \cdot q_u}{\sqrt{v_n^2 n}},$$

where v_n^2 is a consistent estimator for $v^2 := \int_0^1 \Psi_1(u)du + \int_0^1 \int_0^1 \Psi_2(u,v)dudv$. Here, q_u and v_n can be determined by the model assumptions. For example, in infinite dimensional MCMD estimation, $q_u = 1$ and $v^2 = 4$ as we show in Section 2.4. The U-test is motivated from Donald et al. (2003) and Dovonon and Gospodinov (2024) by noting that the J-test may not be bounded under the null hypothesis. Specifically, they examined

$$T_n := \frac{J_n - (s_n - d)}{\sqrt{2(s_n - d)}},$$

and showed that its null limit distribution is a standard normal under their model setup. Note that T_n is defined by supposing that $q_u = 1$ and $v^2 = 2$, but the U-test supposes that q_u and v^2 do not necessarily satisfy this condition. The following result gives the null limit behavior of the tests.

Theorem 2. *Given Assumption 1,*

(i) if Assumptions 2 (i), 3 (i), and 4 (i) hold, $J_n \Rightarrow \mathcal{J}_d := (\mathbf{\Pi}_d \mathcal{G}(\cdot), \mathcal{G}(\cdot))$ under $\mathcal{H}_0$, where $\mathbf{\Pi}_d := \mathbf{\Xi} - \mathbf{\Lambda}_d$, $\mathbf{\Lambda}_d$ is an integral transform operator with kernel $\lambda(\cdot)' A_d^{-1} \lambda(\circ)$, $\lambda(\circ) := \mathbf{\Xi} H(\cdot)$, and $\mathbf{\Xi}$ is an integral operator such that for $b(\cdot) \in \mathcal{C}^{(2)}([0,1])$, $\mathbf{\Xi} b(\cdot) = -b''(\cdot)$; and

(ii) if Assumptions 2 (ii), 3 (ii) and 4 (ii) hold for $\widehat{\Sigma}_n = \ddot{\Sigma}_n$ or $\widehat{\Sigma}_n = \widetilde{\Sigma}_n$ with $\mathcal{G}(1) = 0$ and $H(1) = 0$ such that $[C_2(\cdot)\tau(\cdot)\Phi_2\phi_1', \sigma(\cdot)] = 0$ with prob. 1 and for some v_n, $v_n^2 \to v^2 < \infty$ with prob. converging to 1, then $U_n \overset{\text{A}}{\sim} \mathcal{N}(0,1)$ under $\mathcal{H}_0$. □

Remarks 5. (i) Carrasco and Florens (2000) also provide an overidentification test having a structure similar to U_n under their GMM estimation framework.

(ii) The null limit distribution of the J-test in Theorem 2 (i) is provided under the same structure as in Theorem 1 (i). The only difference lies in the fact that the limiting inverse kernel operator is fixed to $\mathbf{\Pi}_d$ in Theorem 2 (i). Note that $\mathcal{J}_d = (\mathcal{G}'(\cdot), \mathcal{G}'(\cdot)) - [H'(\cdot)', \mathcal{G}'(\cdot)] A_d^{-1} [H'(\cdot), \mathcal{G}'(\cdot)]$ by the definition of $\mathbf{\Pi}_d$.

(iii) We cannot apply the J-test when the conditions in Theorem 2 (ii) hold as it converges to a constant q_u as stated in Lemma 3 (ii.a). For this reason we need to apply the U-test for overidentification.

(iv) Finally, the J-test acquires asymptotic power when the weak limit of $\widetilde{g}(\cdot)$ is unbounded in prob. Under $\mathcal{H}_1$, there is no θ such that $\mathbb{E}[\bar{g}_{n,t}(\theta)] \neq 0$, and it is reasonable to suppose that for some $\nu(\cdot) \in L^2([0,1])$ and $\theta_o \in \Theta$, $\sqrt{n}(g_n(\cdot,\theta_o) - \nu(\cdot)) = O_{\mathbb{P}}(1)$, where θ_o is the probability limit of BM-GMM or BB-GMM. Then $J_n = O_{\mathbb{P}}(n)$ under $\mathcal{H}_1$ so that the J-test has nontrivial asymptotic power. Power of the U-test is acquired in a similar way to the J-test. Therefore, the U-test increases under the alternative, implying that its rejection region is determined by one-sided testing. □

2.4 Applications of BB-GMM and BM-GMM

This section proceeds to examine the running examples using the theory in Sections 2.2 and 2.3.

Example 1: Infinite-Dimensional MCMD Estimation The asymptotics of the MCMD estimator are modified when observations are from a continuous distribution and GMM estimation is used. Let x_t be a continuous random variable with a distribution function $G(\cdot)$, and $p_{n,t} := G(x_{(t)})$, where $x_{(t)}$ is the t-th smallest realization of an IID data set: $\{x_t : t = 1,\dots,n\}$. First, focus on $\{\widehat{p}_{n,t} - F(x_{(t)},\theta)\}$ as the moment condition corresponding to Pollard (1980) and Cho et al. (2018). Note that $\widehat{p}_{n,t} = \widehat{p}_n(p_{n,t}) := n^{-1}\sum_{j=1}^n \mathbb{I}(G(x_j) \leq p_{n,t}) = t/n$, so that $\widehat{p}_{n,t}$ is trivially obtained without estimating any quantity. Next, let $\widehat{c}_n(\cdot,\theta) := F(G^{-1}(\widehat{p}_n^{-1}(\cdot)),\theta)$ and then $F(x_{(t)},\theta) = \widehat{c}_n(t/n,\theta)$ noting that $t/n = \widehat{p}_n(p_{n,t})$, which implies that $\{\widehat{p}_{n,t} - F(x_{(t)},\theta)\} = \{t/n - \widehat{c}_n(t/n,\theta)\}$. Further, suppose that $F(\cdot,\theta) \equiv G(\cdot)$ if and only if $\theta \neq \theta_*$. Then, $\widetilde{g}_n(\cdot) := \sqrt{n}\{(\cdot) - \widehat{c}_n(\cdot,\theta_*)\} \Rightarrow \mathcal{B}^o(\cdot)$; and $\widetilde{g}_n(\cdot)$ is not bounded for $\theta \neq \theta_*$, so that we can use $\{(\cdot) - \widehat{c}_n(\cdot,\theta)\}$ as the moment condition for GMM.

The moment condition can also be stated via order statistics. Note that $F(x_t,\theta_*)$ is a standard uniform IID random variable, so that $F(x_{(t)},\theta_*)$ is the t-th smallest observation of $(n-1)$ IID uniform random variables. Hence, for each t, $\mathbb{E}[F(x_{(t)},\theta_*)] = t/n = \widehat{p}_{t,n}$ by theorem d of Hájek and Šidák (1967, p. 39) which implies that, for each t, $\widehat{p}_{t,n} - F(x_{(t)},\theta_*)$ can serve as a proper moment condition for GMM.

Next estimate the unknown parameter θ_* by BB-GMM. To do so let $\widehat{P}_n := [\widehat{p}_{n,1},\dots,\widehat{p}_{n,n-1}]' = [\frac{1}{n},\dots,\frac{n-1}{n}]'$ and $F_n(\theta) := [F(x_{(1)},\theta),\dots,F(x_{(n-1)},\theta)]'$, and further let

$$\widetilde{\theta}_n := \arg\min_{\theta\in\Theta} \bar{q}_n(\theta), \quad \text{where} \quad \bar{q}_n(\cdot) := \bar{G}_n(\cdot)'\widetilde{\Sigma}_n^{-1}\bar{G}_n(\cdot) \quad \text{and} \quad \bar{G}_n(\cdot) := \widehat{P}_n - F_n(\cdot).$$

Therefore, letting $g_n(\cdot,\theta) := \widehat{p}_n(\cdot) - \widehat{d}_n(\cdot,\theta)$, where

$$\widehat{d}_n(u,\theta) := \begin{cases} \widehat{c}_n(j_n,\theta), & \text{if } u \in [(j-1)/n, j_n) \text{ for } j = 1,2,\dots,n-1; \\ 1, & \text{if } u \in [(n-1)/n, 1], \end{cases}$$

it follows that $\sqrt{n}g_n(\cdot,\theta_*) = \widetilde{g}_n(\cdot)$ and $\bar{q}_n(\theta) = \int_0^1\int_0^1 g_n(u_1,\theta)\widetilde{\xi}_n(u_1,u_2)g_n(u_2,\theta)du_1du_2$. We further note that $\widehat{d}_n(\cdot,\circ) \to d(\cdot,\circ) := F(G^{-1}(\cdot),\circ)$ uniformly on $[0,1]\times\Theta$ by the definition of $\widehat{d}_n(\cdot,\circ)$ and from the fact that $\widehat{p}_n(\cdot) \to (\cdot)$ with prob. converging to 1, so that $g_n(\cdot,\circ) \to g(\cdot,\circ) := (\cdot) - d(\cdot,\circ)$ uniformly on $[0,1]\times\Theta$ with prob. converging to 1 such that $g_n(0,\cdot) \equiv 0$ and $g_n(1,\cdot) \equiv 0$ uniformly in n, and $g(0,\cdot) \equiv 0$ and $g(1,\cdot) \equiv 0$.

Under these regularity conditions for the infinite dimensional MCMD estimator, the following asymptotic properties hold.

Theorem 3. *Given the regularity conditions for the infinite dimensional MCMD estimator and* $\mathcal{H}_0$*,*

(i) $\widetilde{\theta}_n \to \theta_*$ *with prob. converging to 1;*

(ii) $\bar{q}_n(\theta_*) \to 1$ *with prob. converging to 1;*

(iii) $\sqrt{n}(\widetilde{\theta}_n - \theta_*) \overset{\text{A}}{\sim} \mathcal{N}(0, 2[H'(\cdot),H'(\cdot)]^{-1})$*, where* $H(\cdot) := -\nabla_\theta d(\cdot,\theta_*)$*; and*

(iv) $U_n := (J_n - n)/\sqrt{4n} \overset{\text{A}}{\sim} \mathcal{N}(0,1)$. □

Remarks 6. (i) Theorem 3 (i) is shown by noting that $q(\cdot) := -\int_0^1\int_0^1 \delta''(u_1-u_2)g(u_1,\cdot)g(u_2,\cdot)du_1du_2$ is minimized at θ_*. Theorem 3 (ii) holds by applying Lemma 3 (ii.a).

(ii) To show Theorem 3 (iii), we first approximate the infinite dimensional MCMD estimator as $\sqrt{n}(\widetilde{\theta}_n - \theta_*) = -\bar{A}_n^{-1}D_n + o_{\mathbb{P}}(1)$, where $\bar{A}_n := \nabla'_\theta F_n(\theta_*)\widetilde{\Sigma}_n^{-1}\nabla_\theta F_n(\theta_*) = [\widetilde{\Xi}_n H_n(\cdot), H_n(\cdot)]$ and $D_n := \nabla'_\theta F_n(\theta_*)\widehat{\Sigma}_n^{-1}\sqrt{n}(\widehat{P}_n - F_n(\theta_*)) = [\widehat{\Xi}_n H_n(\cdot), \widetilde{g}_n(\cdot)]$ with $H_n(\cdot) := \nabla_\theta g_n(\cdot,\theta_*)$, implying that we can let $h_n(\cdot)$ in Assumption 3 be identical to $g_n(\cdot)$. Next, we show that $\bar{A}_n = [\widehat{\Xi}_n H_n(\cdot), H_n(\cdot)] \to A := 2[H'(\cdot),H'(\cdot)]$ and $[\widehat{\Xi}_n H_n(\cdot), \widetilde{g}_n(\cdot)] \overset{\text{A}}{\sim} \mathcal{N}(0, 8[H'(\cdot),H'(\cdot)])$, so that the desired result follows. Here, the distribution of $(\Delta\widetilde{g}_n(\cdot))^2$ plays a crucial role when deriving the limit distribution of D_n. We note that $(\Delta\widetilde{g}_n(\cdot))^2 = n(\Delta\widehat{d}_n(\cdot))^2 - 2\Delta\widehat{d}_n(\cdot) + n^{-1}$ and that each $\Delta\widehat{d}_n(i_n) := \widehat{d}_n(i_n,\theta_*)$ is an increment of the order statistics constructed by IID uniform random variables (e.g., David and Nagaraja, 2003, section 6.4) which is referred to as the elementary coverage or the spacing (e.g., Wilks, 1948; Rao and Kuo, 1984). From this feature, $(\Delta\widehat{d}_n(\frac{1}{n}),\ldots,\Delta\widehat{d}_n(1))'$ follows a Dirichlet distribution with parameter ι_n. We use this feature to derive the limit distribution of D_n.

(iii) Theorem 3 (ii) implies that we cannot apply J-test for overidentification testing. Instead, U-test is applied. The goodness-of-fit test proposed by Greenwood (1946) is related to the U-test. We note that $q_n(\theta_*) - n = n\{\sum_{i=1}^{n-1}(\Delta\widetilde{g}_n(i_n))^2 - 1\} = n\{n\sum_{i=1}^{n-1}(\Delta\widehat{d}_n(i_n))^2 - 2\} + o_{\mathbb{P}}(n^{-1})$, where the first equality follows from (A.31) in Section A.1 of the Online Supplement, and the second equality holds by the fact that $\widetilde{g}_n(\cdot) := \sqrt{n}((\cdot) - \widehat{d}_n(\cdot))$. Here, $n^2\sum_{i=1}^{n-1}(\Delta\widehat{d}_n(i_n))^2$ is the goodness-of-fit test proposed by Greenwood (1946) with each $\Delta\widehat{d}_n(i_n)$ being the elementary coverage or spacing described above. Using the distributional condition of the elementary coverage, Section A.3.2 in the Online Supplement shows that $\mathrm{var}(\sum_{i=1}^{n-1}(\Delta\widetilde{g}_n(i_n))^2 - 1) = 4n^{-1} + o(n^{-1})$, implying that $\sqrt{n}\{\sum_{i=1}^{n-1}(\Delta\widetilde{g}_n(i_n))^2 - 1\} \overset{\text{A}}{\sim} \mathcal{N}(0,4)$, so that $(q_n(\theta_*) - n)/\sqrt{n} \overset{\text{A}}{\sim} \mathcal{N}(0,4)$.

(iv) The T-test proposed by Donald et al. (2003) does not follow the standard normal distribution under the null hypothesis. That is, T_n follows $\mathcal{N}(0,2)$ because $T_n = \sqrt{2}U_n + o_{\mathbb{P}}(1)$ under the null. We also note that the T-test could be useful if the martingale difference array (MDA) CLT could have been applied to $J_n - n$. Although this is not feasible under the current DGP condition, if we could let n of $(\Delta\widetilde{g}_n(\cdot))^2$ tend to infinity before applying the CLT, we could approximate $(\Delta\widetilde{g}_n(\cdot))^2$ by $(\Delta\mathcal{W}(\cdot))^2 + o_{\mathbb{P}}(1)$ by noting that $\widetilde{g}_n(\cdot) \Rightarrow \mathcal{B}^0(\cdot)$ and $d\mathcal{B}^0(u) = -(1-u)^{-1}\mathcal{B}^0(u)du + d\mathcal{W}(u)$, so that it would follow that

$\sqrt{n}\{\sum_{i=1}^{n-1}(\Delta\mathcal{W}(i_n))^2 - 1\} = n^{-1/2}\sum_{i=1}^{n-1}\{n(\Delta\mathcal{W}(i_n))^2 - 1\}$. Note here that $n(\Delta\mathcal{W}(i_n))^2 - 1$ is an MDA, so that the MDA CLT leads to $\sqrt{n}\{\sum_{i=1}^{n-1}(\Delta\mathcal{W}(i_n))^2 - 1\} \overset{\text{A}}{\sim} \mathcal{N}(0,2)$. This property implies that if $J_n - n$ were an MDA, the T-test would follow a standard normal asymptotically under the null hypothesis. Nonetheless, the sample size n of $(\Delta\widetilde{g}_n(\cdot))^2$ has to tend to infinity along with the application of the CLT, making it impossible to apply the MDA CLT here. It is necessary to take the serial correlation structure of $(\Delta\widetilde{g}_n(\cdot))^2$ into account when applying the CLT, ensuring that the U-test is a valid test asymptotically.

(v) The U-test is distribution-free. Note that the same null hypothesis is commonly tested by the KS-test, but its null limit distribution is affected by parameter estimation error, which makes its application inconvenient (e.g., Durbin, 1973). □

Example 2: Regression Using Integrated Series The DGP condition satisfies the regularity conditions in Assumptions 2 (ii) and 3 (ii). In view of the joint weak convergence $\left(n^{-1/2}\sum_{t=1}^{\lfloor(\cdot)n\rfloor} x_t, n^{-1/2}\sum_{t=1}^{\lfloor(\cdot)n\rfloor} u_t\right) \Rightarrow (\mathcal{B}_x(\cdot), \mathcal{B}_u(\cdot)) = \left(\Omega_x^{1/2}\mathcal{W}_x(\cdot), \sigma_u\mathcal{W}_u(\cdot)\right)$, we set $\mu(\cdot) \equiv 0$, $\sigma(\cdot) \equiv 1$, $\nu(\cdot) \equiv 0$, $\tau(\cdot) \equiv I_k$, $C_1(\cdot) \equiv 0$, $C_2(\cdot) \equiv I_k$, $C_3(\cdot) \equiv 0$, and $C_4(\cdot) \equiv 0$, so that $\Phi_2 = (0_{k\times 1}, \Omega_x^{1/2})$ and $\phi_1 = (\sigma_u, 0_{1\times k})$ from the fact that

$$\Phi = \begin{bmatrix} \sigma_u & 0_{1\times k} \\ 0_{k\times 1} & \Omega_x^{1/2} \end{bmatrix}.$$

The zero off-diagonal blocks in Φ follow from the independence of x_t and u_t. Therefore, Lemma 3 (ii.b) implies that $\bar{A}_n := n^{-2}X'\ddot{\Sigma}_n^{-1}X \to \Omega_x$ in prob. Further, we note that $\Phi_2\phi_1' = 0_{k\times 1}$, so that Lemma 3 (ii.d) implies that $D_n \overset{\text{A}}{\sim} \mathcal{N}(0,\Gamma)$ with $\Gamma = \int_0^1 \Gamma_1(u)du + \int_0^1\int_0^1 \Gamma_2(u,v)dudv$, the asymptotic covariance matrix of $n^{-1/2}\sum_{t=1}^n \Delta u_t \Delta x_t$. The matrix Γ can be consistently estimated by standard HAC methods under mild regularity conditions. Combining all these results, we have $\sqrt{n}(\widehat{\beta}_n - \beta_*) \overset{\text{A}}{\sim} \mathcal{N}(0, \Omega_x^{-1}\Gamma\Omega_x^{-1})$ by Theorem 1 (ii). Although the BM-GMM estimator is consistent and asymptotically normal, it is not an asymptotically efficient estimator. The asymptotic covariance matrix has a sandwich form, meaning that efficiency can be improved by selecting a weight matrix that exploits the structure of Γ. We leave this development in a general setting to future research.

Finally, using these conditions, it also follows from Lemma 3 (ii.a) that $q_u = \sigma_u^2$. Further, $v^2 := \int_0^1 \Psi_1(u)du + \int_0^1\int_0^1 \Psi_2(u,v)dudv$, which is the asymptotic covariance matrix of $n^{-1/2}\sum_{t=1}^n(\Delta u_t^2 - \sigma_u^2)$ and is consistently estimable by HAC methods. Therefore, $U_n \overset{\text{A}}{\sim} \mathcal{N}(0,1)$ under $\mathcal{H}_0 : \mathbb{E}[y_t - \beta_* x_t] = 0$ for all $t = 1, 2, \ldots, n$. □

3 Monte Carlo Simulation

This section reports the results of Monte Carlo simulations on the finite sample performance of the BB-GMM and BM-GMM procedures in the running examples used above. The simulations were designed with the infinite dimensional MCMD estimator to corroborate the properties of GMM estimation. Addressing Theorems 1 (ii) and 2 (ii) specifically, two different DGP conditions were considered, with x_t following exponential or normal distributions. Distributional hypotheses were tested employing the U-test and the limit distribution of the infinite dimensional MCMD estimator was used to test hypotheses on the unknown parameter.

The plan for the simulation is as follows. First, if x_t is exponentially distributed, then $\mathbb{P}(x_t \leq x) = 1-\exp(-\theta_* x)$, which is denoted as $x_t \sim \text{Exp}(\theta_*)$. Likewise, if $x_t \sim \mathcal{N}(\theta_*, 1)$, we have $\mathbb{P}(x_t \leq x) = \Phi(x-\theta_*)$, where $\Phi(\cdot)$ is the standard normal CDF. The unknown parameter is estimated by infinite dimensional MCMD using

$$\widehat{\theta}_n := \arg\min_{\theta\in\Theta} (\widehat{P}_n - F_n(\theta))' \widehat{\Sigma}_n^{-1} (\widehat{P}_n - F_n(\theta)).$$

For the exponential distribution the j-th row element of $F_n(\theta)$ is given be $1 - \exp(-\theta x_{(j)})$; and for the normal distribution the j-th row element of $F_n(\theta)$ is $\Phi(x_{(j)} - \theta)$. In the Online Supplement, we demonstrate that $\sqrt{n}(\widehat{\theta}_n - \theta_*) \overset{\text{A}}{\sim} \mathcal{N}(0, 2\theta_*^2)$ for the exponential distribution and $\sqrt{n}(\widehat{\theta}_n - \theta_*) \overset{\text{A}}{\sim} \mathcal{N}(0, 2)$ for the normal distribution.

Second, we conduct simulations by supposing null DGPs for testing hypotheses with the U-test. For this purpose, we let $\theta_* = 1$ and 0, so that $x_t \sim \text{Exp}(1)$ and $x_t \sim \mathcal{N}(0, 1)$ for the exponential and normal cases, respectively. These parameter values are selected arbitrarily. In each DGP setting, we compute the empirical rejection rates of the U-test for significance levels of 1%, 5%, and 10% with 10,000 independent repetitions. The empirical rejection rates under the null hypothesis for each test are reported in Tables 1 and 2.

Third, we compare the U-test with a corresponding test involving Tikhonov regularization. In particular, applying Carrasco and Florens (2000, theorem 10), we have the following τ-test that corresponds to the U-test

$$\tau_n := \frac{\dot{J}_n - \dot{p}_n}{\sqrt{\dot{q}_n}},$$

where $\dot{J}_n := n\dot{q}_n(\dot{\theta}_n; \alpha_n)$, $\dot{\theta}_n := \arg\min_{\theta\in\Theta} \dot{q}_n(\theta; \alpha_n)$, $\dot{q}_n(\theta; \alpha_n) := (\widehat{P}_n - F_n(\theta))' \widehat{\Sigma}_n^{1/2} (\widehat{\Sigma}_n + \alpha_n I)^{-1} \widehat{\Sigma}_n^{1/2}$ $(\widehat{P}_n - F_n(\theta))$, $\dot{p}_n := \sum_{j=1}^{n-1} \widehat{a}_j$, $\dot{q}_n := 2\sum_{j=1}^{n-1} \widehat{a}_j^2$, and $\widehat{a}_j := \widehat{\lambda}_j^2/(\widehat{\lambda}_j^2 + \alpha_n)$ where $\widehat{\lambda}_j$ is the j-th largest eigenvalue of $\widehat{\Sigma}_n$. Note that this test is identical to T_n if $\alpha_n = 0$ for every n. Following theorem 10 in

Test	Distribution	Level \ n	50	100	200	300	400	500	1,000
U-test	Exponential	1%	0.50	0.58	0.87	1.06	1.02	0.76	1.04
		5%	1.70	2.43	3.70	3.73	4.00	4.09	4.62
		10%	4.19	6.28	7.75	8.26	8.65	8.50	9.44
	Normal	1%	0.34	0.79	0.76	0.88	0.95	0.93	1.02
		5%	1.27	2.85	3.24	3.72	3.91	4.00	4.72
		10%	3.92	6.26	7.51	8.23	8.30	8.97	9.54
τ-test	Exponential	1%	0.31	0.60	0.79	0.82	0.92	1.04	0.93
		5%	0.84	1.46	2.06	2.31	2.56	2.74	3.60
		10%	1.42	2.34	4.42	5.54	6.24	6.94	8.00
	Normal	1%	0.29	0.64	0.88	0.84	0.87	0.84	0.94
		5%	0.67	1.45	2.16	2.49	2.64	2.74	3.46
		10%	1.18	2.35	4.58	5.83	6.37	6.39	8.17

Table 1: EMPIRICAL REJECTION RATES OF THE U- AND τ-TESTS UNDER THE NULL (IN PERCENT). This table shows the empirical rejection rates of the U- and τ-tests under the exponential and normal distributional hypotheses.

Carrasco and Florens (2000), we let $\alpha_n = n^{-1/4}$ for asymptotic optimality and the test is then asymptotically standard normal under the null. The simulation findings under the null are summarized as follows.

(a) For each case, as the sample size n increases, the distribution of the U-test converges to the standard normal. Table 1 demonstrates that the empirical rejection rates are close to 1%, 5%, and 10% for the exponential and normal distribution cases when $n = 1,000$. This observation confirms that the U-test follows the null limit distribution predicted in Theorem 2 (ii). The empirical distributions of the U-test provide further support: the left column of Figure 1 displays these distributions and in each case the empirical distribution approaches the CDF of the standard normal as n increases. Section A.4 of the Online Supplement also provides QQ-plots of the empirical distributions to corroborate convergence.

(b) The empirical distribution of the infinite dimensional MCMD estimator provides further support. The right column of Figure 1 displays the empirical distributions of the infinite dimensional MCMD estimators and these evidently closely approach the $\mathcal{N}(0, 2)$ CDF as n increases.

(c) When comparing the U-test with the τ-test, it is apparent that the empirical rejection rates of the U-test converge to the nominal levels faster than the τ-test. When n is small, the level distortions of the τ-test are large. Even for $n = 1,000$, the empirical rejection rates of τ-test are still far from nominal levels, although they appear to be converging to nominal levels. These findings indicate that the U-test controls type-I errors better than the τ-test. □

Finally, simulations were conducted to examine the local power properties of the U-test. For this purpose, the DGP conditions were modified as follows: (i) for the exponential case, $x_{t,n} := y_t + \frac{1}{2}\sqrt{z_t/n}$, with

Test	Distribution	Level \ n	50	100	200	300	400	500	1,000
U-test	Exponential	1%	0.59	1.86	4.44	7.53	12.30	16.42	39.23
		5%	1.61	4.65	10.93	17.62	24.90	31.88	59.70
		10%	3.33	7.71	16.82	25.33	33.88	41.61	70.51
	Normal	1%	1.63	2.96	4.90	5.81	5.50	6.05	4.11
		5%	4.15	7.83	12.06	13.41	13.84	14.53	11.91
		10%	6.96	12.23	18.25	20.17	21.02	22.02	18.69
τ-test	Exponential	1%	1.10	2.85	4.64	5.75	7.61	9.18	14.20
		5%	2.53	5.85	9.10	11.24	14.25	16.63	24.95
		10%	3.87	7.76	12.92	15.74	19.48	22.68	32.07
	Normal	1%	0.56	1.28	1.81	2.33	2.46	2.99	3.83
		5%	1.26	2.71	4.00	5.02	5.91	6.79	9.13
		10%	1.96	3.92	6.37	7.97	9.43	11.01	14.31

Table 2: EMPIRICAL REJECTION RATES OF THE U-TEST AND τ-TESTS UNDER THE LOCAL ALTERNATIVE (IN PERCENT). This table shows the empirical rejection rates of the U- and τ-tests under local alternatives. For the exponential case, $x_{t,n} := y_t + \frac{1}{2}\sqrt{z_t/n}$, where $y_t \sim \text{Exp}(1)$ and $z_t \sim \mathcal{U}[0.5, 1.5]$; and for the normal case, $x_{t,n} := y_t + \frac{1}{4}y_t^4/\sqrt{n}$, where $y_t \sim \mathcal{N}(0,1)$.

$y_t \sim \text{Exp}(1)$ and $z_t \sim \mathcal{U}[0.5, 1.5]$; and (ii) for the normal case, $x_{t,n} := y_t + \frac{1}{4}y_t^4/\sqrt{n}$, with $y_t \sim \mathcal{N}(0,1)$.[2] Importantly, as n increases the empirical distribution of $x_{t,n}$ gets closer to that of y_t but the finite sample distribution of $x_{t,n}$ is not the same as that of y_t in each case. Similar to the null simulations, 10,000 independent experiments were conducted under the local alternatives and empirical rejection rates of the tests are reported in Table 2. These results are summarized as follows.

(a) The U-test demonstrates non-negligible local power in each case. As the sample size n increases, the empirical rejection rates of the U-test exceed the nominal significance levels. Notably, the empirical local power of the U-test remains relatively stable as n increases for the normal case compared to the exponential case. This suggests that the U-test performs well in detecting local departures from the null hypothesis, especially for the normal distribution case.

(b) When comparing powers of the U- and τ-tests, the empirical rejection rates of the U-test are higher than those of the τ-test. □

This simulation comparison shows that use of the exact inverse operator for the BB-kernel can reduce finite sample size distortion and increase local power.

Beyond the above reported results, further simulations were conducted and the findings are discussed in the Online Supplement. Comparisons of the U-test with the test proposed by Amengual et al. (2020) were also considered. Under the same local alternatives as given in the present section, the empirical rejection rates of the U-test were found to be greater than those of the test in Amengual et al. (2020). The Online

[2]For the normal distribution case, we generated the local-to-zero component by $y_t^4/\sqrt{n}$. When the local-to-zero component was generated by $\sqrt{z_t/n}$ as for the exponential case, simulations showed that the deviations were insufficient to produce non-negligible local power for both the U- and τ-tests.

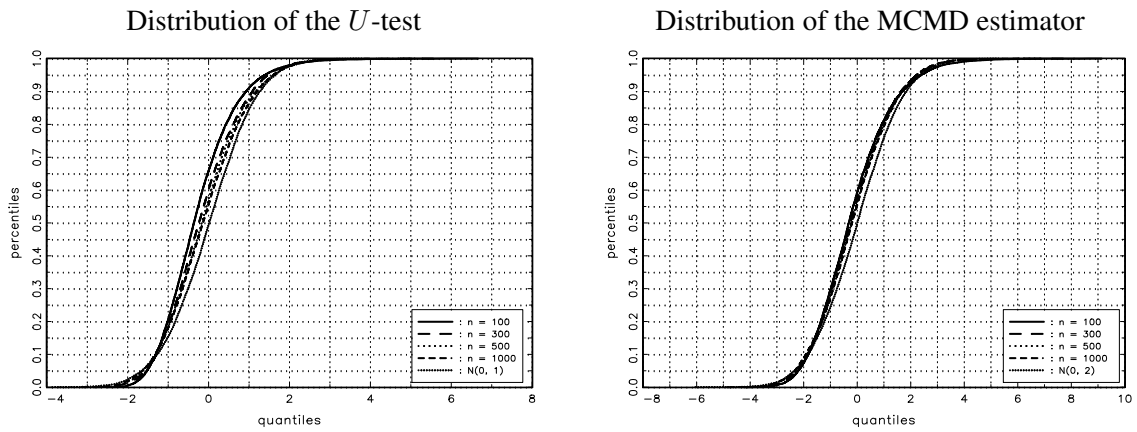

(a) Exponential distribution case

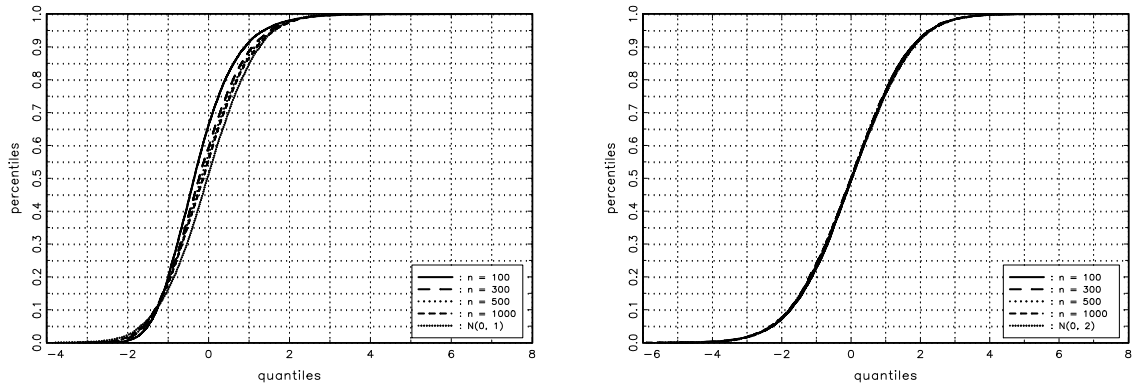

(b) Normal distribution case

Figure 1: EMPIRICAL DISTRIBUTIONS OF THE U-TEST UNDER THE NULL AND THE MCMD ESTIMATOR. For $n = 100, 300, 500$, and $1,000$, each figure shows the null distributions of the U-test or the empirical distributions of the MCMD estimator. The distributions are obtained by repeating 10,000 independent experiments, and the limit distributions are drawn together for comparison purpose.

Supplement also reports simulation evidence using the model in the second running example.

4 Empirical Application

This section reports the findings of an empirical implementation of infinite dimensional MCMD estimation to examine distributional hypotheses concerning labor income data in the U.S. The Pareto distribution has been popular in research on income distributions throughout a large body literature. Since Kuznets (1953, 1955) first examined top income shares in U.S. income data, this statistic has commonly been used for an income inequality index supplementing the Gini coefficient, as the latter does not focus on income inequality associated with the tail of the distribution. In particular, Piketty (2003), Piketty and Saez (2003), Atkinson (2005, 2007), Atkinson and Leigh (2007, 2008), and Moriguchi and Saez (2008), among others, use the Pareto distribution in measuring the top x-percent income shares of many countries such as Australia,

France, Japan, New Zealand, U.K., and the U.S. over long periods to reveal how the estimated top income shares have evolved over time. The findings indicate that the top income shares have increased since the 1970s, signaling a general deterioration in income equality. The results are based on the Pareto distribution assumption and top income share estimates obtained from the methodologies in these studies could be biased unless the Pareto distribution condition holds for the data.

Our empirical application is motivated by much ongoing research on income distributions and inequality where there is a need to test underlying distributional assumptions on which empirical findings are often based. In particular, we utilize this paper's infinite dimensional MCMD methodology to test the Pareto distribution hypothesis and investigate the evolution of income inequality in the U.S over time. Previous studies, such as Piketty and Saez (2003), have pointed out that the recent increase in top income shares is primarily driven by the rise of the capital income share. This means that a small segment of the population has a significant proportion of total income, mainly by way of capital income. Apart from capital income share, Piketty and Saez (2003) highlight a persistent rise of labor income inequality in the U.S. since the 1970s. This aspect of labor income inequality has also been studied by Katz and Murphy (1995); Katz and Autor (1999); Ciccone and Peri (2005); Eisenbarth and Chen (2022) and others, who examine labor market inequality by analyzing the distribution of wage structures. Their findings consistently show that wage inequality has continuously increased in the U.S. labor market. For instance, Katz and Autor (1999) report that earnings inequality has risen for both males and females, and wage disparities based on education, occupation, and age have also widened. Moreover, wage dispersion has expanded within demographic and skill groups, providing valuable insights into the dynamics of labor income inequality in the U.S.

Our main focus is to investigate how labor income inequality has evolved within the same cohort over time. The overall distribution of the wage structure is influenced not only by the inherent demand characteristics of the labor market but also by various heterogeneous factors, such as race, gender, education, and other determinants. This observation leads us to examine labor market inequality by isolating and removing the effects of heterogeneity from the data. By doing so, we aim to gain a better understanding of the contributions of these heterogeneous effects to overall income inequality. This involves comparing inequality indices obtained from different cohorts to discern the changes in labor income inequality over time while accounting for the impact of various demographic and socioeconomic factors. By controlling for these factors and focusing on the evolution of labor income inequality within specific cohorts, we can uncover important insights into the dynamics of income inequality in the U.S. labor market.

Our empirics utilize the Continuous Work History Sample (CWHS) database, which contains annual labor income data before tax for 15,000 individuals in the U.S. from 1980 to 2018. The individuals in

the CWHS database were born between 1960 and 1962, and their gender, education, and race information is also provided. Leveraging this information, we classify the observations into cohorts based on gender, education, and race to ensure that individuals within the same cohort share certain degrees of homogeneity without losing a significant number of observations. Table A.9 in the Online Supplement presents the distribution of the cohorts. A similar data analysis was conducted by d'Albis and Badji (2022) using French data, albeit with a different research objective. Their study used aggregate data pertaining to the same generation to estimate the functional shape of Gini coefficients over time and evaluate income inequality within that generation. Our empirical research goal differs in that we utilize the cohort datasets to focus on labor income inequality dynamics within specific cohorts in the U.S. labor market.[3]

To do so the infinite dimensional MCMD methodology of Section 2.4 is employed. Our focus is in top income shares as in Piketty and Saez (2003) and Atkinson et al. (2011). But prior to computing the top income shares we test the hypothesis that the labor income datasets follow a Pareto law. The test is applied for each annual labor income data set that belongs to the same cohort and the Pareto parameter is fitted using the infinite dimensional MCMD estimator. If the U-test does not reject the Pareto distribution condition, then we proceed to compute the top 5% income share of each data set and apply the methodology developed by Piketty and Saez (2003) and Atkinson et al. (2011). This approach ensures that we apply the top income share methodology only when the data satisfy the Pareto distribution condition. Otherwise, the methodology may be inconsistent for the desired top income share.

The present methodology can suffer from pre-testing bias because a type-I error from estimating the top income share carries over to testing the Pareto hypothesis. Hence, the level of significance needs to be set as small as possible to reduce the type-I error. If the sample size is large, the significance level can be safely decreased (type-II error of the U-test is not a concern). But if n is small or moderate, the estimated top income share should be analyzed with caution.

We conduct specific procedures for each cohort in the CWHS data, classified by the following characteristics: gender (female and male); education (high school or below, which also includes some college but no degree cases, Bachelor (BA) or equivalent degrees which includes associate degrees, Master (MA) or equivalent degrees, and Doctorate or equivalent degrees, which includes professional degrees); and race (white or Caucasian, black or African American, Asian, and others including American Indian, Native Hawaiian or other Pacific Islander, and two or more race individuals).

[3] Although degrees of freedom reduce when focusing on specific cohorts, this issue is not critical for the CWHS data because the sample size of each group is fairly large as Table A.9 reports. In case degrees of freedom are substantially reduced, we can instead specify a mixture of Pareto distributions such that each Pareto distribution is specified for a particular cohort income distribution, thereby enabling use of all observations without losing degrees of freedom.

For each cohort data, we test the Pareto distribution hypothesis using the U-test. The null hypothesis $\mathcal{H}_0$ is formulated as follows: $\mathcal{H}_0 : \mathbb{P}(y_t \leq y) = 1 - (b_x/y)^\theta$, where y_t denotes the t-th individual's labor income, and b_x represents the minimum value of the income variable, ensuring that y_t is distributed on $[b_x, \infty)$. The Pareto distribution hypothesis is intended to capture the right tail distribution of the income data. Our focus is on the top 10% of income observations and the top 5% income shares are estimated from each cohort data.

Application of the U-test for each cohort using the datasets from 1980 to 2018 leads to the results reported in Table A.10 of the Online Supplement. We summarize the inferential findings as follows. First, we cannot find evidence that the Pareto distribution is inappropriate when labor income data are collected from more homogeneous sectors of individuals. Second, the Pareto hypothesis appears appropriate at higher income levels that are obtained by increasing b_x. These findings together imply that the Pareto distribution can be regarded as a dominant feature for the top 10%-income observations.

The next step in the analysis involves estimating the Pareto parameter θ_* using infinite dimensional MCMD.[4] Estimation results are presented in Figures 2, 3, 4, and 5. Figure 2 displays the estimated top 5% income shares as functions of time between 1980 and 2018 for female and male cohorts. Each series is classified based on individual birth years. Missing points in the figures indicate that the U-test rejects the Pareto hypothesis for the data of that year. The level of significance is set to 1% for the U-test. Most missing values occur in the early 1980s, which is the time before the majority of individuals entered the job market.[5] Similarly, Figures 3 and 4 show the estimated top 5% labor income shares for datasets classified by education and race. Additionally, Figure 5 illustrates the estimated top 5% income share when the datasets are not classified. We summarize the findings and implications as follows.

(a) In general, the top 5% income share functions depicted in Figures 2 to 5 exhibit a hump-shaped pattern. For each cohort, the top income share index reaches its lowest values around 1980 and then sharply rises until around 1992. However, since then, it gradually decreases. This trend is consistently observed across all cohorts, and the peak level of top 5% labor income inequality is typically reached when most workers are in the early stages of their careers and are actively seeking jobs. During this transitional period, it is expected that labor income inequality would increase, which can be termed as "frictional inequality." Notably, labor income inequality tends to reach its highest level before workers reach the age of 60, reflecting the passage to retirement during the latter period of a working life.

[4] In the Online Supplement we discuss how θ_* is associated with the top x-percent income share and the Gini coefficient under the Pareto distribution assumption; and use of the top x-percent income share for income inequality is justified.

[5] If the Pareto hypothesis is rejected, an alternative distribution can be used to estimate the top income share. For example, log-normal and S_U distributions are popularly assumed for income distribution. In the current study we focus on the Pareto distribution, following the approach in Piketty and Saez (2003).

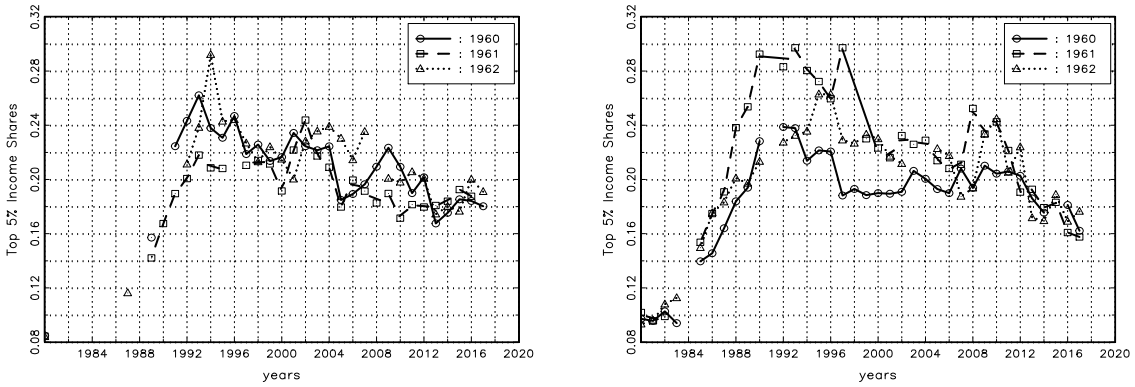

(a) Female (b) Male

Figure 2: TOP 5% INCOME SHARES OF GENDER COHORTS BETWEEN 1980 AND 2018. The figures show the top 5% income share coefficients of gender cohorts estimated by imposing the Pareto distribution to the top 10% CWHS observations. Missing values signify the p-value of the U-test less than 1%.

(b) The hump-shaped top 5% income share trends observed in Figures 2 to 5 have important implications for reducing labor income inequality. In addition to the policy implications derived from the labor market inequality literature (e.g., Katz and Murphy, 1995; Katz and Autor, 1999; Ciccone and Peri, 2005; Eisenbarth and Chen, 2022), the hump-shaped indices suggest that labor income inequality can be significantly reduced by targeting the frictional inequality observed during early career years. To achieve this, economic policies aimed at reducing unemployment, setting a minimum wage, or increasing welfare benefits could be more effective for workers in the early stages of their careers, as frictional income inequality is commonly observed across all cohorts. By implementing such targeted policies during this transitional period overall labor income inequality could be mitigated.

(c) When analyzing the gender effect, we observe from Figure 2 that males generally exhibit more volatile top 5% income shares than females. After reaching the maximum top income share, it decreases gradually for females, while it declines more rapidly for males. For instance, focusing on the 1960 cohort, the maximum top 5% income share is around 0.26 for females and 0.24 for males, and it decreases at a slower rate for females compared to males. This suggests that labor income inequality is more pronounced for females than males within the 1960 cohort. Similar results are found for the 1962 cohort, with males showing a higher maximum index value than females for the 1961 cohort.

(d) When analyzing the education effect, we observe from Figure 3 that individuals with an MA or equivalent degree show the most volatile top 5% income shares compared to other degree holders. The maximum top income share values of individuals with an MA or equivalent degree are higher than those of other degree holders, and they maintain relatively higher top 5% income share values for

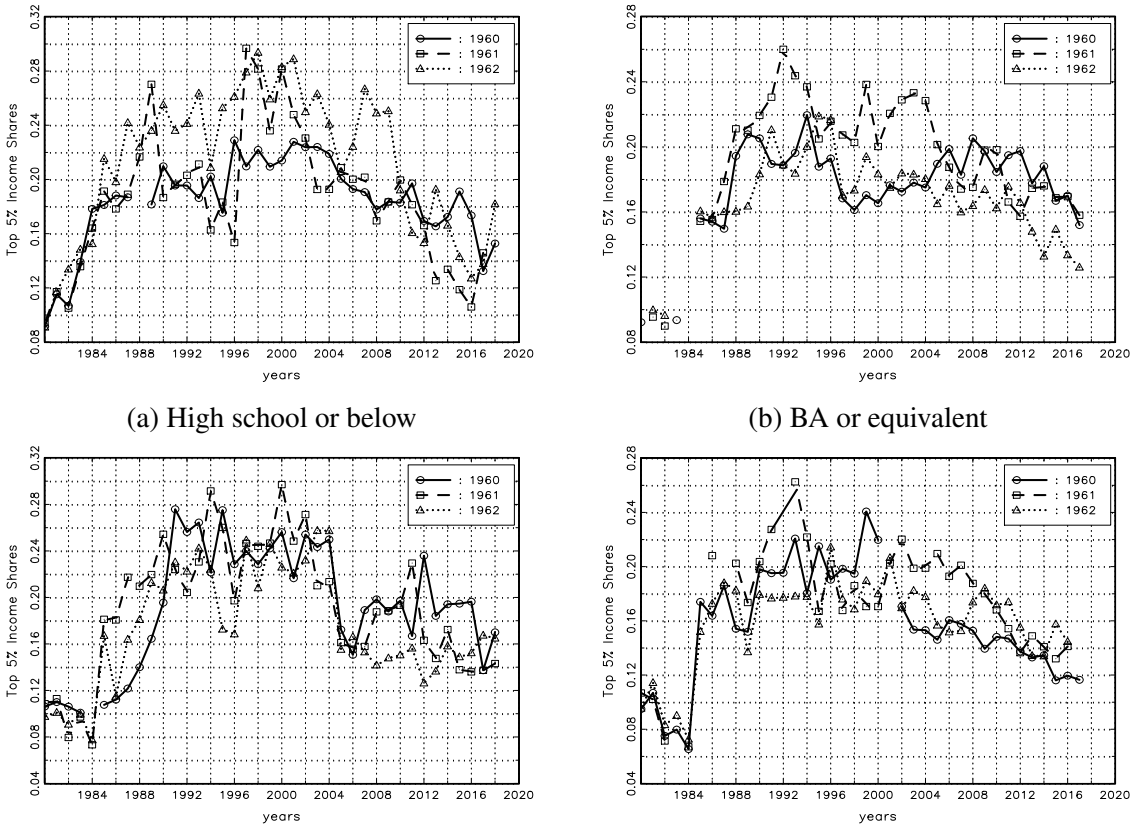

(a) High school or below

(b) BA or equivalent

(c) MA or equivalent

(d) Doctorate or equivalent

Figure 3: TOP 5% INCOME SHARES WITHIN THE SAME EDUCATION COHORTS BETWEEN 1980 AND 2018. The figures show the top 5% income share coefficients within the same education cohorts estimated by imposing the Pareto distribution to the top 10% CWHS observations. Missing values signify the p-value of the U-test less than 1%.

some time. In contrast, the top 5% income share values of individuals with a doctorate or equivalent degree are generally less volatile and smaller than those of other degree holders. The top income share values obtained using all observations, as shown in Figure 5, are roughly between those of individuals with an MA and doctorate or equivalent degree. This finding implies that labor income for individuals with an MA or equivalent degree is more unequally distributed than that of individuals with a doctorate or equivalent degree.

(e) Another notable feature of the education effect is observed from Figure 3, where we see that it takes more years for individuals with a high school diploma or lower education levels to reach the maximum top income share compared to individuals with higher education levels. Additionally, the maximum values are not reached rapidly for the former group. For instance, the 1960 cohort reaches its maximum in 2002, and there are other years before 2002 with slightly smaller index values. This aspect implies that unequal labor income is persistently distributed over a long period for individuals with a

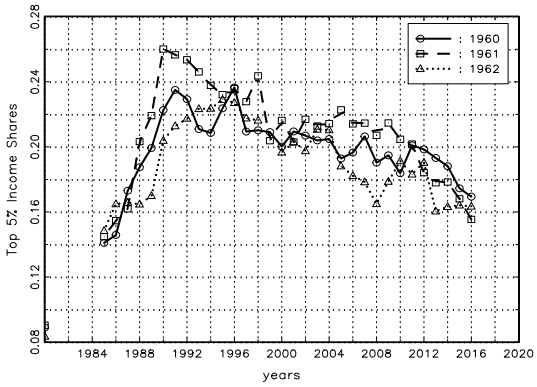

(a) White or Caucasian

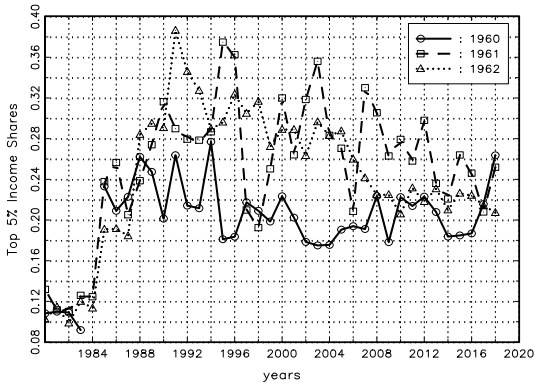

(b) Black or African American

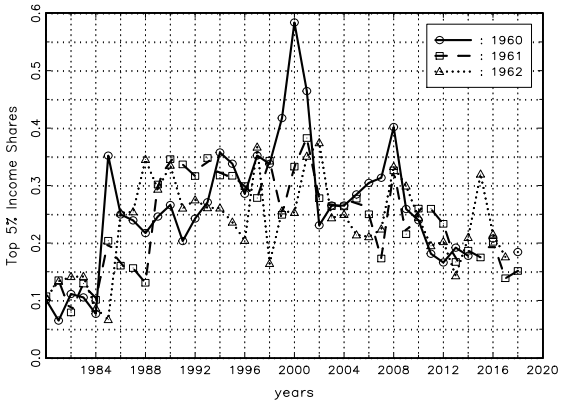

(c) Asian

Figure 4: TOP 5% INCOME SHARES WITHIN THE SAME RACE COHORTS BETWEEN 1980 AND 2018. The figures show the top 5% income share coefficients within the same race cohorts estimated by imposing the Pareto distribution to the top 10% CWHS observations. Missing values signify the p-value of the U-test less than 1%.

high school diploma or lower education levels. A similar feature is observed for individuals with a BA or equivalent degree, although it is not as strong as for those with a high school diploma or lower education levels.

(f) When examining the race effect, we observe from Figure 5 that different races exhibit different patterns in their top 5% labor income shares. White and Caucasian cohorts generally show lower top income shares compared to the other races, and their coefficients remain more or less stable across different birth years, indicating a relatively stable pattern. On the other hand, black and African American cohorts show varying patterns depending on the birth year. Specifically, the cohort born in 1960 maintains lower and stable top income shares, whereas the cohort born in 1962 shows the more typical income share pattern. That is, the top income share sharply increases during their early career years

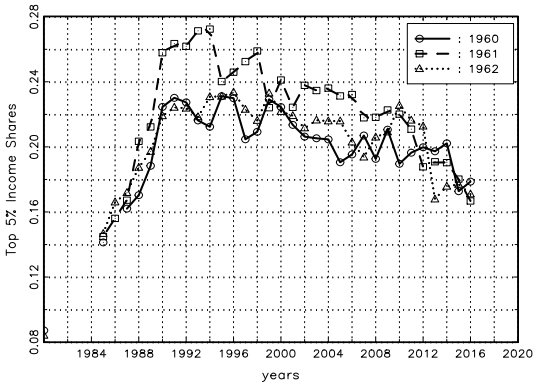

Figure 5: TOP 5% INCOME SHARES USING AGGREGATED OBSERVATIONS FOR EACH YEAR BETWEEN 1980 AND 2018. The figures show the top 5% income share coefficients of aggregated observations estimated by imposing the Pareto distribution to the top 10% CWHS observations. Missing values signify the p-value of the U-test less than 1%.

but slowly improves as the cohort members age.[6] For the Asian case, the cohort born in 1960 exhibits a distinct pattern from the others, with its index sharply increasing between 1999 and 2000, and again in 2008, during the Asian and the subprime financial crises. The other Asian cohorts are less sensitive to the financial crises and show more stable top income shares.

(g) When examining the birth year effect, we observe that the top income share values of the 1960 cohort are generally lower than those of the other cohorts. For each cohort, the index of the 1960 cohort remains persistently lower than the other cohorts, while the 1961 cohort shows consistently but slightly higher values than the 1960 cohort. This finding suggests that the income inequality is influenced by the birth year, and there are differences in income distribution patterns across different cohorts. □

From this empirical analysis we infer that labor income inequality is influenced by heterogeneous factors such as gender, education, race, and year of birth. Further, for each group the income inequality among the same group members typically worsens during early career years but slowly improves with time. These inferential findings have different policy implications for reducing labor income inequality within the same group. In Section A.6.3 of the Online Supplement, we also provide estimated Gini coefficients in parallel with Figures 2 to 5 to affirm the empirical results of this section in a different manner.

[6] Although we do not report the results here, these different patterns between the 1960 and 1962 cohorts were supported by confidence bands for the estimated top income share series.

5 Concluding Summary

If the moment dimension in GMM estimation expands to infinity proportional to the sample size, the limit properties of GMM differ from standard case where the number of moment conditions is fixed. Specifically, the limit properties are influenced by the stochastic properties of the moment conditions and the employed weight matrix. This study has derived the asymptotic properties of GMM when inverse Brownian motion or Brownian bridge kernels are used for the weight matrix. These kernels arise in a natural way in econometric work such as minimum Cramér-von Mises distance estimation, which arises in testing distributional specification. We consider different scenarios where the moment conditions converge to either a smooth Gaussian or a non-differentiable Gaussian process. By leveraging the individual properties of the Brownian motion and Brownian bridge kernels, we show how asymptotic behavior can be fully characterized using the inner products of functionals derived from these Gaussian processes.

The paper also explores conditions under which the standard J-test can serve as an appropriate statistic for testing overidentification. In cases where the standard conditions do not hold, we propose an alternative test called the U-test, inspired by the T-test introduced by Donald et al. (2003) and Dovonon and Gospodinov (2024). Throughout the discussions on GMM estimation, we use the infinite dimensional MCMD estimation and regression analysis using integrated series as the running examples. In particular, we illustrate the usefulness of the infinite dimensional MCMD approach extending the MCMD estimation in Pollard (1980) and Cho et al. (2018) through Monte Carlo simulations and apply it in an empirical study.

Our empirical application analyzes labor income based on the CWHS database. We estimate the top 5% income shares of labor income as a function of time, covering the period from 1980 to 2018. These cohort datasets are classified based on gender, education, race, and birth year. These data are analyzed using the new U-test to test the Pareto distribution hypothesis and estimate the Pareto parameter using infinite dimensional MCMD estimation. The results show that labor income inequality within the same cohort tends to be maximized during early career years for most of the cohort data. This observation suggests that economic policies aimed at reducing income inequality will likely be more effective if they specifically target workers in their early career years. Such policies can play a crucial role in reducing frictional inequality and contribute to a more equitable distribution of labor income.

Acknowledgments

The co-editor, Giuseppe Cavaliere, an anonymous associated editor and two anonymous referees provided helpful comments for which we are most grateful. A comment of a referee on one of our earlier papers

prompted us to pursue our thinking on the research presented here. We have further benefited from discussions with Chirok Han, Dukpa Kim, Seo Jeong Lee, Lin Liu, Ruixuan Liu, Xun Lu, Juwon Seo, Zhentao Shi, Yang Zu, and participants at the Allied Economic Associations Annual Meeting in Korea (2024) and the CUHK Workshop on Econometrics (2024).

Funding Sources

Cho acknowledges research support from the R. K. Cho Memorial Fellowship, and Phillips acknowledges research support from the Kelly Fund at the University of Auckland and a KLC Fellowship at Singapore Management University.

Data Availability

Due to privacy or security reasons, the raw data used for the empirical application remains confidential and is not shared.

References

AMENGUAL, D., M. CARRASCO, AND E. SENTANA (2020): "Testing Distributional Assumptions Using a Continuum of Moments," *Journal of Econometrics*, 218, 655–689. 3, 4, 8, 22, 6, 14

ANDERSEN, L. B. G. AND V. V. PITERBARG (2010): *Interest Rate Modeling*, London: Atlantic Financial Press. 2

ANGRIST, J. D. AND A. B. KEUEGER (1991): "Does Compulsory School Attendance Affect Schooling and Earnings?" *Quarterly Journal of Economics*, 106, 979–1014. 1

ATKINSON, A. (2005): "Top Incomes in the UK over the 20th Centry," *Journal of the Royal Statistical Society. Series A*, 168, 325–343. 23

——— (2007): "Measuring Top Incomes: Methodological Issues," in *Top Incomes over the Twentieth Century : a Contrast between Continental European and English-Speaking Countries*, ed. by A. B. Atkinson and T. Piketty, Oxford, UK: Oxford University Press, 18–42. 23

ATKINSON, A. AND A. LEIGH (2007): "The Distribution of Top Incomes in Australia," *Economic Record*, 83, 247–261. 23

——— (2008): "Top Incomes in New zealand 1921–2005: Understanding the Effects of Marginal Tax Rates, Migration Threat, and the Macroeconomy," *Review of Income and Wealth*, 54, 149–165. 23

ATKINSON, A., T. PIKETTY, AND E. SAEZ (2011): "Top Incomes in the Long Run of History," *Journal of Economic Literature*, 49, 3–71. 1, 4, 25

BAI, J. AND S. NG (2010): "Instrumental Variable Estimation in a Data Rich Environment," *Econometric Theory*, 26, 1577–1606. 9

BATES, C. AND H. WHITE (1985): "A Unified Theory of Consistent Esetimation for Parametric Model," *Econometric Theory*, 1, 151–178. 6

BELLONI, A., D. CHEN, V. CHERNOZHUKOV, AND C. HANSEN (2012): "Sparse Models and Methods for Optimal Instruments with an Application to Eminent Domain," *Econometrica*, 80, 2369–2429. 9

BONTEMPS, C. AND N. MEDDAHI (2012): "Testing Distributional Assumptions: A GMM aproach," *Journal of Applied Econometrics*, 27, 978–1012. 6

CARRASCO, M. (2012): "A Regularization Approach to the Many Instruments Problem," *Journal of Econometrics*, 170, 383–398. 1

CARRASCO, M. AND J.-P. FLORENS (2000): "Generalization of GMM to a Continuum of Moment Conditions," *Econometric Theory*, 16, 797–834. 3, 4, 8, 16, 20, 21, 9

CARRASCO, M., J.-P. FLORENS, AND E. RENAULT (2007): "Linear Inverse Problems in Structural Econometrics Estimation Based on Spectral Decomposition and Regularization," in *Handbook of Econometrics*, ed. by J. J. Heckman and E. E. Leamer, Elsevier, vol. 6, chap. 77, 5633–5751. 3, 4, 12

CHO, J. S., M.-H. PARK, AND P. C. B. PHILLIPS (2018): "Practical Kolmogorov-Smirnov Testing by Minimum Distance Applied to Measure Top Income Shares in Korea," *Journal of Business & Economic Statistics*, 36, 523–537. 1, 6, 17, 31

CHO, J. S. AND H. WHITE (2011): "Generalized Runs Tests for the IID Hypothesis," *Journal of Econometrics*, 162, 326–344. 9

CHUI, C. K. (1971): "Concerning Rates of Convergence of Riemann Sums," *Journal of Approximation Theory*, 4, 279–287. 4, 6, 26, 27, 30

CICCONE, A. AND G. PERI (2005): "Long-Run Substitutability netween More and Less Educated Workers: Evidence from U.S. States," *Review of Economcis & Statistics*, 87, 652–663. 24, 27

D'ALBIS, H. AND I. BADJI (2022): "Inequality within generation: Evidence from France," *Research in Economics*, 76, 69–83. 25

DAVID, H. A. AND H. N. NAGARAJA (2003): *Order Statistics*, New Jersey: John Wiley & Sons. 18

DONALD, S., G. IMBENS, AND N. NEWEY (2003): "Empirical Likelihood Estimation and Consistent Tests with Conditional Moment Restrictions," *Journal of Econometrics*, 69, 1161–1191. 4, 16, 18, 31

DONALD, S. AND W. NEWEY (2001): "Choosing the Number of Instruments," *Econometrica*, 69, 1161–1191. 9

DOVONON, P. AND N. GOSPODINOV (2024): "Specification testing for conditional moment restrictions under local identification failure," *Quantitative Economics*, 15, 849–891. 16, 31

DURBIN, J. (1973): "Weak Convergence of the Sample Distribution Function when Parameters are Estimated," *Annals of Statistics*, 1, 279–290. 19

EISENBARTH, A. AND Z. CHEN (2022): "The Evolution of Wage Inequality within Local U.S. Labor Markets," *Journal for Labor Market Research*, 56, 2. 24, 27

ENGLE, R. F. AND C. W. J. GRANGER (1987): "Co-Integration and Error Correction: Representation, Estimation, and Testing," *Econometrica*, 55, 251–276. 7

GREENWOOD, M. (1946): "The Statistical Study of Infectious Diseases," *Journal of the Royal Statistical Society. Series A*, 109, 185–186. 18

GRENANDER, U. (1981): *Abstract Inference*, New York: John Wiley & Sons. 8

HÁJEK, J. AND Z. ŠIDÁK (1967): *Theory of Rank Tests*, New York: Academic Press. 17

HANSEN, L. P. (1982): "Large Sample Properties of Generalized Method of Moments Estimators," *Econometrica*, 50, 1029–1054. 4, 6, 16

HIRSA, A. AND S. N. NEFTCI, eds. (2014): *An Introduction to the Mathematics of Financial Derivatives (Third Edition)*, San Diego: Academic Press, third edition ed. 2

KATZ, L. AND D. AUTOR (1999): "Changes in the Wage Structure and Earnings Inequality," in *Handbook of Labor Economics*, ed. by O. Ashenfelter and D. Card, Amsterdam: Elsevier, 1453–1555. 24, 27

KATZ, L. AND K. MURPHY (1995): "Changes in Relative Wages: Supply and Demand Factors," *Quarterly Journal of Economics*, 107, 35–78. 24, 27

KIRSCH, A. (1996): *An Introduction to the Mathematical Theory of Inverse Problems*, Applied Mathematical Sciences, Springer New York. 4, 8

KUZNETS, S. (1953): *Shares of Upper Income Groups in Income and Savings*, New York: National Bureau of Economic Research. 23

——— (1955): "Economic Growth and Economic Inequality," *American Economic Review*, 45, 1–28. 23

LIGHTHILL, M. J. (1959): *Introduction to Fourier analysis and generalized functions*, Cambridge University Press. 17

MORIGUCHI, C. AND E. SAEZ (2008): "The Evolution of Income Concentration in Japan, 1886-2005: Evidence from Income Tax Statistics," *Review of Economics and Statistics*, 90, 713–734. 23

PHILLIPS, P. C. B. (1986): "Understanding spurious regressions in econometrics," *Journal of Econometrics*, 33, 311–340. 7

——— (1987): "Time Series Regression with a Unit Root," *Econometrica*, 55, 277–301. 9

——— (1991): "A Shoartcut to LAD Estimator Asymptotics," *Econometric Theory*, 7, 450–463. 3, 17

PHILLIPS, P. C. B. AND S. N. DURLAUF (1986): "Multiple Time Series Regression with Integrated Processes," *Review of Economic Studies*, 53, 473–495. 7, 8

PICARD, E. (1910): "Sur un Théorème Général Relatif aux Équations Intégrales de Premiére Espéce et sur Quelques Problèmes de Physique Mathématique," *Rendiconti del Cicolo Matematico di Palermo*, 29, 79–97. 4, 8

PIKETTY, T. (2003): "Income Inequality in France, 1901–1998," *Journal of Political Economy*, 111, 1004–1042. 1, 4, 23

PIKETTY, T. AND E. SAEZ (2003): "Income Inequality in the United States, 1913–1998," *Quarterly Journal of Economics*, 118, 1–39. 1, 4, 23, 24, 25, 26

POLLARD, D. (1980): "The Minimum Distance Method of Testing," *Metrika*, 27, 43–70. 1, 6, 17, 31

RAO, J. AND M. KUO (1984): "Asymptotic Results on the Greenwood Statistic and Some of its Generalizations," *Journal of the Royal Statistical Society. Series B*, 46, 228–237. 18

SARGAN, J. D. (1958): "The Estimation of Economic Relationships Using Instrumental Variables," *Econometrica*, 26, 393–415. 4, 16

SHI, Z. (2016): "Econometric Estimation with High-Dimensional Moment Equalities," *Journal of Econometrics*, 195, 104–119. 9

WHITE, H. (2001): *Asymptotic Theory for Econometricians*, Orlando, FL: Academic Press. 8, 27

WILKS, S. S. (1948): "Order Statistics," *Bulletin of the American Mathematical Statistics*, 5, 6–50. 18

Online Supplement for 'GMM Estimation by the Brownian Kernels Applied to Measuring the Income Inequality'[1]

by

Jin Seo Cho[a,*] and Peter C. B. Phillips[b,c,d]

[a]Yonsei University

[b]University of Auckland, [c]Yale University, [d]Singapore Management University

This Online Supplement is an Appendix that provides technical and empirical supplements to the main text.

A Appendix

The Appendix has six sections. Sections A.1 and A.2 explore the limit behavior of the quantities formed by transforming an Itô Process and a smooth Gaussian process. Section A.3 presents the moments of the statistics forming the infinite dimensional MCMD estimator, and Sections A.4 and A.5 provide additional simulation evidence and proofs of the main results, respectively. Section A.6 offers supplementary empirical studies to those in the paper.

A.1 Limit Difference of Transformed Itô Process

We derive the differential of a transformed Itô process. For this examination, suppose that a limit of a process is constructed as follows: $\bar{X}_n(\cdot) := \sqrt{n}(X(\cdot) - \widehat{X}_n(\cdot)) \Rightarrow \mathcal{G}(\cdot)$, where $\widehat{X}_n(\cdot)$ is a sample average of random processes defined on $[0,1]$, $X(\cdot)$ is its population mean, and $\mathcal{G}(\cdot)$ is an Itô process satisfying Assumption 2 (ii) in the main paper. Here, we suppose that $X(\cdot)$ is differentiable on $[0,1]$ and $\widehat{X}_n(\cdot)$ converges to $X(\cdot)$ uniformly on $[0,1]$. For example, we can consider an empirical process as a specific example: $\widetilde{g}_n(\cdot) := \sqrt{n}\{(\cdot) - \widehat{d}_n(\cdot)\} \Rightarrow \mathcal{B}^0(\cdot)$, where $\widehat{d}_n(\cdot) := \widehat{d}_n(\cdot, \theta_*)$, which determines the limit distribution of the infinite dimensional MCMD estimator. For this case, $\widehat{X}_n(\cdot) = \widehat{d}_n(\cdot)$, $X(\cdot) = (\cdot)$, and $\mathcal{G}(\cdot) = \mathcal{B}^0(\cdot)$, such that $\mu(u, \mathcal{G}(u)) = -(1-u)^{-1}\mathcal{B}^0(\cdot)$ and $\sigma(u, \mathcal{G}(\cdot)) = 1$. As before, we let $\mu(\cdot)$ and $\sigma(\cdot)$ abbreviate $\mu(\cdot, \mathcal{G}(\cdot))$ and $\sigma(\cdot, \mathcal{G}(\cdot))$, respectively.

[1]The co-editor, Giuseppe Cavaliere, an anonymous associated editor and two anonymous referees provided many helpful comments for which we are most grateful. A comment of a referee on one of our earlier papers prompted us to pursue our thinking on the research presented here. We have further benefited from discussions with Chirok Han, Dukpa Kim, Seo Jeong Lee, Lin Liu, Ruixuan Liu, Xun Lu, Juwon Seo, Zhentao Shi, Yang Zu, and participants at the Allied Economic Associations Annual Meeting in Korea (2024) and the CUHK Workshop on Econometrics (2024). Cho acknowledges research support from the R. K. Cho Memorial Fellowship, and Phillips acknowledges research support from the Kelly Fund at the University of Auckland and a KLC Fellowship at Singapore Management University. Due to privacy or security reasons, the raw data used in the empirical application remains confidential and is not shared. *: Corresponding author.

Given this, for a function $f : \mathbb{R} \mapsto \mathbb{R}$ in $\mathcal{C}^{(2)}([0,1])$, we let $Q_n(\cdot) := f(\widehat{X}_n(\cdot))$ and derive the limits of the quantities associated with $\Delta Q_n(i_n)$ for $i = 0, 1, 2, \ldots, n$. Here, for each $t = 0, 1, 2, \ldots, n$ and a function $h : [0,1] \mapsto \mathbb{R}$, we let $\Delta h(i_n) := h(i_n) - h(\frac{i-1}{n})$ for notational simplicity.

A.1.1 Limit Behavior of $\sqrt{n}\Delta Q_n(\cdot)$

We obtain the limit behavior of $\sqrt{n}\Delta Q_n(\cdot)$ by applying Itô's lemma. Note that

$$\Delta Q_n(\cdot) = f'(\widehat{X}_n(\cdot))\Delta\widehat{X}_n(\cdot) + o_{\mathbb{P}}(1) \tag{A.1}$$

by Taylor expansion. Now $\Delta\widehat{X}_n(\cdot) = \Delta X(\cdot) - n^{-1/2}\bar{X}_n(\cdot)$ and $\Delta X(\cdot)$ can be approximated by $X'(\cdot)/n$. Therefore, we obtain that

$$\Delta\widehat{X}_n(\cdot) = \frac{1}{n}X'(\cdot) - \frac{1}{\sqrt{n}}\Delta\bar{X}_n(\cdot) + o_{\mathbb{P}}(1), \tag{A.2}$$

implying that

$$\sqrt{n}\Delta Q_n(\cdot) = f'(\widehat{X}_n(\cdot))\{n^{-1/2}X'(\cdot) - \Delta\bar{X}_n(\cdot)\} + o_{\mathbb{P}}(1) \tag{A.3}$$

by plugging (A.2) into (A.1). The stochastic differential equation of $\sqrt{n}\Delta Q_n(\cdot)$ is obtained from this limit. Note that $\widehat{X}_n(\cdot)$ converges to $X(\cdot)$ uniformly on $[0,1]$, and $\Delta\bar{X}_n(\cdot)$ is approximated by $d\mathcal{G}(\cdot)$. Therefore, if we let $d\mathcal{Q}(\cdot)$ denote the limit of $\sqrt{n}\Delta Q_n(\cdot)$, it follows that $d\mathcal{Q}(\cdot) = -f'(X(\cdot))\mu(\cdot)du - f'(X(\cdot))\sigma(\cdot)d\mathcal{W}(\cdot)$.

For example, for the infinite dimensional MCMD estimator we have $H_n(\cdot) = H(\widehat{d}_n(\cdot))$. This fact implies that

$$\sqrt{n}\Delta H_n(\cdot) = H'(\cdot)\{n^{-1/2} - \sqrt{n}\Delta\widehat{d}_n(\cdot)\} + o_{\mathbb{P}}(1) = n^{-1/2}H'(\cdot) - H'(\cdot)\Delta\widetilde{g}_n(\cdot) + o_{\mathbb{P}}(1) \tag{A.4}$$

by noting the definition of $\widetilde{g}_n(\cdot) := \sqrt{n}\{(\cdot) - \widehat{d}_n(\cdot)\}$ and that $\widehat{d}_n(\cdot) \to (\cdot)$ uniformly on $[0,1]$ with prob. converging to 1. This fact can be related to Assumption 3 by noting that $C_1(\cdot) = H'(\cdot)$, $C_2(\cdot) = -H'(\cdot)$ and $\widetilde{h}(\cdot) = \widetilde{g}_n(\cdot)$.

A.1.2 Limit Behavior of $n\sum_{t=1}^{n}\{\Delta Q_n(i_n)\}^2$

We examine the limit of $n\sum_{t=1}^{n}\{\Delta Q_n(i_n)\}^2$. From the first equality of (A.3), we note that $\sum_{i=1}^{n}\{\sqrt{n}\Delta Q_n(i_n)\}^2 = \sum_{i=1}^{n}\{f'(\widehat{X}_n(i_n))\}^2\{\frac{1}{n}(X'(i_n))^2 + (\Delta\bar{X}_n(i_n))^2\} + o_{\mathbb{P}}(1) = \frac{1}{n}\sum_{i=1}^{n}\{f'(X(i_n))\}^2\{(X'(i_n))^2 + \sigma^2(i_n)\} + o_{\mathbb{P}}(1)$, where the second equality holds by noting that $\widehat{X}_n(\cdot)$ converges to $X(\cdot)$ uniformly on $[0,1]$ and that $\sum_{i=1}^{n}\{f'(\widehat{X}_n(i_n))\}^2(\Delta\bar{X}_n(i_n))^2 = \sum_{i=1}^{n}\{f'(X(i_n))\}^2(\Delta\mathcal{G}(i_n))^2 + o_{\mathbb{P}}(1) = \frac{1}{n}\sum_{i=1}^{n}\{f'(X(i_n))\}^2\sigma^2(i_n) + o_{\mathbb{P}}(1)$. From this we derive $n\sum_{i=1}^{n}\{\Delta Q_n(i_n)\}^2 \Rightarrow \int_0^1\{f'(X(u))\}^2\{(X'(u))^2 + \sigma^2(u, \mathcal{G}(u))\}du$.

This result can also be generalized. If we let $\widetilde{Q}_n(\cdot) := h(\widehat{X}_n(\cdot))$ for a function $h : \mathbb{R} \mapsto \mathbb{R}$ in $\mathcal{C}^{(2)}([0,1])$, then we have $n\sum_{i=1}^n\{\Delta Q_n(i_n)\}\{\Delta\widetilde{Q}_n(i_n)\} \Rightarrow \int_0^1 f'(X(u))h'(X(u))\ \{(X'(u))^2 + \sigma^2(u, \mathcal{G}(u))\}du$. For example, for the infinite dimensional MCMD estimator, $H_n(\cdot) = H(\widehat{d}_n(\cdot))$ and $\widehat{d}_n(\cdot) \to (\cdot)$ uniformly on $[0,1]$ with prob. converging to 1, and $X(\cdot) = (\cdot)$. Hence, $n\sum_{i=1}^n \Delta H_n(i_n)\Delta H_n(i_n)' \to 2\int_0^1 H'(u)H'(u)'du$ with prob. converging to 1 by noting that $X'(\cdot) \equiv 1$ and $\sigma(\cdot) \equiv 1$ for the Brownian bridge.

A.1.3 Limit Behavior of $n\sum_{t=1}^n \Delta Q_n(i_n)\Delta\bar{X}_n(i_n)$

Here we examine the limit behavior of $n\sum_{t=1}^n \Delta Q_n(i_n)\Delta\bar{X}_n(i_n)$. Note that (A.3) implies that

$$\begin{aligned} n\Delta Q_n(\cdot) =& f'(\widehat{X}_n(\cdot))\{X'(\cdot) - \sqrt{n}\Delta\bar{X}_n(\cdot)\} \\ &+ \frac{1}{2}f''(\widehat{X}_n(\cdot))\left(\frac{1}{n}(X'(\cdot))^2 - \frac{2}{\sqrt{n}}X'(\cdot)\Delta\bar{X}_n(\cdot) + (\Delta\bar{X}_n(\cdot))^2\right) + o_{\mathbb{P}}(1) \end{aligned} \tag{A.5}$$

by a second-order Taylor expansion. This expansion is obtained by using the following approximation: $(\Delta\widehat{X}(\cdot))^2 = \frac{1}{n^2}(X'(\cdot))^2 - \frac{2}{n\sqrt{n}}X'(\cdot)\Delta\bar{X}_n(\cdot) + \frac{1}{n}(\Delta\bar{X}_n(\cdot))^2 + o_{\mathbb{P}}(1)$ based on (A.2). From this, we now obtain that

$$\begin{aligned} n\sum_{t=1}^n \left\{\Delta Q_n\left(i_n\right)\Delta\bar{X}_n\left(i_n\right)\right\} =& \sum_{i=1}^n f'\left(\widehat{X}_n\left(i_n\right)\right)X'\left(i_n\right)\Delta\bar{X}_n\left(i_n\right) \\ &- \sqrt{n}\sum_{i=1}^n f'\left(\widehat{X}_n\left(i_n\right)\right)\left(\Delta\bar{X}_n\left(i_n\right)\right)^2 + o_{\mathbb{P}}(1), \end{aligned} \tag{A.6}$$

using the fact that $(\Delta\bar{X}_n(\cdot))^2 = n^{-1}\sigma^2(\cdot) + o_{\mathbb{P}}(1)$. Note that the second-order term of (A.5) vanishes to 0 with prob. converging to 1. This fact implies that the limit behavior of $n\sum_{t=1}^n \Delta Q_n(i_n)\Delta\bar{X}_n(i_n)$ by focusing on the first-order approximation of $n\Delta Q_n(\cdot)$. Therefore

$$n\sum_{t=1}^n \left\{\Delta Q_n\left(i_n\right)\Delta\bar{X}_n\left(i_n\right)\right\} + \sqrt{n}\sum_{i=1}^n f'\left(\widehat{X}_n\left(i_n\right)\right)\left(\Delta\bar{X}_n\left(i_n\right)\right)^2 \Rightarrow \int_0^1 f'(X(u))X'(u)d\mathcal{G}(u). \tag{A.7}$$

We derive the weak limit of $n\sum_{t=1}^n\{\Delta Q_n\left(i_n\right)\Delta\bar{X}_n\left(i_n\right)\}$ by elaborating the second term of the left side in (A.6). Here, $\sum_{i=1}^n f'(\widehat{X}_n(i_n))(\Delta\bar{X}_n(i_n))^2 = \frac{1}{n}\sum_{i=1}^n f'(\widehat{X}_n(i_n))\sigma^2(i_n) + o_{\mathbb{P}}(1) \Rightarrow \int_0^1 f'(X(u))\sigma^2(u)du$. Therefore, if we further suppose that $\int_0^1 f'(X(u))\sigma^2(u)du = 0$ and that $n^{-1/2}\sum_{i=1}^n f'(X(i_n))\sigma^2(i_n) \to 0$ with prob. converging to 1, we can derive the weak limit of $n\sum_{t=1}^n\{\Delta Q_n(i_n)\Delta\bar{X}_n(i_n)\}$ more

specifically. For this derivation, first note that

$$\sqrt{n}\sum_{i=1}^{n} f'\left(\widehat{X}_n\left(i_n\right)\right)\left(\Delta\bar{X}_n\left(i_n\right)\right)^2 = \sqrt{n}\sum_{i=1}^{n} f'\left(X\left(i_n\right)\right)\left(\Delta\bar{X}_n\left(i_n\right)\right)^2 - \sum_{i=1}^{n} f''\left(X\left(i_n\right)\right)\sqrt{n}\left(X\left(i_n\right)-\widehat{X}_n\left(i_n\right)\right)\left(\Delta\bar{X}_n\left(i_n\right)\right)^2 + o_{\mathbb{P}}(1), \tag{A.8}$$

using the fact that

$$f'(\widehat{X}_n(\cdot)) = f'(X(\cdot)) - f''(X(\cdot))(X(\cdot)-\widehat{X}_n(\cdot)) + o_{\mathbb{P}}(1). \tag{A.9}$$

Next, note that $\sqrt{n}\sum_{i=1}^{n} f'(X(i_n))(\Delta\bar{X}_n(i_n))^2 = \sqrt{n}\sum_{i=1}^{n} f'(X(i_n))\{(\Delta\bar{X}_n(i_n))^2 - \frac{1}{n}\sigma^2(i_n)\} + o_{\mathbb{P}}(1)$ from the supposition that $n^{-1/2}\sum_{i=1}^{n} f'(X(i_n))\sigma^2(i_n) = o_{\mathbb{P}}(1)$; and applying a CLT to the right side gives $\sqrt{n}\sum_{i=1}^{n} f'(X(i_n))(\Delta\bar{X}_n(i_n))^2 \Rightarrow \mathcal{Z} \sim \mathcal{N}(0,\Gamma)$, where $\Gamma := \lim_{n\to\infty} n\sum_{i=1}^{n}\sum_{j=1}^{n} f'(X(i_n))f'(X(j_n))\mathbb{E}[\{(\Delta\bar{X}_n(i_n))^2 - \frac{1}{n}\sigma^2(i_n)\}\{(\Delta\bar{X}_n(j_n))^2 - \frac{1}{n}\sigma^2(j_n)\}]$. Third, note that $(\Delta\bar{X}_n(\cdot))^2 = n^{-1}\sigma^2(\cdot) + o_{\mathbb{P}}(1)$, and this implies that $\sum_{i=1}^{n} f''(X(i_n))\sqrt{n}(X(i_n)-\widehat{X}_n(i_n))(\Delta\bar{X}_n(i_n))^2 = \frac{1}{n}\sum_{i=1}^{n} f''(X(i_n))\sqrt{n}(X(i_n)-\widehat{X}_n(i_n))\sigma^2(i_n) + o_{\mathbb{P}}(1) \Rightarrow \int_0^1 f''(X(u))\mathcal{G}(u)\sigma^2(u)du$ from the supposition that $\sqrt{n}(X(\cdot)-\widehat{X}_n(\cdot)) \Rightarrow \mathcal{G}(\cdot)$. Combining these two weak limits with (A.8) gives $\sqrt{n}\sum_{i=1}^{n} f'(\widehat{X}_n(i_n))(\Delta\bar{X}_n(i_n))^2 \Rightarrow \mathcal{Z} - \int_0^1 f''(X(u))\,\mathcal{G}(u)\sigma^2(u)du$, which further implies that $n\sum_{t=1}^{n}\{\Delta Q_n(i_n)\Delta\bar{X}_n(i_n)\} \Rightarrow -\mathcal{Z} + \int_0^1 f''(X(u))\mathcal{G}(u)\sigma^2(u)du + \int_0^1 f'(X(u))X'(u)d\mathcal{G}(u)$ by (A.7).

For example, if we consider the infinite dimensional MCMD estimator, $H_n(\cdot) = H(\widehat{d}_n(\cdot))$ and $\widehat{d}_n(\cdot) \to (\cdot)$ uniformly on $[0,1]$ with prob. converging to 1. If we further elaborate on (A.4) expanding it by using the fact that $H'(\widehat{d}_n(\cdot)) = H'(\cdot) - H''(\cdot)((\cdot)-\widehat{d}_n(\cdot)) + o_{\mathbb{P}}(1)$, it follows that $\sqrt{n}\Delta H_n(\cdot) = n^{-1/2}H'(\cdot) - H'(\cdot)\Delta\widetilde{g}_n(\cdot) - n^{-1/2}H''(\cdot)\widetilde{g}_n(\cdot)\Delta\widetilde{g}_n(\cdot) + o_{\mathbb{P}}(n^{-1})$. Furthermore, $\widetilde{g}_n(\cdot) := \sqrt{n}\{(\cdot)-\widehat{d}_n(\cdot)\} \Rightarrow \mathcal{B}^0(\cdot)$, so that $\sigma^2(\cdot) \equiv 1$, and the proof of Theorem 3 shows that $\int_0^1 H'(u)du = 0$ and $n^{-1/2}\sum_{i=1}^{n} H'(i_n) = o(1)$ using theorem 1 (c) of Chui (1971). Hence, $n\sum_{t=1}^{n-1}\{\Delta H_n(i_n)\Delta\widetilde{g}_n(i_n)\} \Rightarrow -\mathcal{Z} + \int_0^1 H''(u)\mathcal{B}^0(u)du + \int_0^1 H'(u)d\mathcal{B}^0(u)$, where $\mathcal{Z} \overset{\text{A}}{\sim} \mathcal{N}(0, 8[H'(\cdot), H'(\cdot)])$, and $\int_0^1 H''(u)\mathcal{B}^0(u)du + \int_0^1 H'(u)d\mathcal{B}^0(u) = 0$ as the proof of Theorem 3 verifies.

A.2 Limit Differences of Smooth Gaussian Processes

This section derives the limit behavior of the same quantities examined in Section A.1 by supposing that $\mathcal{G}(\cdot)$ satisfies the condition in Assumption 2 (i). That is, $\mathcal{G}(\cdot)$ is differentiable with prob. 1 instead of being an Itô process. Note that the convergence rate of $\Delta\bar{X}_n(\cdot)$ is different from that of Section A.1. Specifically, Assumption 2 (i) implies that $n\Delta\bar{X}_n(\cdot) = \mathcal{G}'(\cdot) + o_{\mathbb{P}}(1)$. This different feature produces different limit behavior in the quantities involved.

A.2.1 Limit Behavior of $\sum_{i=1}^{n} \Delta Q_n(i_n)$

We first examine the limit behavior of $\sqrt{n}\Delta Q_n(\cdot)$. If we combine (A.2), (A.3), and (A.9), we can derive the following:

$$\sqrt{n}\Delta Q_n(\cdot) = \frac{1}{\sqrt{n}} f'(\cdot)X'(\cdot) - f'(\cdot)\Delta\bar{X}_n(\cdot) - \frac{1}{\sqrt{n}} f''(\cdot)\bar{X}_n(\cdot)\Delta\bar{X}_n(\cdot) + o_{\mathbb{P}}(1), \tag{A.10}$$

so that $n\Delta Q_n(\cdot) = f'(\cdot)X'(\cdot) + o_{\mathbb{P}}(1)$. Therefore, it follows that $\sum_{i=1}^{n} \Delta Q_n(\cdot) = \frac{1}{n}\sum_{i=1}^{n} f'(i_n)X'(i_n) + o_{\mathbb{P}}(1) \to \int_0^1 f'(u)X'(u)du$ with prob. converging to 1.

A.2.2 Limit Behavior of $n\sum_{t=1}^{n}\{\Delta Q_n(i_n)\}^2$

By (A.10), $n\sum_{i=1}^{n}\{\Delta Q_n(i_n)\}^2 = \frac{1}{n}\sum_{i=1}^{n}\{f'(i_n)X'(i_n)\}^2 + o_{\mathbb{P}}(1) \to \int_0^1\{f'(u)X'(u)\}^2du$ with prob. converging to 1. The limit is identical to $(f'(\cdot)X'(\cdot), f'(\cdot)X'(\cdot))$.

A.2.3 Limit Behavior of $n\sum_{t=1}^{n}\Delta Q_n(i_n)\Delta\bar{X}_n(i_n)$

By (A.10) and the fact that $n\Delta\bar{X}_n(\cdot) = \mathcal{G}'(\cdot) + o_{\mathbb{P}}(1)$, it follows that $n\sum_{i=1}^{n}\Delta Q_n(i_n)\Delta\bar{X}_n(i_n) = \frac{1}{n}\sum_{i=1}^{n}$ $f'(i_n)X'(i_n)n\Delta\bar{X}_n(i_n) + o_{\mathbb{P}}(1) \Rightarrow \int_0^1 f'(u)X'(u)\mathcal{G}'(u)du = (f'(\cdot)X'(\cdot), \mathcal{G}'(\cdot))$.

A.3 Asymptotics of Quantities involved in Infinite Dimensional MCMD Estimation

This section explores the asymptotic variances of the quantities constituting the infinite dimensional MCMD estimator. For this, we first note that $(\Delta\widehat{d}_n(\frac{1}{n}), \Delta\widehat{d}_n(\frac{2}{n}), \ldots, \Delta\widehat{d}_n(1))'$ follows a Dirichlet distribution with parameter ι_n. Using this condition, the following hold: for each i and $j = 1, 2, \ldots, n-1$ $(i \neq j)$,

$$\mathbb{E}\left[\Delta\widehat{d}_n(i_n)\right] = \frac{1}{n}, \tag{A.11}$$

$$\mathbb{E}\left[\left(\Delta\widehat{d}_n(i_n)\right)^2\right] = \frac{2}{n(n+1)}, \tag{A.12}$$

$$\mathbb{E}\left[\left(\Delta\widehat{d}_n(i_n)\right)^3\right] = \frac{6}{n(n+1)(n+2)}, \tag{A.13}$$

$$\mathbb{E}\left[\left(\Delta\widehat{d}_n(i_n)\right)^4\right] = \frac{24}{n(n+1)(n+2)(n+3)}, \tag{A.14}$$

$$\mathbb{E}\left[\left(\Delta\widehat{d}_n(i_n)\right)^2\Delta\widehat{d}_n(j_n)\right] = \frac{2}{n(n+1)(n+2)}, \tag{A.15}$$

$$\mathbb{E}\left[\left(\Delta\widehat{d}_n(i_n)\right)^2\left(\Delta\widehat{d}_n(j_n)\right)^2\right] = \frac{4}{n(n+1)(n+2)(n+3)}. \tag{A.16}$$

A.3.1 The Variance of $\sqrt{n}\sum_{i=1}^{n-1} H_j'(i_n)\{n(\Delta\widehat{d}_n(i_n))^2 - \frac{2n}{n(n+1)}\}$

The asymptotic variance of $\sqrt{n}\sum_{i=1}^{n-1} H_j'(i_n)\{n(\Delta\widehat{d}_n(i_n))^2 - \frac{2n}{n(n+1)}\}$ is shown to be $20(H_j'(\cdot), H_j'(\cdot))$. For simplicity let $U_{n,i} := n(\Delta\widehat{d}_n(i_n))^2 - \frac{2n}{n(n+1)}$, then $\text{var}[\sqrt{n}\sum_{i=1}^{n-1} H_j'(i_n)\{n(\Delta\widehat{d}_n(i_n))^2 - \frac{2n}{n(n+1)}\}] = n\sum_{i=1}^{n-1}\sum_{\ell=1}^{n-1} H_j'(i_n)H_j'(\ell_n)\mathbb{E}[U_{n,i}U_{n,\ell}]$, where $\ell_n := \frac{\ell}{n}$. Here, note that $\mathbb{E}[U_{n,i}U_{n,\ell}] = n^2\mathbb{E}[(\Delta\widehat{d}_n(i_n))^2 (\Delta\widehat{d}_n(\ell_n))^2] - \frac{4n^2}{n(n+1)}\mathbb{E}[(\Delta\widehat{d}_n(i_n))^2] + \frac{4n^2}{n^2(n+1)^2}$. If $i \neq \ell$, $\mathbb{E}[U_{n,i}U_{n,\ell}] = -16n^{-3} + o(n^{-3})$ by (A.12) and (A.16); and if $i = \ell$, $\mathbb{E}[U_{n,i}U_{n,\ell}] = 20n^{-2} + o(n^{-2})$ by (A.12) and (A.14). Combining these two facts, it follows that $\text{var}[\sqrt{n}\sum_{i=1}^{n-1} H_j'(i_n)\{n(\Delta\widehat{d}_n(i_n))^2 - \frac{2n}{n(n+1)}\}] = \frac{20}{n}\sum_{i=1}^{n-1}(H_j'(i_n))^2 - \frac{16}{n^2}(\sum_{i=1}^{n-1} H_j'(i_n))^2 + o(1) \to 20\int_0^1 (H_j'(u))^2 du = 20(H_j'(\cdot), H_j'(\cdot))$ since $\sum_{i=1}^{n-1} H_j'(i_n) = o(n^{-1})$ by theorem 1 (c) of Chui (1971).

A.3.2 The Variance of $\sum_{i=1}^{n-1}(\Delta\widetilde{g}_n(i_n))^2 - 1$

The asymptotic variance of $\sum_{i=1}^{n-1}(\Delta\widetilde{g}_n(i_n))^2 - 1$ is now shown to be $4n^{-1} + o(n^{-1})$. We first note that $\Delta\widetilde{g}_n(\cdot) = \sqrt{n}(\frac{1}{n} - \Delta\widehat{d}_n(\cdot))$, so that $(\Delta\widetilde{g}_n(\cdot))^2 = n(\Delta\widehat{d}_n(\cdot))^2 - 2\Delta\widehat{d}_n(\cdot) + n^{-1}$. This fact implies that $\sum_{i=1}^{n-1}(\Delta\widetilde{g}_n(i_n))^2 - 1 = n\sum_{i=1}^{n-1}(\Delta\widehat{d}_n(i_n))^2 - 2 + 2\Delta\widehat{d}_n(1) - \frac{1}{n}$ by noting that $\sum_{i=1}^{n-1}\Delta\widehat{d}_n(i_n) = 1 - \Delta\widehat{d}_n(1)$. Hence, it follows that $\mathbb{E}[(\Delta\widetilde{g}_n(i_n))^2] = \frac{n-1}{n(n+1)} = o(n^{-1})$ from (A.11) and (A.12), so that $\text{var}[\sum_{i=1}^{n-1}(\Delta\widetilde{g}_n(i_n))^2 - 1] = n^2\sum_{i=1}^{n-1}\sum_{j=1}^{n-1}\mathbb{E}[(\Delta\widehat{d}_n(i_n))^2(\Delta\widehat{d}_n(j_n))^2] - 4n\sum_{i=1}^{n-1}\mathbb{E}[(\Delta\widehat{d}_n(i_n))^2] + 4 + o(n^{-1})$, implying that $\text{var}[\sum_{i=1}^{n-1}(\Delta\widetilde{g}_n(i_n))^2 - 1] = \frac{4n^3+20n^2+72n}{n(n+1)(n+2)(n+3)} + o(n^{-1}) = \frac{4}{n} + o(n^{-1})$ by (A.12), (A.14), and (A.16).

A.3.3 The Covariance between $\sum_{i=1}^{n-1} H_j'(i_n)\Delta\widetilde{g}_n(i_n)$ and $\sqrt{n}\sum_{i=1}^{n-1} H_j'(i_n)\{n(\Delta\widehat{d}_n(i_n))^2 - \frac{2n}{n(n+1)}\}$

We show that $-4(H_j'(\cdot), H_j'(\cdot))$ is the asymptotic covariance between $\sum_{i=1}^{n-1} H_j'(i_n)\Delta\widetilde{g}_n(i_n)$ and $\sqrt{n}\sum_{i=1}^{n-1} H_j'(i_n)U_{n,i}$, where $U_{n,i} := n(\Delta\widehat{d}_n(i_n))^2 - \frac{2n}{n(n+1)}$ as in Section A.3.1. We note that $\text{cov}[\sum_{i=1}^{n-1} H_j'(i_n)\Delta\widetilde{g}_n(i_n), \sqrt{n}\sum_{i=1}^{n-1} H_j'(i_n)U_{n,i}] = \sum_{i=1}^{n-1}\sum_{\ell=1}^{n-1} H_j'(i_n)H_j'(\ell_n)[n^2\mathbb{E}[(\Delta\widehat{d}_n(i_n))^2\Delta\widehat{d}_n(\ell_n)] - \frac{2n}{n+1}]$ since $\Delta\widetilde{g}_n(\cdot) = n^{-1/2} - \sqrt{n}\widehat{d}_n(\cdot)$ and using (A.11) and (A.12), where $\ell_n := \frac{\ell}{n}$. We further use the moment conditions in (A.13) and (A.15) to obtain that $\text{cov}[\sum_{i=1}^{n-1} H_j'(i_n)\Delta\widetilde{g}_n(i_n), \sqrt{n}\sum_{i=1}^{n-1} H_j'(i_n)U_{n,i}] = -\frac{4n}{(n+1)(n+2)}\sum_{i=1}^{n-1} H_j'(i_n)^2 + \frac{4n^2}{(n+1)(n+2)}(\frac{1}{n}\sum_{i=1}^{n-1} H_j'(i_n))^2 \to -4(H_j'(\cdot), H_j'(\cdot))$, because $\sum_{i=1}^{n-1} H_j'(i_n) = o(n^{-1})$ by theorem 1 (c) of Chui (1971).

A.4 Additional Simulation Evidence

In this section, we provide additional simulation evidence for the infinite dimensional MCMD estimator. We also compare the U-test with the distributional specification test proposed by Amengual et al. (2020).

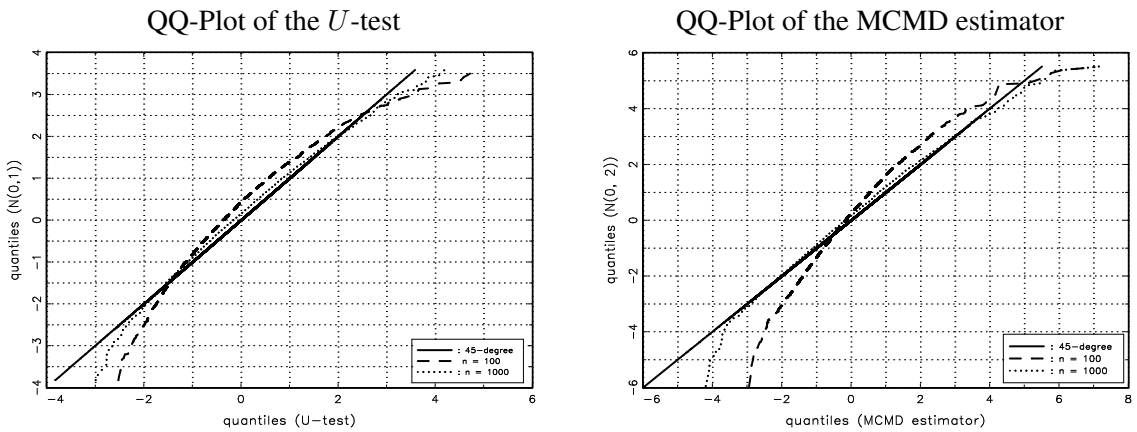

(a) Exponential distribution case

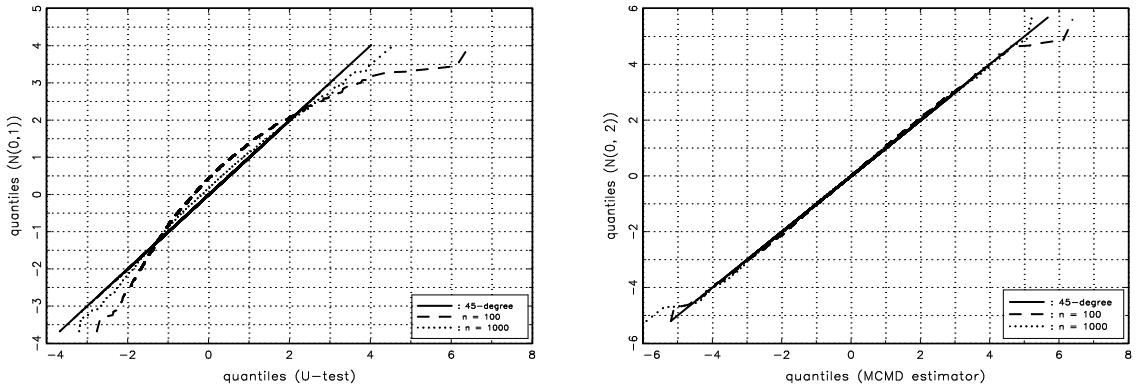

(b) Normal distribution case

Figure A.1: QQ-PLOTS OF THE U-TEST UNDER THE NULL AND THE MCMD ESTIMATOR. For $n = 100$ and $1,000$, each figure shows the QQ-plots the U-test and the MCMD estimator against their limit distributions. The QQ-plots are obtained by repeating 10,000 independent experiments.

Before proceeding with our discussion, we provide additional evidence in support of the simulation results in Section 3. Figure 1 provides the finite sample distributions of the U-test under the null and the MCMD estimator together with their limit distributions. Here, we provide their QQ-plots in Figure A.1. For $n = 100$ and $1,000$, the QQ-plots are drawn, and the figures demonstrate that the QQ-plots approach the 45-degree line as the sample size increases from 100 to $1,000$. In addition, we note that the null distribution of the U-test converges to the standard normal distribution rather slowly when compared to the distribution of the MCMD estimator. For the normal distribution case, the empirical distribution of the MCMD estimator is almost identical to the limit normal distribution even when $n = 100$.

A.4.1 Simulation Evidence of t-Test

This section provides additional findings in support of the present approach by examining the t-test of the current study in comparison with the t-test based on Tikhonov regularization. Using the infinite dimensional

MCMD estimator we report simulations conducted to elaborate the properties of GMM estimation. For this purpose, we use the two DGP conditions in Section 3, with x_t following an exponential or normal distribution. The simulation design is as follows.

First, if x_t follows an exponential distribution, then $\mathbb{P}(x_t \leq x) = 1 - \exp(-\theta_* x)$, denoted as $x_t \sim \text{Exp}(\theta_*)$. Likewise, for $x_t \sim \mathcal{N}(\theta_*, 1)$, we have $\mathbb{P}(x_t \leq x) = \Phi(x - \theta_*)$, and the unknown parameter is estimated by the infinite dimensional MCMD detailed in Section 3.

Second, we conduct simulations by supposing null DGPs for testing the hypotheses of the t-test. For this purpose, we let $\theta_* = 1$ and 0 for the exponential and normal cases, respectively. In each DGP environment, we compute the empirical rejection rates of t-test for significance levels of 1%, 5%, and 10% with 10,000 independent repetitions.

Third, the t-test is developed from the asymptotic distribution of the infinite dimensional MCMD estimator. For this, using the distributional hypotheses we obtain

$$H(p) = \begin{cases} \frac{1}{\theta_*}(1-p)\log(1-p), & \text{for the exponential distribution;} \\ \phi(\Phi^{-1}(p)), & \text{for the normal distribution,} \end{cases}$$

if the models are correctly specified, where $\phi(\cdot)$ is the probability density function (PDF) of a standard normal distribution. In all cases, $\lim_{p\to 0} H(p) = 0$, $\lim_{p\to 1} H(1) = 0$. Furthermore,

$$\int_0^1 (H'(u))^2 du = \begin{cases} \frac{1}{\theta_*^2}, & \text{for the exponential distribution;} \\ 1, & \text{for the normal distribution.} \end{cases}$$

Therefore, it follows that

$$\sqrt{n}(\widehat{\theta}_n - \theta_*) \overset{\text{A}}{\sim} \begin{cases} \mathcal{N}(0, 2\theta_*^2), & \text{for the exponential distribution;} \\ \mathcal{N}(0, 2), & \text{for the normal distribution} \end{cases}$$

by Theorem 3 (iii), so that if we let

$$t_n := \begin{cases} \frac{\sqrt{n}(\widehat{\theta}_n - c)}{\sqrt{2\widehat{\theta}_n^2}}, & \text{for the exponential distribution;} \\ \frac{\sqrt{n}(\widehat{\theta}_n - c)}{\sqrt{2}}, & \text{for the normal distribution,} \end{cases}$$

it follows $\mathcal{N}(0,1)$ under the joint hypothesis that $\theta_* = c$ and that the distributional condition is correct. For all cases, $U_n \overset{\text{A}}{\sim} \mathcal{N}(0,1)$ under the same conditions. If the t-test rejects the null, it is not evident which specific condition is violated in the joint hypotheses. To address this issue, both the U-test and the t-test need to test the distributional hypothesis. If the U-test rejects the distributional hypothesis, inference from

Test	Distribution	Level \ n	50	100	200	300	400	500	1,000
t-test	Exponential	1%	2.57	1.72	1.62	1.22	1.32	1.22	1.03
		5%	7.87	6.39	5.86	5.50	5.40	5.66	5.14
		10%	13.16	11.52	11.01	10.40	9.91	10.40	10.17
	Normal	1%	0.89	1.02	0.73	1.11	0.91	0.97	1.04
		5%	4.35	4.89	4.46	4.51	4.91	4.88	4.89
		10%	8.67	9.26	9.07	9.18	9.87	9.48	9.74
t'-test	Exponential	1%	2.93	2.05	1.50	1.47	1.45	1.38	1.31
		5%	8.82	7.32	6.48	6.04	6.30	6.12	5.61
		10%	14.54	12.66	12.09	11.44	11.61	11.66	11.02
	Normal	1%	1.43	1.32	1.17	1.25	1.08	1.03	1.13
		5%	6.54	6.23	5.97	5.69	5.48	5.08	5.25
		10%	11.80	11.48	10.88	10.92	10.83	10.25	10.34

Table A.1: EMPIRICAL REJECTION RATES OF THE t- AND t'-TESTS UNDER THE NULL (IN PERCENT). This table shows the empirical rejection rates of the t- and t'-tests under the joint hypothesis that $\theta_* = c$ and that the distributional condition is correct. For the exponential and normal cases, we let $\theta_* = 1$ and 0, respectively.

the t-test is not informative. But if the t-test rejects the null while the U-test does not, it is evident that $\theta_* \neq c$. This combined approach provides a more comprehensive assessment of the hypotheses.

In addition, we define the following test by Tikhonov's regularization method:

$$t'_n := \begin{cases} \frac{\sqrt{n}(\dot{\theta}_n - c)}{\sqrt{\dot{\theta}_n^2}}, & \text{for the exponential distribution;} \\ \sqrt{n}(\dot{\theta}_n - c), & \text{for the normal distribution,} \end{cases}$$

where $\dot{\theta}_n$ is defined in Section 3. This test is defined by noting that theorem 8 in Carrasco and Florens (2000) implies that $\sqrt{n}(\dot{\theta}_n - \theta_*) \overset{\text{A}}{\sim} \mathcal{N}(0, \int_0^1 (H'(u))^2 du)$. Our earlier derivations show that $\int_0^1 (H'(u))^2 du = \theta_*^2$ for the exponential distribution, and $\int_0^1 (H'(u))^2 du = 1$ for the normal distribution. The asymptotic variances are straightforwardly obtained by applying Lemma 1 (i.b) to theorem 8 of Carrasco and Florens (2000), and letting $\alpha_n = n^{-1/4}$ to satisfy the condition in theorem 8. Under the null, t'_n is then asymptotically standard normal.

The null simulation results are given in Table A.1 and are summarized as follows.

(a) As the sample size n increases the distribution of the t-test converges to the standard normal. Table A.1 shows that the empirical rejection rates are close to 1%, 5%, and 10% for the exponential and normal distribution cases when $n = 200$, 300, 400, 500, and 1,000. These results corroborate the limit theory of the t-test under the null given in Theorem 1 (ii).

(b) Comparison of the t-test and t'-test results shows that the empirical rejection rates of the t-test also converge to the nominal levels faster than the t'-test. Although the finite sample distortions are not as

Test	Distribution	Level \ n	50	100	200	300	400	500	1,000
t-test	Exponential	1%	4.53	5.66	7.56	10.61	13.37	15.77	29.30
		5%	12.94	15.59	20.37	26.26	30.33	35.19	52.49
		10%	20.47	24.35	31.05	37.23	43.03	47.09	64.67
	Normal	1%	0.64	0.86	2.14	3.62	5.09	5.84	6.49
		5%	2.68	5.06	11.68	17.30	20.88	23.26	23.67
		10%	5.55	11.31	23.09	31.65	36.58	39.04	39.04
t'-test	Exponential	1%	5.65	5.19	4.67	4.67	4.54	4.61	4.34
		5%	14.03	14.05	12.80	13.32	13.62	13.38	13.66
		10%	20.99	21.28	20.20	20.73	21.54	20.84	21.81
	Normal	1%	1.04	1.33	1.27	1.40	1.17	1.58	1.91
		5%	5.32	5.41	5.57	6.22	6.23	6.36	7.01
		10%	10.19	10.61	10.82	11.10	11.69	12.00	12.81

Table A.2: EMPIRICAL REJECTION RATES OF THE t- AND t'-TESTS UNDER THE LOCAL ALTERNATIVE (IN PERCENT). This table shows the empirical rejection rates of the t- and τ'-tests under local alternatives. For the exponential case, $x_{t,n} := y_t + \frac{1}{2}\sqrt{z_t/n}$, where $y_t \sim \text{Exp}(1)$ and $z_t \sim \mathcal{U}[0.5, 1.5]$; and for the normal case, $x_{t,n} := y_t + \frac{1}{4}y_t^4/\sqrt{n}$, where $y_t \sim \mathcal{N}(0,1)$.

Test	Distribution	Level \ n	50	100	200	300	400	500	1,000
U-test	Pareto	1%	0.47	0.74	0.85	0.89	0.84	0.92	0.97
		5%	1.38	2.71	3.48	4.33	3.87	4.10	4.42
		10%	4.14	6.74	7.69	8.73	8.20	9.16	9.48
τ-test	Pareto	1%	0.35	0.51	0.83	0.94	0.89	0.94	0.91
		5%	0.84	1.58	2.25	2.20	2.68	2.81	3.42
		10%	1.34	2.46	4.52	5.29	6.84	7.29	7.85

Table A.3: EMPIRICAL REJECTION RATES OF THE U- AND τ-TESTS UNDER THE NULL (IN PERCENT). This table shows the empirical rejection rates of the U- and τ-tests under the Pareto distributional hypothesis.

severe as the U-test, the t-test nevertheless controls type-I errors better than the t'-test. □

Finally, simulations were conducted to examine the local power properties of the t-test. For this purpose, we employ the same local DGP conditions in Section 3: (i) for the exponential case, $x_{t,n} := y_t + \frac{1}{2}\sqrt{z_t/n}$, with $y_t \sim \text{Exp}(1)$ and $z_t \sim \mathcal{U}[0.5, 1.5]$; and (ii) for the normal case, $x_{t,n} := y_t + \frac{1}{4}y_t^4/\sqrt{n}$, with $y_t \sim \mathcal{N}(0,1)$. Local powers of the t-test are examined together with those of the t'-test. Similar to the null simulations, 10,000 independent experiments were repeated under the local alternatives and empirical rejection rates of the tests are reported in Table A.2. These results are summarized as follows.

(a) The t-test exhibits non-negligible local power in each case. As the sample size n increases, the empirical rejection rates of the t-test tend to exceed the nominal significance levels, again indicating that the t-test exhibits local power. Similar to the U-test, the empirical local power of the t-test remains relatively stable for the normal distribution case across different sample sizes, suggesting that the t-test performs well in detecting local departures from the null hypothesis, particularly for the

normal distribution case.

(b) When comparing powers of the t- and t'-tests, the empirical rejection rates of the t-test are higher than those of the t'-test for the two distributions. □

This simulation comparing our approach with the t-test based on Tikhonov's regularization method shows that the BB-kernel reduces finite sample size distortion and increases local power.

A.4.2 Testing the Pareto Distributional Hypothesis

We repeat the simulation experiments in Sections 3 and A.4.1 using the Pareto distribution. This separate experiment is conducted by noting that the empirical application in Section 4 exploits testing the Pareto distributional hypothesis. The plan for the simulation parallels earlier simulations.

First, if x_t follows a Pareto distribution bounded from 1, we have $\mathbb{P}(x_t \leq x) = 1 - (1/x)^{\theta_*}$, denoted as $x_t \sim \text{Pa}(\theta_*, 1)$, and the infinite dimensional MCMD is obtained as

$$\widehat{\theta}_n := \arg\min_{\theta \in \Theta} (\widehat{P}_n - F_n(\theta))' \widehat{\Sigma}_n^{-1} (\widehat{P}_n - F_n(\theta)),$$

where the j-th row element of $F_n(\theta)$ is $1 - \left(1/x_{(j)}\right)^{\theta}$.

Second, using the Pareto distributional hypothesis we obtain $H(p) = \frac{1}{\theta_*}(1-p)\log(1-p)$ if the models are correctly specified. Here, $\lim_{p\to 0} H(p) = 0$, $\lim_{p\to 1} H(1) = 0$, and $\int_0^1 (H'(u))^2 du = \frac{1}{\theta_*^2}$. Therefore, it follows that $\sqrt{n}(\widehat{\theta}_n - \theta_*) \overset{\text{A}}{\sim} \mathcal{N}(0, 2\theta_*^2)$ by Theorem 3 (iii), so that t-test can be defined as $t_n := \sqrt{n}(\widehat{\theta}_n - c)/\sqrt{2\widehat{\theta}_n^2}$, which is the same formula as for the t-test applied to the exponential distribution case. It follows $\mathcal{N}(0,1)$ under the joint hypothesis that $\theta_* = c$ and that the distributional condition is correct. Also, $U_n \overset{\text{A}}{\sim} \mathcal{N}(0,1)$ under the same conditions.

Third, we conduct simulations by assuming the null DGP for testing the hypotheses involved in the U- and t-tests. For this purpose, we let $\theta_* = 1$, so that $x_t \sim \text{Pa}(1,1)$. We compute the empirical rejection rates of the U- and t-tests for significance levels of 1%, 5%, and 10% with 10,000 independent repetitions. The empirical rejection rates under the null hypothesis for each test are reported in Table A.3.

Fourth, we compare the U- and t-tests with the corresponding tests based on Tikhonov regularization, viz., the τ- and t'-tests. The formula of the τ_n test is the same as that in Section 3, and that of the t'-test is the same as that for the exponential distribution case. This result is obtained by noting that $\sqrt{n}(\dot{\theta}_n - \theta_*) \overset{\text{A}}{\sim} \mathcal{N}\left(0, \int_0^1 (H'(u))^2 du\right)$ and that $\int_0^1 (H'(u))^2 du = \theta_*^2$. The null simulation results are summarized as follows.

(a) As the sample size n increases, the distribution of the U-test converges to the standard normal. Table A.3 demonstrates that the empirical rejection rates are close to 1%, 5%, and 10% when $n = 1,000$. This observation confirms that the U-test follows the null limit distribution given in Theorem 2 (ii).

Test	Distribution	Level \ n	50	100	200	300	400	500	1,000
t-test	Pareto	1%	2.68	1.87	1.34	1.19	1.23	1.13	1.27
		5%	7.64	6.75	5.60	5.44	5.42	5.58	5.21
		10%	13.24	11.64	10.38	10.58	10.44	10.92	9.66
t'-test	Pareto	1%	2.65	2.09	1.86	1.46	1.51	1.35	1.32
		5%	8.76	7.15	6.60	6.11	6.16	6.21	5.85
		10%	14.55	12.99	12.23	11.55	11.76	11.53	10.74

Table A.4: EMPIRICAL REJECTION RATES OF THE t- AND t'-TESTS UNDER THE NULL (IN PERCENT). This table shows the empirical rejection rates of the t- and t'-tests under the joint hypothesis that $\theta_* = c$ and that the distributional condition is correct under the Pareto distribution condition with $\theta_* = 1$.

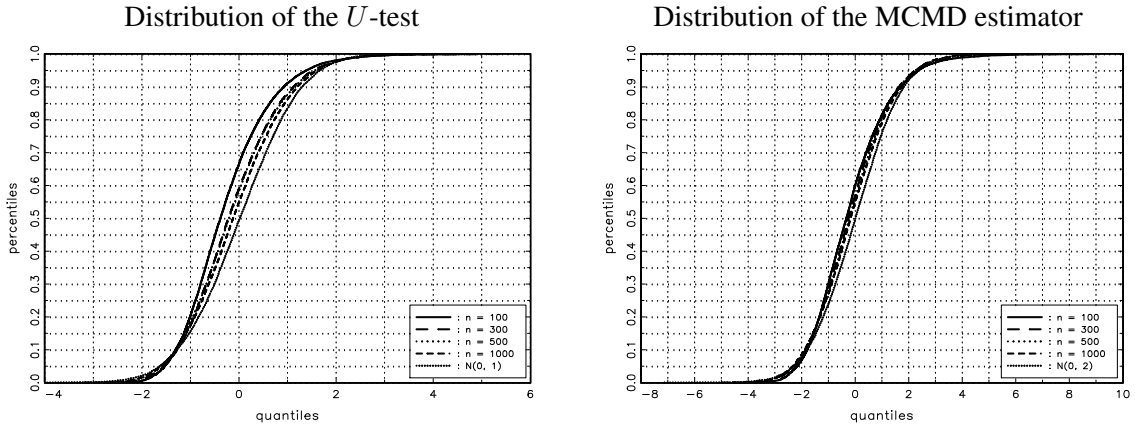

Pareto distribution case

Figure A.2: EMPIRICAL DISTRIBUTIONS OF THE U-TEST UNDER THE NULL AND THE MCMD ESTIMATOR. For $n = 100, 300, 500$, and $1,000$, each figure shows the null distributions of the U-test or the empirical distributions of the MCMD estimator under the Pareto distribution condition. The distributions are obtained by repeating 10,000 independent experiments.

The empirical distributions of the U-test given in the left column of Figure A.2 displays these distributions. The empirical distribution approaches the CDF of the standard normal as n increases.

(b) As the sample size n increases the distribution of the t-test converges to the standard normal. Table A.4 shows that the empirical rejection rates are close to 1%, 5%, and 10% when $n = 200$, 300, 400, 500, and $1,000$. These results corroborate the limit theory of the t-test under the null given in Theorem 1 (ii). Furthermore, the standard normal provides a better approximation of the distribution of the t-test compared to the U-test.

(c) The right column of Figure A.2 displays the empirical distributions of the infinite dimensional MCMD estimator and these evidently closely approach the $\mathcal{N}(0, 2)$ CDF as n increases. This matches the evidence observed in the exponential and normal distribution cases.

(d) When comparing the U-test with the τ-test reported in Table A.3, it is apparent that the empirical

Test	Distribution	Level \ n	50	100	200	300	400	500	1,000
U-test	Pareto	1%	0.61	1.53	4.38	8.04	11.45	15.58	40.30
		5%	2.01	4.33	10.47	17.34	24.28	31.34	60.64
		10%	3.76	7.47	15.99	25.39	34.41	41.38	70.77
τ-test	Pareto	1%	0.80	2.35	4.30	5.52	6.95	8.30	13.90
		5%	2.02	4.93	8.48	10.22	13.58	15.43	24.10
		10%	3.19	7.29	12.56	14.69	18.65	21.24	32.01

Table A.5: EMPIRICAL REJECTION RATES OF THE U-TEST AND τ-TESTS UNDER THE LOCAL ALTERNATIVE (IN PERCENT). This table shows the empirical rejection rates of the U- and τ-tests under local alternatives. For the Pareto case, $x_{t,n} := y_t + \frac{1}{2}\sqrt{z_t/n}$, where $y_t \sim \text{Pa}(1,1)$ and $z_t \sim \mathcal{U}[0.5, 1.5]$.

rejection rates of the U-test converge to the nominal levels faster than the τ-test. When n is small, the level distortions of the τ-test are large. Even for $n = 1,000$, the empirical rejection rates of the τ-test are still far from nominal levels. This outcome is again the same as those for the exponential and normal distribution cases.

(e) Much the same findings as above are obtained in the comparison of the t-test and t'-test. Although the finite sample distortions are not as severe as the U-test, the empirical rejection rates of the t-test are closer to nominal levels than those the t'-test. □

Finally, simulations were conducted to examine the local power properties of the U- and t-tests. For this purpose, we suppose the following DGP condition: $x_{t,n} := y_t + \frac{1}{2}\sqrt{z_t/n}$, with $y_t \sim \text{Pa}(1,1)$ and $z_t \sim \mathcal{U}[0.5, 1.5]$. Note that this is a local alternative DGP condition similar to the exponential distribution case. As before, we examine local powers of the U- and t-tests together with those of the τ- and t'-tests, and the empirical rejection rates of the tests are reported in Tables A.5 and A.6. The performance of the tests under the local departure are summarized as follows.

(a) The U-test demonstrates non-negligible local power. As n increases, the empirical rejection rates of the U-test exceed the nominal significance levels, indicating that the U-test exhibits local power. This suggests that the U-test performs well in detecting local departures, and this is the same observation as for the exponential distribution case.

(b) The t-test also exhibits non-negligible local power. As n increases, the empirical rejection rates of the t-test tend to exceed the nominal significance levels.

(c) As for the exponential and normal distribution cases, the empirical rejection rates of the U- and t-tests are higher than those of the τ- and t'-tests, respectively. □

These simulation results align with those obtained from exponential and normal distributions, confirming applicablility to the Pareto distribution case.

Test	Distribution	Level \ n	50	100	200	300	400	500	1,000
t-test	Pareto	1%	3.20	3.71	5.20	6.98	9.28	11.72	22.57
		5%	9.83	11.82	15.67	19.52	24.78	27.84	44.11
		10%	16.28	19.00	25.06	30.01	35.82	39.11	56.60
t'-test	Pareto	1%	3.60	3.26	2.91	2.61	2.60	2.58	2.48
		5%	10.02	9.07	9.28	8.75	8.81	8.77	9.00
		10%	16.35	14.75	15.98	14.78	15.24	15.74	15.15

Table A.6: EMPIRICAL REJECTION RATES OF THE t- AND t'-TESTS UNDER THE LOCAL ALTERNATIVE (IN PERCENT). This table shows the empirical rejection rates of the t- and τ'-tests under local alternatives for the Pareto distribution case, $x_{t,n} := y_t + \frac{1}{2}\sqrt{z_t/n}$, where $y_t \sim \text{Pa}(1,1)$ and $z_t \sim \mathcal{U}[0.5, 1.5]$.

A.4.3 Comparison with Amengual et al.'s (2020) Test

This section now compares the U-test with the distributional specification test proposed by Amengual et al. (2020) and reports its local power in Table A.7. Amengual et al. (2020) define the test using the GMM distance constructed by moment conditions based on the difference between the estimated characteristic function and the characteristic function hypothesized by the distributional assumption. Since the characteristic function completely defines the distribution, testing the hypothesized characteristic function is equivalent to testing the hypothesized distribution. We denote this test as the ACS-test.

We test the distributional hypothesis for the exponential and normal distributions under the same DGP conditions as given in the section for MCMD simulation. Several remarks are warranted on the testing procedure. First, in computing the ACS-test, the domains of the empirical and hypothetical characteristic functions are set to the interval $[-1, 1]$, which is an arbitrarily selected interval covering the origin. We also apply the parametric bootstrap for the test by following Amengual et al. (2020). The null limit distribution of the ACS-test is nonstandard and the empirical rejection rates are computed by the parametric bootstrap. The empirical rejection rates of the ACS-test are obtained by 10,000 independent experiments. Second, we suppose the same local alternative DGP conditions as those given in Section 3 for the exponential and normal distributions. That is, for the exponential case, $x_{t,n} := y_t + \frac{1}{2}\sqrt{z_t/n}$, with $y_t \sim \text{Exp}(1)$ and $z_t \sim \mathcal{U}[0.5, 1.5]$; and for the normal case, $x_{t,n} := y_t + \frac{1}{4}y_t^4/\sqrt{n}$, with $y_t \sim \mathcal{N}(0,1)$. Since the parametric bootstrap is employed, the empirical rejection rate under the null is almost identical to the nominal level of significance. So we do not examine the empirical rejection rates under the null. Third, for the Pareto distribution, the hypothesized characteristic function involves an incomplete gamma function with imaginary argument, making computation of ACS-test inconvenient. Transformation by a log transform leads to an exponential distribution under the null. Then, testing the exponential distribution hypothesis for log-transformed data becomes equivalent to testing the Pareto distribution hypothesis for the original data.

Distribution	Test	Level \ n	50	100	200	300	400	500	1000
Exponential	U_n	1%	0.59	1.86	4.44	7.53	12.30	16.42	39.23
		5%	1.61	4.65	10.93	17.62	24.90	31.88	59.70
		10%	3.33	7.71	16.82	25.33	33.88	41.61	70.51
	ACS	1%	0.04	0.09	0.13	0.20	0.23	0.19	0.30
		5%	0.83	1.07	1.34	1.34	1.62	1.64	1.84
		10%	2.01	2.41	3.20	3.27	3.48	3.80	4.12
Normal	U_n	1%	1.63	2.96	4.90	5.81	5.50	6.05	4.11
		5%	4.15	7.83	12.06	13.41	13.84	14.53	11.91
		10%	6.96	12.23	18.25	20.17	21.02	22.02	18.69
	ACS	1%	2.83	2.52	1.99	1.97	1.99	1.79	1.79
		5%	9.74	9.01	8.29	7.97	8.05	7.44	6.92
		10%	15.39	15.04	13.81	14.08	13.72	12.93	12.18

Table A.7: EMPIRICAL REJECTION RATES OF THE U- AND ACS-TESTS UNDER THE LOCAL ALTERNATIVE (IN PERCENT). This table shows the empirical rejection rates of the U- and ACS-tests for the exponential case, $x_{t,n} := y_t + \frac{1}{2}\sqrt{z_t/n}$, with $y_t \sim \text{Exp}(1)$ and $z_t \sim \mathcal{U}[0.5, 1.5]$; and for the normal case, $x_{t,n} := y_t + \frac{1}{4}y_t^4/\sqrt{n}$, with $y_t \sim \mathcal{N}(0,1)$. The empirical rejection rates were obtained by 10,000 independent experiments.

Hence, we report the empirical rejection rates of the U- and ACS-tests only for the exponential and normal distribution cases under the local alternatives. The empirical rejection rates are given in Table A.7. Here, the empirical rejection rates of the U-test in Table A.7 are those of Table 2 because the local alternative DGP conditions for the exponential and normal distribution cases are the same as those assumed for Table 2.

The simulation results in Table A.7 are summarized as follows. In comparisions, the U-test is more powerful than the ACS-test for both the exponential and normal distribution cases. The empirical rejection rates of the ACS-test are generally lower than those of the U-test, which has respectable local power for the U-test particularly for $n \geq 100$. We observe, in addition, that applying the U-test is more convenient than the ACS-test because the parametric bootstrap computations can time-consuming.

A.4.4 Monte Carlo Simulation Using Example 2: Regression Using Integrated Series

This section provides simulation evidence for BM-GMM using the second example and the simulations parallel those in Section 4. The following simple DGP is employed: $y_t = x_t\beta_* + u_t$ with $\beta_* = 1$ such that $(\Delta x_t, \Delta u_t)'$ IID$\sim \mathcal{N}(0, I_2)$ and $(x_0, u_0) = 0$ without loss of generality. We estimate the unknown parameter β_* consistently by BM-GMM. The current DGP condition implies that $\Omega_x = 1$ and $\widetilde{A}_n \to 1$. Further, from the IID condition, $\Gamma_1(\cdot) \equiv 1$ and $\Gamma_2(\cdot,\cdot) \equiv 0$, so that $D_n \overset{\text{A}}{\sim} \mathcal{N}(0,1)$. Combining these results, it follows that $\sqrt{n}(\widehat{\beta}_n - \beta_*) \overset{\text{A}}{\sim} \mathcal{N}(0,1)$. We further note that the DGP implies that $q_u = 1$ and $v^2 = 2$ using the fact that $\Psi_1(\cdot) \equiv 2$ and $\Psi_2(\cdot,\cdot) \equiv 0$. Therefore, $U_n \overset{\text{A}}{\sim} \mathcal{N}(0,1)$ under $\mathcal{H}_0 : \mathbb{E}[y_t - \beta_* x_t] = 0$ for all $t = 1, 2, \ldots, n$.

Statistics	Percentile \ n	50	100	200	300	400	500	1,000
$\sqrt{n}(\widehat{\beta}_n - \beta_*)$	1%	1.31	0.92	1.03	1.09	0.93	1.00	0.93
	5%	5.57	4.97	4.82	5.01	5.03	4.98	5.00
	95%	94.76	94.90	95.44	94.97	94.82	94.83	94.70
	99%	98.91	98.93	98.92	99.03	98.82	99.01	98.74
U_n	1%	1.55	1.32	1.27	1.06	1.03	1.42	1.13
	5%	4.96	4.50	4.99	5.08	4.94	5.39	4.73
	10%	9.03	8.54	9.27	9.58	9.29	9.65	9.53

Table A.8: EMPIRICAL DISTRIBUTIONS OF THE BM-GMM ESTIMATOR AND EMPIRICAL REJECTION RATES OF THE U-TEST UNDER THE NULL (IN PERCENT). This table shows the empirical distributions of the BM-GMM estimator $\widehat{\beta}_n$ and the empirical rejection rates of the U-test under the null hypothesis. The empirical percentiles are obtained by conducting 10,000 independent experiments.

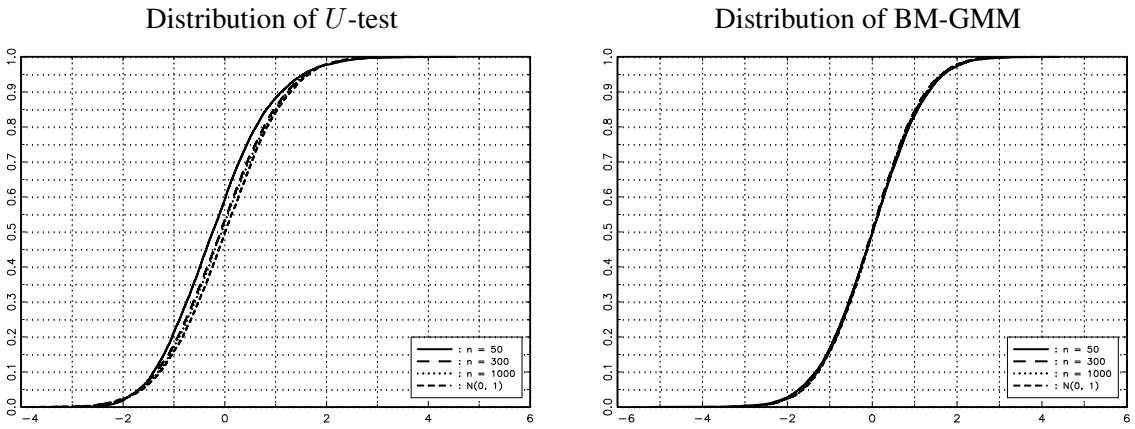

Figure A.3: EMPIRICAL DISTRIBUTIONS OF U-TEST UNDER THE NULL AND BM-GMM ESTIMATOR. The figures show the empirical distributions of the BM-GMM estimator and U-test for $n = 50$, 300, 1,000, and the standard normal distribution.

For $n \in \{50, 100, 200, 300, 400, 500, 1,000\}$, 10,000 replications were conducted and the simulation results are in Table A.8. The first panel reports the empirical distribution of $\sqrt{n}(\widehat{\beta}_n - \beta_*)$. For a given percentile, we select the quantile level from the standard normal distribution and report the empirical percentage for the quantities to be less than the quantile. Evidently, the standard normal distribution approximates the empirical distributions well. Even when the sample size is as small as 50, the results are close to the standard normal distribution. The right panel in Figure A.3 shows the empirical distributions of the BM-GMM estimator for n =50, 300, and 1,000 in addition to the standard normal distribution. From the same figure the empirical distributions are evidently close to the standard normal, corroborating the theory in Section 3.

The second panel in Table A.8 reports empirical rejection rates of the U-tests under the null. Compared to the first panel in Table A.8, larger sample sizes are required to approximate the null limit distribution, but the empirical rejection rates are well approximated by the null limit distribution at small significance levels. The left panel in Figure A.3 further shows the empirical null distributions of the U-tests for $n = 50$, 300,

and 1,000, which again corroborate the limit theory of the U-statistic test.

A.5 Proofs of the Main Claims

In this section we prove the main claims in the paper. To begin we give the functional forms of $\widetilde{\xi}_n(\cdot,\circ)$ and $\ddot{\xi}_n(\cdot,\circ)$. First, if n is finite, it is not difficult to find $\widetilde{\Sigma}_n^{-1}$ and obtain the following inverse kernel function

$$\widetilde{\xi}_n(\cdot,\circ) = n^3\left\{2\widetilde{\mathbb{I}}_n(\cdot,\circ) - \widetilde{\mathbb{J}}_n(\cdot,\circ) - \widetilde{\mathbb{J}}_n(\circ,\cdot)\right\},$$

where

$$\widetilde{\mathbb{I}}_n(\cdot,\circ) := \mathbb{I}\left[(\cdot,\circ) \in \bigcup_{i=1}^{s_n}\left[\frac{i-1}{n}, i_n\right) \times \left[\frac{i-1}{n}, i_n\right)\right] \quad \text{and}$$

$$\widetilde{\mathbb{J}}_n(\cdot,\circ) := \mathbb{I}\left[(\cdot,\circ) \in \bigcup_{i=1}^{s_n}\left[i_n, \frac{i+1}{n}\right) \times \left[\frac{i-1}{n}, i_n\right)\right].$$

Note that $\widetilde{\xi}_n(\cdot,\circ)$ is not uniformly bounded with respect to n. Next, it follows from $\ddot{\Sigma}_n^{-1}$ that

$$\ddot{\xi}_n(\cdot,\circ) = n^3\left\{\ddot{\mathbb{I}}_n(\cdot,\circ) - \ddot{\mathbb{J}}_n(\cdot,\circ) - \ddot{\mathbb{J}}_n(\circ,\cdot)\right\},$$

where

$$\ddot{\mathbb{I}}_n(\cdot,\circ) := 2\mathbb{I}\left[(\cdot,\circ) \in \bigcup_{i=1}^{s_n-1}\left[\frac{i-1}{n}, i_n\right) \times \left[\frac{i-1}{n}, i_n\right)\right] + \mathbb{I}\left[(\cdot,\circ) \in \left[\frac{n-1}{n}, 1\right] \times \left[\frac{n-1}{n}, 1\right]\right] \quad \text{and}$$

$$\ddot{\mathbb{J}}_n(\cdot,\circ) := \mathbb{I}\left[(\cdot,\circ) \in \bigcup_{i=1}^{s_n-2}\left[i_n, \frac{i+1}{n}\right) \times \left[\frac{i-1}{n}, i_n\right)\right] + \mathbb{I}\left[(\cdot,\circ) \in \left[\frac{n-1}{n}, 1\right] \times \left[\frac{n-2}{n}, \frac{n-1}{n}\right)\right].$$

The structure of $\ddot{\xi}(\cdot,\circ)$ is similar to $\widehat{\xi}_n(\cdot,\circ)$ and it too is not bounded, although $\ddot{\mathbb{I}}(\cdot,\circ)$ is not exactly the same as $\widetilde{\mathbb{I}}(\cdot,\circ)$. Mainly, the coefficient of the final diagonal block $\left[\frac{n-1}{n}, 1\right] \times \left[\frac{n-1}{n}, 1\right]$ differs from 1, and the functional values of $\ddot{\xi}_n(1,\circ)$ and $\ddot{\xi}_n(\cdot,1)$ are defined by noting that $s_n = n$. So it follows that

$$\begin{aligned}\ddot{\xi}_n(\cdot,\circ) = \widetilde{\xi}_n(\cdot,\circ) &+ n^3\mathbb{I}\left[(\cdot,\circ) \in \left[\frac{n-1}{n}, 1\right] \times \left[\frac{n-1}{n}, 1\right]\right] \\ &- n^3\mathbb{I}\left[(\cdot,\circ) \in \left[\frac{n-1}{n}, 1\right] \times \left[\frac{n-2}{n}, \frac{n-1}{n}\right)\right] - n^3\mathbb{I}\left[(\circ,\cdot) \in \left[\frac{n-1}{n}, 1\right] \times \left[\frac{n-2}{n}, \frac{n-1}{n}\right)\right].\end{aligned}$$

Next, it is convenient in these proofs to use some basic properties of generalized functions, particularly the Dirac delta function $\delta(x)$ and its derivatives that play certain critical roles in the proofs. Note in particular the following useful properties for functionals involving the delta function.[1]

[1] Readers are referred to Lighthill (1959) and Phillips (1991) for further details.

For a function $f : [0,1] \mapsto \mathbb{R}$ in $\mathcal{C}^{(2)}([0,1])$,

$$\int_0^1 \frac{\delta(x - \cdot - n^{-1}) - \delta(x - \cdot)}{n^{-1}} f(x)dx \to \int_0^1 -\delta'(x - \cdot)f(x)dx = f'(\cdot) \tag{A.17}$$

uniformly on $[0,1]$. Defining $\delta_n(u - v) := n\widetilde{\mathbb{I}}_n(u,v)$, it follows that $\delta_n(x) = n\mathbb{I}_n[x \in [0, \frac{1}{n})]$, whose limit is $\delta(x)$ as n tends to infinity. Further note that $\delta_n(u - \frac{1}{n} - v) = n\widetilde{\mathbb{I}}_n(u - \frac{1}{n}, v) = n\widetilde{\mathbb{J}}_n(u,v)$ since $\widetilde{\mathbb{I}}_n(\cdot - \frac{1}{n}, \circ) = \widetilde{\mathbb{J}}_n(\cdot, \circ)$, so the first-order derivative of the Dirac delta generalized function is obtained as

$$\delta'_n(u - v) := \frac{\delta_n\left(u - v - \frac{1}{n}\right) - \delta_n(u - v)}{-n^{-1}} = n^2\{\widetilde{\mathbb{I}}_n(u,v) - \widetilde{\mathbb{J}}_n(u,v)\} \to \delta'(u - v), \tag{A.18}$$

and if $f_n(\cdot)$ uniformly converges to $f(\cdot)$, it follows that

$$\int_0^1 -\delta'_n(x - \cdot)f_n(x)dx \to \int_0^1 -\delta'(x - \cdot)f(x)dx = f'(\cdot).$$

Also, the first derivative of the Dirac delta generalized function satisfies the property

$$-\delta'(u) = \delta'(-u). \tag{A.19}$$

The second derivative of the Dirac delta generalized function is obtained similar to the first derivative, viz.,

$$\begin{aligned}\delta''_n(u - v) &:= \frac{\delta'_n\left(u - v + \frac{1}{n}\right) - \delta'_n(u - v)}{n^{-1}} \\ &= \frac{n^2\{[\widetilde{\mathbb{J}}_n(u,v) - \widetilde{\mathbb{I}}_n(u,v)] - [\widetilde{\mathbb{I}}_n(v,u) - \widetilde{\mathbb{J}}_n(v,u)]\}}{n^{-1}} \to \delta''(u - v).\end{aligned} \tag{A.20}$$

Proof of Lemma 1: (i) We prove each statement in turn.

(i.a) First note that for any $n > 2$,

$$\widetilde{\Sigma}_n^{-1} = n \begin{bmatrix} 2 & -1 & \cdots & 0 & 0 \\ -1 & 2 & \cdots & 0 & 0 \\ \vdots & \vdots & \ddots & \vdots & \vdots \\ 0 & 0 & \cdots & 2 & -1 \\ 0 & 0 & \cdots & -1 & 2 \end{bmatrix},$$

so that if $\Omega_n := -\Omega_{1n} + \Omega_{2n}$ with

$$\Omega_{1n} = \begin{bmatrix} 1 & 0 & \cdots & 0 \\ 0 & 1 & \cdots & 0 \\ \vdots & \vdots & \ddots & \vdots \\ 0 & 0 & \cdots & 1 \end{bmatrix}, \quad \text{and} \quad \Omega_{2n} = \begin{bmatrix} 0 & 1 & \cdots & 0 \\ \vdots & \vdots & \ddots & \vdots \\ 0 & 0 & \cdots & 1 \\ 0 & 0 & \cdots & 0 \end{bmatrix},$$

it follows that $\widetilde{\Sigma}_n^{-1} = -n\Omega_n - n\Omega_n'$. Now let $B_n := [b_n(\frac{1}{n}), b_n(\frac{2}{n}), \ldots, b_n(\frac{n-1}{n})]'$, so that the first-row and final-row elements of B_n converge to zero since $b(0) = b(1) = 0$ by assumption. Recall that $b_n(\cdot) := b(\lfloor n(\cdot) \rfloor / n)$ with $b(\cdot)$ being continuous on $[0, 1]$. Therefore, for $j = 0, 1, \ldots, (n-1)$, $b_n(\frac{j}{n}) = b_n(\frac{j+s}{n})$ as long as $s \in [0, \frac{1}{n})$, so that if we let $b_n(\cdot)$ be a càdlàg function defined on $[0, 1]$, then $B_n \cup \{b_n(1) = 0\}$ becomes the range of $b_n(\cdot)$. In parallel, using the fact that $b_n(1) = 0$,

$$n\Omega_n B_n = \frac{(\Omega_{2n} - \Omega_{1n})}{n^{-1}} B_n = \frac{1}{n^{-1}} \begin{bmatrix} b_n(\frac{2}{n}) - b_n(\frac{1}{n}) \\ \vdots \\ b_n(1) - b_n(\frac{n-1}{n}) \end{bmatrix}$$

becomes the range of the mapping $\frac{1}{n^{-1}}(b_n((\cdot) + \frac{1}{n}) - b_n(\cdot))$ defined on $[0, 1)$. We further note that for each $r \in [0, 1)$,

$$\frac{1}{n^{-1}} \left\{ b_n \left(r + \frac{1}{n} \right) - b_n(r) \right\} = \frac{1}{n^{-1}} \left\{ b \left(\frac{\lfloor nr + 1 \rfloor}{n} \right) - b \left(\frac{\lfloor nr \rfloor}{n} \right) \right\} \to b'(r).$$

Therefore, the range of $b'(\cdot)$ becomes the limit of $n\Omega_n B_n$:

$$n\Omega_n B_n \to [b'(r) : r \in [0, 1)]. \tag{A.21}$$

Note that this result can be associated with the Dirac delta function as follows

$$\Omega_{2n} B_n = \begin{bmatrix} b_n(\frac{2}{n}) \\ \vdots \\ b_n(1) \end{bmatrix} = \begin{bmatrix} \sum_{i=1}^{n-1} b_n(i_n) \widetilde{\mathbb{J}}_n(i_n, \frac{1}{n}) \\ \vdots \\ \sum_{i=1}^{n-1} b_n(i_n) \widetilde{\mathbb{J}}_n(i_n, \frac{n-1}{n}) \end{bmatrix} = \begin{bmatrix} n \int_0^1 b_n(u) \widetilde{\mathbb{J}}_n(u, \frac{1}{n}) du \\ \vdots \\ n \int_0^1 b_n(u) \widetilde{\mathbb{J}}_n(u, \frac{n-1}{n}) du \end{bmatrix}$$

and

$$\Omega_{1n} B_n = \begin{bmatrix} b_n(\frac{1}{n}) \\ \vdots \\ b_n(\frac{n-1}{n}) \end{bmatrix} = \begin{bmatrix} \sum_{i=1}^{n-1} b_n(i_n) \widetilde{\mathbb{I}}_n(i_n, \frac{1}{n}) \\ \vdots \\ \sum_{i=1}^{n-1} b_n(i_n) \widetilde{\mathbb{I}}_n(i_n, \frac{n-1}{n}) \end{bmatrix} = \begin{bmatrix} n \int_0^1 b_n(u) \widetilde{\mathbb{I}}_n(u, \frac{1}{n}) du \\ \vdots \\ n \int_0^1 b_n(u) \widetilde{\mathbb{I}}_n(u, \frac{n-1}{n}) du \end{bmatrix}.$$

Therefore, if we let $\delta_n'(u-v) := n^2\{\widetilde{\mathbb{I}}_n(u,v) - \widetilde{\mathbb{J}}_n(u,v)\}$, it follows that

$$n\Omega_n B_n = n(\Omega_{2n} - \Omega_{1n})B_n = \begin{bmatrix} n^2 \int_0^1 b_n(u)\{\widetilde{\mathbb{J}}_n(u, \frac{1}{n}) - \widetilde{\mathbb{I}}_n(u, \frac{1}{n})\}du \\ \vdots \\ n^2 \int_0^1 b_n(u)\{\widetilde{\mathbb{J}}_n(u, \frac{n-1}{n}) - \widetilde{\mathbb{I}}_n(u, \frac{n-1}{n})\}du \end{bmatrix}$$
$$= \begin{bmatrix} -\int_0^1 b_n(u)\delta_n'(u - \frac{1}{n})du \\ \vdots \\ -\int_0^1 b_n(u)\delta_n'(u - \frac{n-1}{n})du \end{bmatrix}.$$

by applying (A.17) and (A.18). Here, we done that for $j = 0, 1, \ldots, (n-1)$, $\delta_n'(u - \frac{j}{n}) = \delta_n'(u - \frac{\lfloor j+s \rfloor}{n})$ as long as $s \in [0, \frac{1}{n})$. Therefore, the right side becomes the range of the mapping $-\int_0^1 b_n(u)\delta_n'(u - \frac{\lfloor n(\cdot) \rfloor}{n})du$ defined on $[0,1)$. Furthermore, for each $r \in [0,1)$,

$$-\int_0^1 b_n(u)\delta_n'\left(u - \frac{\lfloor nr \rfloor}{n}\right)du = -\int_0^1 b\left(\frac{\lfloor un \rfloor}{n}\right)\delta_n'\left(u - \frac{\lfloor nr \rfloor}{n}\right)du \to -\int_0^1 b(u)\delta'(u-r)du = b'(r),$$

where the limit convergence is achieved by (A.18) and the fact that $b_n(\cdot)$ converges to $b(\cdot)$ uniformly on $[0,1]$. Further, the last equality holds by (A.17). Therefore, the limit of $n\Omega_n B_n$ becomes the range of $b'(\cdot)$, implying (A.21).

In a similar manner, we obtain

$$n\Omega_n' B_n = \frac{(\Omega_{2n}' - \Omega_{1n})}{n^{-1}} B_n = \frac{1}{n^{-1}} \begin{bmatrix} b_n(0) - b_n(\frac{1}{n}) \\ \vdots \\ b_n(\frac{n-2}{n}) - b_n(\frac{n-1}{n}) \end{bmatrix} \to [-b'(r) : r \in [0,1)]. \tag{A.22}$$

We here use the fact that $b_n(0) = 0$.

As before, (A.22) can be associated with the Dirac delta generalized function, viz.,

$$\Omega_{2n}' B_n = \begin{bmatrix} 0 \\ \vdots \\ b_n(\frac{n-2}{n}) \end{bmatrix} = \begin{bmatrix} \sum_{i=1}^{n-1} b_n(i_n)\widetilde{\mathbb{J}}_n(\frac{1}{n}, i_n) \\ \vdots \\ \sum_{i=1}^{n-1} b_n(i_n)\widetilde{\mathbb{J}}_n(\frac{n-1}{n}, i_n) \end{bmatrix} = \begin{bmatrix} n\int_0^1 b_n(u)\widetilde{\mathbb{J}}_n(\frac{1}{n}, u)du \\ \vdots \\ n\int_0^1 b_n(u)\widetilde{\mathbb{J}}_n(\frac{n-1}{n}, u)du \end{bmatrix},$$

$$\Omega_{1n} B_n = \begin{bmatrix} b_n(\frac{1}{n}) \\ \vdots \\ b_n(\frac{n-1}{n}) \end{bmatrix} = \begin{bmatrix} \sum_{i=1}^{n-1} b_n(i_n)\widetilde{\mathbb{I}}_n(\frac{1}{n}, i_n) \\ \vdots \\ \sum_{i=1}^{n-1} b_n(i_n)\widetilde{\mathbb{I}}_n(\frac{n-1}{n}, i_n) \end{bmatrix} = \begin{bmatrix} n\int_0^1 b_n(u)\widetilde{\mathbb{I}}_n(\frac{1}{n}, u)du \\ \vdots \\ n\int_0^1 b_n(u)\widetilde{\mathbb{I}}_n(\frac{n-1}{n}, u)du \end{bmatrix},$$

and

$$n\Omega_n' B_n = n(\Omega_{2n}' - \Omega_{1n})B_n = \begin{bmatrix} n^2 \int_0^1 b_n(u)\{\widetilde{\mathbb{J}}_n(\frac{1}{n}, u) - \widetilde{\mathbb{I}}_n(\frac{1}{n}, u)\}du \\ \vdots \\ n^2 \int_0^1 b_n(u)\{\widetilde{\mathbb{J}}_n(\frac{n-1}{n}, u) - \widetilde{\mathbb{I}}_n(\frac{n-1}{n}, u)\}du \end{bmatrix}$$
$$= \begin{bmatrix} -\int_0^1 b_n(u)\delta_n'(\frac{1}{n} - u)du \\ \vdots \\ -\int_0^1 b_n(u)\delta_n'(\frac{n-1}{n} - u)du \end{bmatrix}.$$

Therefore, the right side becomes the range of the mapping $-\int_0^1 b_n(u)\delta_n'(\frac{\lfloor n(\cdot)\rfloor}{n} - u)du$ defined on $[0, 1)$. Furthermore, for each $r \in [0, 1)$,

$$-\int_0^1 b_n(u)\delta_n'\left(\frac{\lfloor nr\rfloor}{n} - u\right)du = -\int_0^1 b\left(\frac{\lfloor un\rfloor}{n}\right)\delta_n'\left(\frac{\lfloor nr\rfloor}{n} - u\right)du \to -\int_0^1 b(u)\delta'(r-u)du$$

by applying (A.18) and the fact that $b_n(\cdot)$ converges to $b(\cdot)$ uniformly on $[0, 1]$. Furthermore, (A.19) implies that $-\int_0^1 b(u)\delta'(r-u)du = \int_0^1 b(u)\delta'(u-r)du = -b'(r)$, where the last equality follows from (A.17). Therefore, the limit of $n\Omega_n' B_n$ becomes the range of $-b'(\cdot)$, implying (A.22).

Before stating the limit of $n\widetilde{\Sigma}_n^{-1}B_n$, we note that

$$\begin{aligned}\delta_n'(j_n - u) &= n^2\left\{\widetilde{\mathbb{I}}_n(j_n, u) - \widetilde{\mathbb{J}}_n(j_n, u)\right\} \\ &= -n^2\left\{\widetilde{\mathbb{J}}_n\left(u, \frac{j-1}{n}\right) - \widetilde{\mathbb{I}}_n\left(u, \frac{j-1}{n}\right)\right\} = -\delta_n'\left(u - \frac{j-1}{n}\right)\end{aligned} \tag{A.23}$$

using the definition of $\widetilde{\mathbb{I}}_n(\cdot, \circ)$ and $\widetilde{\mathbb{J}}_n(\cdot, \circ)$.

We now combine the two results in (A.21) and (A.22) to obtain the the limit of $n\widetilde{\Sigma}_n^{-1}B_n$, leading to

$$n\widetilde{\Sigma}_n^{-1}B_n = -n^2(\Omega_n + \Omega_n')B_n = -\frac{1}{n^{-2}}\begin{bmatrix} \vdots \\ b_n(\frac{j+1}{n}) - 2b_n(j_n) + b_n(\frac{j-1}{n}) \\ \vdots \end{bmatrix},$$

and the right side is the range of the mapping $b_n((\cdot) + \frac{1}{n}) - 2b_n(\cdot) + b_n((\cdot) - \frac{1}{n})$ defined on $[0, 1)$. We further note that for each $r \in [0, 1)$,

$$\begin{aligned}&\frac{1}{n^{-2}}\left[b_n\left(r + \frac{1}{n}\right) - 2b_n(r) + b_n\left(r - \frac{1}{n}\right)\right] \\ &\quad = \frac{1}{n^{-1}}\left[\frac{1}{n^{-1}}\left\{b_n\left(r + \frac{1}{n}\right) - b_n(r)\right\} - \frac{1}{n^{-1}}\left\{b_n(r) - b_n\left(r - 1n\right)\right\}\right] \to b''(r).\end{aligned}$$

Therefore, the limit of $n\widetilde{\Sigma}_n^{-1}B_n$ is the range of $-b''(\cdot)$. That is, $n\widetilde{\Sigma}_n^{-1}B_n \to [-b''(r) : r \in [0,1)]$.

This result can also be related to the Dirac delta generalized function as follows:

$$-n^2(\Omega_n + \Omega_n')B_n = -\frac{1}{n^{-1}}\begin{bmatrix} \vdots \\ n^2\int_0^1 b_n(u)\{[\widetilde{\mathbb{J}}_n(u,j_n) - \widetilde{\mathbb{I}}_n(u,j_n)] - [\widetilde{\mathbb{I}}_n(j_n,u) - \widetilde{\mathbb{J}}_n(j_n,u)]\}du \\ \vdots \end{bmatrix}$$

$$= -\frac{1}{n^{-1}}\begin{bmatrix} \vdots \\ \int_0^1 b_n(u)\{-\delta_n'(u-j_n) + \delta_n'(u-\frac{j-1}{n})\}du \\ \vdots \end{bmatrix} = -\begin{bmatrix} \vdots \\ \int_0^1 b_n(u)\delta_n''(u-j_n)du \\ \vdots \end{bmatrix},$$

where the second equality holds by (A.23), and the third equality holds by noting that $\frac{1}{n^{-1}}[-\delta_n'(u-j_n) + \delta_n'(u-\frac{j-1}{n})] = \frac{1}{n^{-1}}[\delta_n'(u-j_n+\frac{1}{n}) - \delta_n'(u-j_n)] = \delta_n''(u-j_n)$ using (A.20). From this, we can see that the right side is the range of the mapping $-\int_0^1 b_n(u)\delta_n''(u-(\cdot))du$ defied on $[0,1)$, and for each $r \in [0,1)$,

$$-\int_0^1 b_n(u)\delta_n''(u-r)du = -\int_0^1 b\left(\frac{\lfloor nu \rfloor}{n}\right)\delta_n''(u-r)du \to -\int_0^1 b(u)\delta''(u-r)du = -b''(r),$$

implying that the limit of $n\widetilde{\Sigma}_n^{-1}B_n = -n^2(\Omega_n + \Omega_n')B_n$ is the range of $-b''(\cdot)$.

Furthermore we can see that $n^3\{[\widetilde{\mathbb{J}}_n(u,j_n) - \widetilde{\mathbb{I}}_n(u,j_n)] - [\widetilde{\mathbb{I}}_n(j_n,u) - \widetilde{\mathbb{J}}_n(j_n,u)]\} = -\widetilde{\xi}_n(u,j_n)$ by noting that $\widetilde{\mathbb{I}}_n(u,j_n) = \widetilde{\mathbb{I}}_n(j_n,u)$, so it also follows that

$$\widetilde{\xi}_n(u,j_n) = -\delta_n''(u-j_n), \tag{A.24}$$

implying that

$$n\widetilde{\Sigma}_n^{-1}B_n = \widetilde{\mathbf{\Xi}}_n b_n(\cdot) = [-b''(r) : r \in [0,1)] + o(1). \tag{A.25}$$

(i.b) Next note that if we let $C_n := [c_n(\frac{1}{n}), c_n(\frac{2}{n}), \ldots, c_n(\frac{n-1}{n})]'$,

$$C_n'\widetilde{\Sigma}_n^{-1}B_n = \frac{1}{n}C_n' n\widetilde{\Sigma}_n^{-1}B_n = \frac{1}{n}\sum_{j=1}^{n-1} c_n(j_n)\int_0^1 \widetilde{\xi}_n(j_n,u)\, b_n(u)du = \int_0^1\int_0^1 \widetilde{\xi}_n(v,u)\, b_n(u)c_n(v)dudv$$

$$= -\int_0^1\int_0^1 \delta_n''(v,u)\, b_n(u)c_n(v)dudv \to -\int_0^1 c(u)b''(u)du = \int_0^1 c'(u)b'(u)du, \tag{A.26}$$

where the second and fourth equalities follow from (A.24) and (A.25), and the last equality holds since $c(1)b'(1) - c(0)b'(0) = \int_0^1 d\{c(u)b'(u)\} = \int_0^1 c'(u)b'(u)du + \int_0^1 c(u)b''(u)du$. Note that $c(0) = c(1) = 0$, so that the left side is zero, leading to (A.26). Therefore, it follows that

$$(\widetilde{\mathbf{\Xi}}_n b_n(\cdot), c_n(\cdot)) = \int_0^1\int_0^1 \widetilde{\xi}_n(v,u)b_n(u)c_n(v)dudv = \int_0^1 c'(u)b'(u)du + o(1) = (b'(\cdot), c'(\cdot)) + o(1).$$

In addition, note that

$$(b'(\cdot), c'(\cdot)) = \int_0^1 \int_0^1 \delta(u-v) c'(u) b'(v) du dv, \tag{A.27}$$

where the last equality follows from the fact that $\int_0^1 \delta(u_1 - u_2) f'(u_1) du_1 = f'(u_2)$.

(ii) Using the fact that $\widetilde{\Sigma}_n^{-1} = -n\Omega_n - n\Omega_n'$, we obtain

$$\begin{aligned} \frac{1}{n} C_n' \widetilde{\Sigma}_n^{-1} B_n = & - \sum_{i=2}^{n-1} c_n\left(\frac{i-1}{n}\right) \left\{ b_n\left(i_n\right) - b_n\left(\frac{i-1}{n}\right) \right\} \\ & - \sum_{i=2}^{n-1} b_n\left(\frac{i-1}{n}\right) \left\{ c_n\left(i_n\right) + c_n\left(\frac{i-1}{n}\right) \right\} + 2 b_n\left(\frac{n-1}{n}\right) c_n\left(\frac{n-1}{n}\right). \end{aligned} \tag{A.28}$$

Also note that

$$b_n\left(\frac{i-1}{n}\right) = \frac{1}{2}\left(\left\{ b_n\left(i_n\right) + b_n\left(\frac{i-1}{n}\right) \right\} - \left\{ b_n\left(i_n\right) - b_n\left(\frac{i-1}{n}\right) \right\} \right), \tag{A.29}$$

$$c_n\left(\frac{i-1}{n}\right) = \frac{1}{2}\left(\left\{ c_n\left(i_n\right) + c_n\left(\frac{i-1}{n}\right) \right\} - \left\{ c_n\left(i_n\right) - c_n\left(\frac{i-1}{n}\right) \right\} \right), \tag{A.30}$$

so that if we plug these two equations into (A.28), it follows that $\frac{1}{n} C_n' \widetilde{\Sigma}_n^{-1} B_n = b_n(\frac{1}{n}) c_n(\frac{1}{n}) + \sum_{i=2}^{n-1} \{b_n(i_n) - b_n(\frac{i-1}{n})\}\{c_n(i_n) - c_n(\frac{i-1}{n})\} + b_n(\frac{n-1}{n}) c_n(\frac{n-1}{n})$. We here note that $b_n(0) = c_n(0) = b_n(1) = c_n(1) = 0$, so that $b_n(\frac{1}{n}) c_n(\frac{1}{n}) = (b_n(\frac{1}{n}) - b_n(0))(c_n(\frac{1}{n}) - c_n(0))$ and $b_n(\frac{n-1}{n}) c_n(\frac{n-1}{n}) = (b_n(1) - b_n(\frac{n-1}{n}))(c_n(1) - c_n(\frac{n-1}{n}))$. This fact implies

$$\frac{1}{n} C_n' \widetilde{\Sigma}_n^{-1} B_n = \sum_{i=1}^{n} \left\{ b_n\left(i_n\right) - b_n\left(\frac{i-1}{n}\right) \right\} \left\{ c_n\left(i_n\right) - c_n\left(\frac{i-1}{n}\right) \right\} \to \int_0^1 db(u) dc(u), \tag{A.31}$$

which is $(db(\cdot), dc(\cdot))$. Furthermore, (A.26) implies that $n^{-1} C_n' \widetilde{\Sigma}_n^{-1} B_n = n^{-1} (\widetilde{\Xi}_n b_n(\cdot), c_n(\cdot))$. Therefore, $n^{-1}(\widetilde{\Xi}_n b_n(\cdot), c_n(\cdot)) \to (db(\cdot), dc(\cdot))$. ■

Proof of Lemma 2: (i) First note that for $n \geq 2$,

$$\ddot{\Sigma}_n^{-1} = \left[\begin{array}{ccc:c} & & & 0 \\ & \widetilde{\Sigma}_n^{-1} & & \vdots \\ & & & 0 \\ & & & -n \\ \hdashline 0 & \cdots & 0 & -n \quad n \end{array} \right],$$

so that $\ddot{\Sigma}_n^{-1}$ is almost identical to $\widetilde{\Sigma}_n^{-1}$ except that the n-th row and n-th column element of $\ddot{\Sigma}_n^{-1}$ is n,

whereas the $(n-1)$-th row and $(n-1)$-th column element of $\widetilde{\Sigma}_n^{-1}$ is $2n$. Therefore, the limit kernel of $\ddot{\Sigma}_n^{-1}$ can be similarly obtained to that of $\widetilde{\Sigma}_n^{-1}$. We again prove the statements in turn.

(i.a) Let $\ddot{B}_n := [B_n, b_n(1)]'$ and $\ddot{b}_n := [0'_{n-2}, b_n(1)]'$ and note that

$$n\ddot{\Sigma}_n^{-1}\ddot{B}_n = \begin{bmatrix} n\widetilde{\Sigma}_n^{-1}B_n - n^2\ddot{b}_n \\ \hdashline -\frac{1}{n^{-2}}[b_n(\frac{n-1}{n}) - b_n(1)] \end{bmatrix} = \begin{bmatrix} \vdots \\ -\int_0^1 b_n(u)\delta_n''(u-j_n)du \\ \vdots \\ \hdashline -\frac{1}{n^{-2}}[b_n(\frac{n-1}{n}) - b_n(1)] \end{bmatrix}.$$

Here, Lemma 1 (i) shows that $-\int_0^1 b_n(u)\delta_n''(u-j_n)du \to -b''(\cdot)$, and we further note that $-\frac{1}{n^{-2}}\{b_n(\frac{n-1}{n}) - b_n(1)\} \to -b''(1)$ because $b_n(1-\frac{1}{n}) = b_n(1) - b_n'(1)\frac{1}{n} + b_n''(1)\frac{1}{n^2} + o(1)$ such that $b'(1) = 0$ and $b(\cdot) \in \mathcal{C}^{(2)}([0,1])$. Therefore, even the last row element converges to the negative second-order derivative of $b(\cdot)$, and this implies that

$$n\ddot{\Sigma}_n^{-1}\ddot{B}_n \to [-b''(r) : r \in [0,1)]. \tag{A.32}$$

Note further that $\frac{-1}{n^{-2}}[b_n(1-\frac{1}{n}) - b_n(1)] = \frac{-1}{n^{-3}}\int_0^1 b_n(u)\{\ddot{\mathbb{J}}_n(1,u) + \ddot{\mathbb{J}}(u,1) - \ddot{\mathbb{I}}_n(1,u)\}du = \int_0^1 b_n(u)\ddot{\xi}_n(u,1)du$ using the definition of $\ddot{\xi}_n(\cdot,\circ)$. Therefore, it follows that

$$\begin{bmatrix} \vdots \\ -\int_0^1 b_n(u)\delta_n''(u-j_n)du \\ \vdots \\ \hdashline -\frac{1}{n^{-2}}[b_n(\frac{n-1}{n}) - b_n(1)] \end{bmatrix} = \begin{bmatrix} \vdots \\ \int_0^1 b_n(u)\widetilde{\xi}_n(u,j_n)du \\ \vdots \\ \hdashline \int_0^1 b_n(u)\ddot{\xi}_n(u,1)du \end{bmatrix} = \begin{bmatrix} \vdots \\ \int_0^1 b_n(u)\ddot{\xi}_n(u,j_n)du \\ \vdots \end{bmatrix} = \ddot{\mathbf{\Xi}}_n b_n(\cdot), \tag{A.33}$$

where the first equality holds by (A.24), and the second equality holds by the fact that for $j = 1, 2, \ldots, n-1$, $\widetilde{\xi}_n(\cdot, j_n) = \ddot{\xi}_n(\cdot, j_n)$. Combining (A.32) and (A.33), it follows that $n\ddot{\Sigma}_n^{-1}\ddot{B}_n = \ddot{\mathbf{\Xi}}_n b_n(\cdot) \to -b''(\cdot)$.

(i.b) Let $\ddot{C}_n := [C_n, c_n(1)]'$ and obtain

$$\begin{aligned} \ddot{C}_n'\ddot{\Sigma}_n^{-1}\ddot{B}_n &= \frac{1}{n}\ddot{C}_n' n\ddot{\Sigma}_n^{-1}\ddot{B}_n = \frac{1}{n}\sum_{j=1}^{n} c_n(j_n)\int_0^1 \ddot{\xi}_n(j_n,u)\, b_n(u)du \\ &= \int_0^1\int_0^1 \ddot{\xi}_n(v,u)\, b_n(u)c_n(v)dudv = -\int_0^1\int_0^2 \delta_n''(v,u)\, b_n(u)c_n(v)dudv \\ &\to -\int_0^1 c(u)b''(u)du = \int_0^1 c'(u)b'(u)du, \end{aligned} \tag{A.34}$$

where the last equality holds by noting that $c(1)b'(1) - c(0)b'(0) = \int_0^1 d\{c(u)b'(u)\} = \int_0^1 c'(u)b'(u)du + \int_0^1 c(u)b''(u)du$. Note that $c(0) = b'(1) = 0$, so that the left side is zero, leading to (A.34). Therefore, it

follows that $(\ddot{\Xi}_n b_n(\cdot), c_n(\cdot)) = \int_0^1 \int_0^1 \ddot{\xi}_n(v,u) b_n(u) c_n(v) du dv = \int_0^1 c'(u) b'(u) du + o(1) = (b'(\cdot), c'(\cdot)) + o(1)$.

(ii) Note that

$$\frac{1}{n}\ddot{C}_n'\ddot{\Sigma}_n^{-1}\ddot{B}_n = -\sum_{i=2}^{n} c_n\left(\frac{i-1}{n}\right)\left\{b_n\left(i_n\right) - b_n\left(\frac{i-1}{n}\right)\right\} - \sum_{i=2}^{n} b_n\left(\frac{i-1}{n}\right)\left\{c_n\left(i_n\right) + c_n\left(\frac{i-1}{n}\right)\right\} + b_n\left(1\right) c_n\left(1\right). \tag{A.35}$$

Here, we plug (A.29) and (A.30) in (A.35) to obtain $\frac{1}{n}\ddot{C}_n'\ddot{\Sigma}_n^{-1}\ddot{B}_n = b_n(\frac{1}{n})c_n(\frac{1}{n}) + \sum_{i=2}^n \{b_n(i_n) - b_n(\frac{i-1}{n})\}$ $\{c_n(i_n) - c_n(\frac{i-1}{n})\} = \sum_{i=1}^n \{b_n(i_n) - b_n(\frac{i-1}{n})\}\{c_n(i_n) - c_n(\frac{i-1}{n})\}$ by noting that $b_n(0) = c_n(0) = 0$. This fact implies that as n tends to infinity,

$$\frac{1}{n}\ddot{C}_n'\ddot{\Sigma}_n^{-1}\ddot{B}_n = \sum_{i=1}^{n}\left\{b_n\left(i_n\right) - b_n\left(\frac{i-1}{n}\right)\right\}\left\{c_n\left(i_n\right) - c_n\left(\frac{i-1}{n}\right)\right\} \to \int_0^1 (db(u)dc(u)) \tag{A.36}$$

that is identical to $(db(\cdot), dc(\cdot))$. Furthermore, (A.34) implies that $n^{-1}\ddot{C}_n'\ddot{\Sigma}_n^{-1}\ddot{B}_n = n^{-1}(\ddot{\Xi}_n b_n(\cdot), c_n(\cdot))$. Therefore, $n^{-1}(\ddot{\Xi}_n b_n(\cdot), c_n(\cdot)) \to (db(\cdot), dc(\cdot))$. This completes the proof. ■

Proof of Lemma 3: (i) Given the conditions, we use Lemmas 1 and 2 to prove the statements in turn.

(i.a) Using the definition of $q_n(\theta_*)$, note that $q_n(\theta_*) = \widetilde{G}_n(\theta_*)'\widehat{\Sigma}_n^{-1}\widetilde{G}_n(\theta_*) = (\widehat{\Xi}_n\widetilde{g}_n(\cdot), \widetilde{g}_n(\cdot)) \Rightarrow (\Xi\mathcal{G}(\cdot), \mathcal{G}(\cdot))$ by Assumption 2 (i). Further, Lemmas 1 (i and ii) or 2 (i and ii) imply that $(\Xi\mathcal{G}(\cdot), \mathcal{G}(\cdot)) = -(\mathcal{G}''(\cdot), \mathcal{G}(\cdot)) = (\mathcal{G}'(\cdot), \mathcal{G}'(\cdot)) =: \mathcal{Q}_d$. Therefore, $q_n(\theta_*) \Rightarrow \mathcal{Q}_d$.

(i.b) Using the definition of $\bar{A}_n$, note that $\bar{A}_n = \nabla_\theta \bar{G}_n(\theta_*)\widehat{\Sigma}_n^{-1}\nabla_\theta'\bar{G}_n(\theta_*) = [\widehat{\Xi}_n H_n(\cdot), H_n(\cdot)] \to [\Xi H(\cdot), H(\cdot)]$ with prob. converging to 1 by Assumption 3 (i). Further, Lemmas 1 (i and ii) or 2 (i and ii) imply that $[\Xi H(\cdot), H(\cdot)] = -[H''(\cdot), H(\cdot)] = [H'(\cdot), H'(\cdot)]$; and Assumption 3 (i) implies that $n\Delta H_n(\cdot) = C_1(\cdot) + o_{\mathbb{P}}(1)$ and $n\Delta H_n(\cdot) = H'(\cdot) + o_{\mathbb{P}}(1)$. Therefore, $[H'(\cdot), H'(\cdot)] = [C_1(\cdot), C_1(\cdot)] =: A_d$. Hence, $\bar{A}_n \to A_d$.

(i.c) By definition $D_n = \nabla_\theta \bar{G}_n(\theta_*)\widehat{\Sigma}_n^{-1}\widetilde{G}_n(\theta_*) = [H_n(\cdot), \widehat{\Xi}_n\widetilde{g}_n(\cdot)] \Rightarrow [H(\cdot), \Xi\mathcal{G}(\cdot)]$ by Assumptions 2 (i) and 3 (i). Note that Lemmas 1 (i and ii) or 2 (i and ii) imply that $[H(\cdot), \Xi\mathcal{G}(\cdot)] = -[H(\cdot), \mathcal{G}''(\cdot)] = [H'(\cdot), \mathcal{G}'(\cdot)]$; and further $H'(\cdot) = C_1(\cdot)$ by Assumption 3 (i). Therefore, $[H'(\cdot), \mathcal{G}'(\cdot)] = [C_1(\cdot), \mathcal{G}'(\cdot)] =: \mathcal{D}_d$ and so $D_n \Rightarrow \mathcal{D}_d$.

(ii) We prove each statement in turn.

(ii.a) Given the conditions, we apply the proof of Lemma 1 (ii) or 2 (ii). For this, we note that $\frac{1}{n}q_n(\theta_*) = \frac{1}{n}\widetilde{G}_n(\theta_*)'\widehat{\Sigma}_n^{-1}\widetilde{G}_n(\theta_*) = \frac{1}{n}(\widehat{\Xi}_n\widetilde{g}_n(\cdot), \widetilde{g}_n(\cdot)) = \sum_{i=1}^{s_n}(\Delta\widetilde{g}_n(i_n))^2 \Rightarrow \int_0^1 (d\mathcal{G}(u))^2$, where the third equality holds by (A.27) or (A.36), and the weak convergence follows from Assumption 2 (ii). Furthermore, the

same condition implies that $\int_0^1 (d\mathcal{G}(u))^2 = \int_0^1 \sigma^2(u)(d\bar{\mathcal{B}}(u))^2 = (\phi_{11}^2 + \phi_{12}\phi_{12}')\int_0^1 \sigma^2(u)du = (\phi_{11}^2 + \phi_{12}\phi_{12}')(\sigma(\cdot),\sigma(\cdot))$, where the second last equality holds by noting that $\mathcal{G}(\cdot)$ is an Itô process such that $d\bar{\mathcal{B}}(\cdot) = \phi_{11}d\bar{\mathcal{W}}(\cdot) + \phi_{12}d\widetilde{\mathcal{W}}(\cdot)$.

(ii.b) Given the conditions, it follows from (A.27) or (A.36) that $\frac{1}{n}\bar{A}_n = \frac{1}{n}\nabla_\theta \bar{G}_n(\theta_*)\widehat{\Sigma}_n^{-1}\nabla_\theta' \bar{G}_n(\theta_*) = \sum_{i=1}^{s_n}\Delta H_n(i_n)\Delta H_n(i_n)'$. Therefore, if we combine this equation with Assumption 3 (ii), it further follows that $\bar{A}_n = \frac{1}{n}\sum_{i=1}^{s_n} C_1(i_n)C_1(i_n)' + \sum_{i=1}^{s_n} C_2(i_n)\Delta\widetilde{h}_n(i_n)\Delta\widetilde{h}_n(i_n)'C_2(i_n)' + \frac{1}{\sqrt{n}}[\sum_{i=1}^{s_n} C_1(i_n)\Delta\widetilde{h}_n(i_n)'C_2(i_n)' + \sum_{i=1}^{s_n} C_2(i_n)\Delta\widetilde{h}_n(i_n)C_1(i_n)'] + o_{\mathbb{P}}(1)$. Next examine the asymptotic behavior of each element on the right side. First, note that $\frac{1}{n}\sum_{i=1}^{s_n} C_1(i_n)C_1(i_n)' \to \int_0^1 C_1(u)C_1(u)'du = [C_1(\cdot), C_1(\cdot)]$.

Second, $(d\mathcal{H}(u))(d\mathcal{H}(u))' = \tau(u)d\widetilde{\mathcal{B}}(u)d\widetilde{\mathcal{B}}(u)'\tau(u)' = \tau(u)\Phi_2\Phi_2'\tau(u)'du$, so that $\sum_{i=1}^{s_n} C_2(i_n)\Delta\widetilde{h}_n(i_n)\Delta\widetilde{h}_n(i_n)'C_2(i_n)' = n^{-1}\sum_{i=1}^{s_n} C_2(i_n)\tau(i_n)\Phi_2\Phi_2'\tau(i_n)'C_2(i_n) + o_{\mathbb{P}}(1) \to \int_0^1 C_2(u)\tau(u)\Phi_2\Phi_2'\tau(u)'C_2(u)'du = [C_2(\cdot)\tau(\cdot)\Phi_2, C_2(\cdot)\tau(\cdot)\Phi_2]$.

Finally, we examine the asymptotic behavior of $n^{-1/2}\sum_{i=1}^{s_n} C_2(i_n)\Delta\widetilde{h}_n(i_n)'C_1(i_n)'$. Note that $\Delta\widetilde{h}_n(\cdot)$ can be approximated by $d\mathcal{H}(\cdot)$ if n is sufficiently large, so that it follows that $\frac{1}{\sqrt{n}}\sum_{i=1}^{s_n} C_1(i_n)\Delta\widetilde{h}_n(i_n)'C_2(i_n)' = \frac{1}{\sqrt{n}}\int_0^1 C_1(u)\nu(u)'C_2(u)'du + \frac{1}{\sqrt{n}}\int_0^1 C_1(u)(\tau(u)d\widetilde{\mathcal{B}}(u))'C_2(u)' + o_{\mathbb{P}}(1)$. Note that the first two terms on the right side are $o_{\mathbb{P}}(1)$, implying that $\bar{A}_n = \frac{1}{n}\sum_{i=1}^{s_n} C_1(i_n)C_1(i_n)' + \sum_{i=1}^{s_n} C_2(i_n)\Delta\widetilde{h}_n(i_n)\Delta\widetilde{h}_n(i_n)'C_2(i_n)' + o_{\mathbb{P}}(1) \to [C_1(\cdot), C_1(\cdot)] + [C_2(\cdot)\tau(\cdot)\Phi_2, C_2(\cdot)\tau(\cdot)\Phi_2]$ with prob. converging to 1.

(ii.c) Given the conditions, (A.27) or (A.36) implies that $D_n = n\sum_{i=1}^{s_n}\Delta H_n(i_n)\Delta\widetilde{g}_n(i_n)$, and Assumption 3 implies that $\Delta H_n(\cdot) = n^{-1}C_1(\cdot) + n^{-1/2}C_2(\cdot)\Delta\widetilde{h}_n(\cdot) + n^{-1}C_3(\cdot)(\widetilde{h}_n(\cdot)\odot\Delta\widetilde{h}_n(\cdot)) + o_{\mathbb{P}}(n^{-1})$, so that $D_n - \sqrt{n}\sum_{i=1}^{s_n} C_2(i_n)\Delta\widetilde{h}_n(i_n)\Delta\widetilde{g}_n(i_n) = \sum_{i=1}^{s_n} C_1(i_n)\Delta\widetilde{g}_n(i_n) + \sum_{i=1}^{s_n} C_3(i_n)\{\widetilde{h}_n(i_n)\odot(\Delta\widetilde{h}_n(i_n)\Delta\widetilde{g}_n(i_n))\} + o_{\mathbb{P}}(1) \Rightarrow \int_0^1 C_1(u)d\mathcal{G}(u) + \int_0^1 C_3(u)(\mathcal{H}(u)\odot\tau(u)\Phi_2\phi_1')\sigma(u)du =: \mathcal{D}_u$ by noting that $\widetilde{h}_n(\cdot) \Rightarrow \mathcal{H}(\cdot)$ and $\Delta\widetilde{h}_n(\cdot)\Delta\widetilde{g}_n(\cdot) = n^{-1}\tau(\cdot)\Phi_2\phi_1'\sigma(\cdot) + o_{\mathbb{P}}(1)$. We further note that $\int_0^1 C_1(u)d\mathcal{G}(u) = [C_1(\cdot), d\mathcal{G}(\cdot)]$ and $\int_0^1 C_3(u)(\mathcal{H}(u)\odot\tau(u)\Phi_2\phi_1')\sigma(u)du = [C_3(\cdot)(\mathcal{H}(\cdot)\odot\tau(\cdot)\Phi_2\phi_1'), \sigma(\cdot)]$.

(iii.d) Given Assumption 2 (ii), it follows that $(d\mathcal{G}(u)d\mathcal{H}(u)) = \sigma(u)\tau(u)du\Phi_2\phi_1'$. Approximate $\Delta\widetilde{g}_n(\cdot)$ by $d\mathcal{G}(\cdot)$ and then $\sum_{i=1}^{s_n} C_2(i_n)\Delta\widetilde{g}_n(i_n)\Delta\widetilde{h}_n(i_n) = \int_0^1 \sigma(u)C_2(u)\tau(u)du\Phi_2\phi_1' + o_{\mathbb{P}}(1) = o_{\mathbb{P}}(1)$ from the condition that $\int_0^1 C_2(u)\sigma(u)\tau(u)du\Phi_2\phi_1' = [C_2(\cdot)\tau(\cdot)\Phi_2\phi_1', \sigma(\cdot)] = 0$ with prob. 1, implying that $n^{-1/2}\sum_{i=1}^{s_n} C_2(i_n)\sigma(i_n)\tau(i_n)\Phi_2\phi_1' = o_{\mathbb{P}}(1)$ by applying theorem 1 (c) of Chui (1971). This also implies that $n^{-1/2}\sum_{i=1}^{s_n} C_2(i_n)\mathbb{E}[\sigma(i_n)\tau(i_n)]\Phi_2\phi_1' = o(1)$. Therefore, $\sqrt{n}\sum_{i=1}^{s_n} C_2(i_n)\Delta\widetilde{g}_n(i_n)\Delta\widetilde{h}_n(i_n) = \frac{1}{\sqrt{n}}\sum_{i=1}^{s_n} C_2(i_n)\{n\Delta\widetilde{g}_n(i_n)\Delta\widetilde{h}_n(i_n) - \mathbb{E}[\sigma(i_n)\tau(i_n)]\Phi_2\phi_1'\} + o_{\mathbb{P}}(1)$. We here note that $\{n\Delta\widetilde{g}_n(i_n)\Delta\widetilde{h}_n(i_n)\}$ is a mixingale process of size -1 by Assumption 3 (ii.c) such that $\mathrm{var}[\frac{1}{\sqrt{n}}\sum_{i=1}^{s_n} C_2(i_n)\{n\Delta\widetilde{g}_n(i_n)\Delta\widetilde{h}_n(i_n) - \mathbb{E}[\sigma(i_n)\tau(i_n)]\Phi_2\phi_1'\}] = \frac{1}{n}\sum_{i=1}^{s_n}\Gamma_1(i_n)C_2(i_n)C_2(i_n)' + \frac{1}{n^2}\sum_{i=1}^{s_n}\sum_{j=1_{i\neq j}}^{s_n}\Gamma_2(i_n,j_n)C_2(i_n)C_2(j_n)' + o(1) \to \int_0^1\Gamma_1(u)C_2(u)C_2(u)'du + \int_0^1\int_0^1\Gamma_2(u,v)C_2(u)C_2(v)'dudv =: \Gamma$, which is finite by Assumption 3 (ii.c). Therefore, $\mathrm{var}[\frac{1}{\sqrt{n}}\sum_{i=1}^{s_n} C_2(i_n)\{n\Delta\widetilde{g}_n(i_n)\Delta\widetilde{h}_n(i_n) - \mathbb{E}[\sigma(i_n)\tau(i_n)]\Phi_2\phi_1'\}] \to \Gamma$, and it follows

from the mixingale CLT (e.g., White, 2001, theorem 5.16) that $\frac{1}{\sqrt{n}}\sum_{i=1}^{s_n} C_2(i_n)\{(n\Delta\widetilde{g}_n(i_n))\Delta\widetilde{h}_n(i_n)) - \sigma(i_n)\tau(i_n)\Phi_2\phi_1'\} \Rightarrow \mathcal{Z} \sim \mathcal{N}(0,\Gamma)$ by noting that Γ is positive definite. This implies $\sqrt{n}\sum_{i=1}^{s_n} C_2(i_n)\Delta\widetilde{h}_n(i_n)\Delta\widetilde{g}_n(i_n) \Rightarrow \mathcal{Z}$. Combining this result with (ii.c) gives $D_n = \sqrt{n}\sum_{i=1}^{s_n} C_2(i_n)\Delta\widetilde{h}_n(i_n)\Delta\widetilde{g}_n(i_n) + \sum_{i=1}^{s_n} C_1(i_n)\Delta\widetilde{h}_n(i_n) + \sum_{i=1}^{s_n} C_3(i_n)(\widetilde{h}_n(i_n) \odot \Delta\widetilde{h}_n(i_n))\Delta\widetilde{g}_n(i_n) + o_{\mathbb{P}}(1) \Rightarrow \mathcal{Z} + \mathcal{D}_u =: \mathcal{D}_w$. This completes the proof. ■

Proof of Theorem 1: (i) Given Lemma 3 (i) and the fact that $\sqrt{n}(\widehat{\theta}_n - \theta_*) = -\bar{A}_n^{-1}D_n + o_{\mathbb{P}}(1)$, $\sqrt{n}(\widehat{\theta}_n - \theta_*) \Rightarrow -A_d^{-1}\mathcal{D}_d$.

(ii) Given Lemma 3 (ii.d), the desired results follow from the fact that $\sqrt{n}(\widehat{\theta}_n - \theta_*) = -\bar{A}_n^{-1}D_n + o_{\mathbb{P}}(1) \Rightarrow -A_u^{-1}\mathcal{D}_w$. ■

Proof of Theorem 2: (i) We first apply a second-order Taylor expansion to $q_n(\cdot)$ around θ_* and obtain that

$$J_n := q_n(\widehat{\theta}_n) = q_n(\theta_*) - \sqrt{n}(\widehat{\theta}_n - \theta_*)'(\nabla_\theta \bar{G}_n(\theta_*)\widehat{\Sigma}_n^{-1}\nabla_\theta'\bar{G}_n(\theta_*))\sqrt{n}(\widehat{\theta}_n - \theta_*) + o_{\mathbb{P}}(1). \tag{A.37}$$

It now follows from (1) that $J_n = q_n(\theta_*) - \widetilde{G}_n(\theta_*)'\widehat{\Sigma}_n^{-1}\nabla_\theta'\bar{G}_n(\theta_*)(\nabla_\theta\bar{G}_n(\theta_*)\widehat{\Sigma}_n^{-1}\nabla_\theta'\bar{G}_n(\theta_*))^{-1}\nabla_\theta\bar{G}_n(\theta_*)\widehat{\Sigma}_n^{-1}\widetilde{G}_n(\theta_*) + o_{\mathbb{P}}(1) = q_n(\theta_*) - D_n'\bar{A}_n^{-1}D_n + o_{\mathbb{P}}(1) \Rightarrow \mathcal{Q}_d - \mathcal{D}_d'A_d^{-1}\mathcal{D}_d$ by Lemma 3 (i). We further note that $\mathcal{Q}_d - \mathcal{D}_d'A_d^{-1}\mathcal{D}_d = (\mathbf{\Xi}\mathcal{G}(\cdot),\mathcal{G}(\cdot)) - [\lambda_d(\cdot)',\mathcal{G}(\cdot)]A_d^{-1}[\lambda_d(\cdot),\mathcal{G}(\cdot)] = (\mathbf{\Xi}\mathcal{G}(\cdot),\mathcal{G}(\cdot)) - [\lambda_d(\cdot)'A_d^{-1}[\lambda_d(\circ),\mathcal{G}(\circ)], \mathcal{G}(\cdot)] = (\mathbf{\Xi}\mathcal{G}(\cdot),\mathcal{G}(\cdot)) - ((\lambda_d(\cdot)'A_d^{-1}\lambda_d(\circ),\mathcal{G}(\circ)),\mathcal{G}(\cdot)) = (\mathbf{\Pi}_d\mathcal{G}(\cdot),\mathcal{G}(\cdot)) =: \mathcal{J}_d$, where the last equality holds from the fact that $(\lambda_d(\cdot)'A_d^{-1}\lambda_d(\circ),\mathcal{G}(\circ)) = \lambda_d(\cdot)'A_d^{-1}\int_0^1 \lambda_d(u)\mathcal{G}(u)du = \mathbf{\Lambda}_d\mathcal{G}(\cdot)$, so that $(\mathbf{\Xi}\mathcal{G}(\cdot),\mathcal{G}(\cdot)) - ((\lambda_d(\cdot)'A_d^{-1}\lambda_d(\circ),\mathcal{G}(\circ)),\mathcal{G}(\cdot)) = (\mathbf{\Xi}\mathcal{G}(\cdot),\mathcal{G}(\cdot)) - (\mathbf{\Lambda}_d\mathcal{G}(\cdot),\mathcal{G}(\cdot)) = ((\mathbf{\Xi} - \mathbf{\Lambda}_d)\mathcal{G}(\cdot),\mathcal{G}(\cdot)) = (\mathbf{\Pi}_d\mathcal{G}(\cdot),\mathcal{G}(\cdot))$.

(ii) Given (A.37), it follows that $n^{-1}J_n = n^{-1}q_n(\theta_*) + o_{\mathbb{P}}(1)$. Furthermore, Lemma 3 (ii.a) implies that $n^{-1}q_n(\theta_*) \to q_u := \varphi_q\int_0^1 \sigma^2(u)du$ with prob. converging to 1, which is identical to $\varphi_q\int_0^1 \mathbb{E}[\sigma^2(u)]du$. Now $n^{-1}q_n(\theta_*) = n^{-1}\sum_{i=1}^{s_n}(\sqrt{n}\Delta\widetilde{g}_n(i_n))^2$. It follows that $\sqrt{n}(\frac{1}{n}J_n - q_u) = \frac{1}{\sqrt{n}}\sum_{i=1}^{s_n}[(\sqrt{n}\Delta\widetilde{g}_n(i_n))^2 - \varphi_q\mathbb{E}[\sigma^2(i_n)]] + o_{\mathbb{P}}(1)$ by noting that $\left|\frac{1}{n}\sum_{i=1}^{s_n}\varphi_q\sigma^2(i_n) - q_u\right| = o_{\mathbb{P}}(n^{-1/2})$, which is implied by theorem 1 (c) of Chui (1971). Now $\{(\sqrt{n}\Delta\widetilde{g}_n(i_n))^2 - \varphi_q\mathbb{E}[\sigma^2(i_n)]\}$ is a mixingale of size -1, as assumed by Assumption 2 (ii). Therefore, $\mathrm{var}[\frac{1}{\sqrt{n}}\sum_{i=1}^{s_n}\{(\sqrt{n}\Delta\widetilde{g}_n(i_n))^2 - \varphi_q\mathbb{E}[\sigma^2(i_n)]\}] = \frac{1}{n}\sum_{i=1}^{s_n}\gamma_1(i_n) + \frac{1}{n^2}\sum_{i=1}^{s_n}\sum_{j=1_{i\neq j}}^{s_n}\gamma_2(i_n,j_n) + o_{\mathbb{P}}(1) \to \int_0^1\gamma_1(u)du + \int_0^1\int_0^1\gamma_2(u,v)dudv =: v^2$, which is finite by Assumptions 2 (ii). Therefore, it follows from the mixingale CLT that $\frac{1}{\sqrt{n}}\sum_{i=1}^{s_n}\{(\sqrt{n}\Delta\widetilde{g}_n(i_n))^2 - \varphi_q\mathbb{E}[\sigma^2(i_n)]\} \overset{A}{\sim} \mathcal{N}(0,v^2)$, which also implies that $\sqrt{n}(\frac{1}{n}J_n - q_u) + o_{\mathbb{P}}(1) = \frac{(J_n - nq_u)}{\sqrt{n}} + o_{\mathbb{P}}(1) \overset{A}{\sim} \mathcal{N}(0,v^2)$. From this, we obtain that $U_n \overset{A}{\sim} \mathcal{N}(0,1)$ under $\mathcal{H}_0$, as required. ■

Proof of Theorem 3: (i) We first note that $\bar{q}_n(\theta) = \int_0^1\int_0^1 g_n(u_1,\theta)\widetilde{\xi}_n(u_1,u_2)g_n(u_2,\theta)du_1du_2$. We further

note that $\widehat{d}_n(\cdot,\circ) \to d(\cdot,\circ)$ uniformly on $[0,1]\times\Theta$ by the definition of $\widehat{d}_n(\cdot,\circ)$, so that $g_n(\cdot,\circ) \to g(\cdot,\circ) := (\cdot) - d(\cdot,\circ)$ uniformly on $[0,1]\times\Theta$ such that $g_n(0,\cdot)\equiv 0$ and $g_n(1,\cdot)\equiv 0$ uniformly in n, and $g(0,\cdot)\equiv 0$ and $g(1,\cdot)\equiv 0$. These properties are useful in characterizing the limit properties of infinite dimensional MCMD estimation. Note that Lemma 1 (i) implies that

$$q(\cdot) = -\int_0^1\int_0^1 \delta''(u_1-u_2)g(u_1,\cdot)g(u_2,\cdot)du_1du_2 = \int_0^1\{(\partial/\partial u)g(u,\cdot)\}^2du$$
$$= \int_0^1\{1-(\partial/\partial u)d(u,\cdot)\}^2du = \int_0^1\{(\partial/\partial u)d(u,\cdot)\}^2du - 1,$$

where the last equality holds because $\int_0^1(\partial/\partial u)d(u,\cdot)du = d(1,\cdot)-d(0,\cdot)\equiv 1$. Here, $\int_0^1\{(\partial/\partial u)d(u,\theta)\}^2 du - 1 = \int_0^1\{(\partial/\partial u)u\}^2du - 1 = 0$ if and only if $\theta=\theta_*$. Furthermore, $\int_0^1\{1-(\partial/\partial u)d(u,\cdot)\}^2du$ cannot be less than zero, so that $q(\cdot)$ is minimized at θ_*. From this fact, the GMM estimator must converge to θ_* with prob. converging to 1.

(ii) Lemma 1 (i) implies that

$$\bar{q}_n(\theta_*) = n^{-1}q_n(\theta_*) = \bar{G}_n(\theta_*)'\widehat{\Sigma}_n^{-1}\bar{G}_n(\theta_*) \to \int_0^1\{d\mathcal{B}^0(u)\}^2 = 1 \tag{A.38}$$

with prob. converging to 1, because $\sqrt{n}\bar{G}_n(\theta_*)$ can be translated to $\widetilde{g}_n(\cdot)$ which converges weakly to $\mathcal{B}^o(\cdot)$ so that $\mathcal{B}^0(0)=\mathcal{B}^0(1)=0$ with prob. 1, where the last equality of (A.38) follows from the fact that $d\mathcal{B}^0(u) = -(1-u)^{-1}\mathcal{B}^0(u)du + d\mathcal{W}(u)$, implying that $\mu(\cdot) = -\mathcal{B}^0(\cdot)(1-(\cdot))^{-1}$ and $\sigma(\cdot)\equiv 1$. Therefore, $n^{-1}q_n(\theta_*)\to 1$ with prob. converging to 1.

(iii) We examine the asymptotic distribution of the infinite dimensional MCMD estimator. For finite n, $\sqrt{n}(\widetilde{\theta}_n-\theta_*) = -\bar{A}_n^{-1}D_n + o_{\mathbb{P}}(1)$, and $\bar{A}_n := \nabla_\theta'F_n(\theta_*)\widetilde{\Sigma}_n^{-1}\nabla_\theta F_n(\theta_*) = [\widetilde{\Xi}_nH_n(\cdot),H_n(\cdot)]$ such that the j'-th row and j-th column element of $[\widetilde{\Xi}_nH_n(\cdot),H_n(\cdot)]$ is obtained as $(\widetilde{\Xi}_nH_{n,j'}(\cdot),H_{n,j}(\cdot)) = n\sum_{i=1}^{n-1}\Delta H_{n,j'}(i_n)\Delta H_{n,j}(i_n)$ by applying Lemma 1 (ii), where $H_{n,j}(\cdot)$ denotes the j-th row function of $H_n(\cdot) := \nabla_\theta g_n(\cdot,\theta_*)$. In Section A.1.2, we separately show that $n\sum_{i=1}^{n-1}\Delta H_{n,j'}(i_n)\Delta H_{n,j}(i_n) \to \int_0^1 H_j'(u)H_{j'}'(u)\{\frac{dd(u,\theta_*)}{du}+\sigma^2(u)\}du$ with prob. converging to 1, where $H_j(\cdot)$ and $H_{j'}(\cdot)$ are the j-th row and j'-th row functions of $H(\cdot) := -\nabla_\theta d(\cdot,\theta_*)$, respectively, and $d(\cdot,\theta_*)=(\cdot)$ and $\sigma(\cdot)\equiv 1$, so that it follows that $\frac{dd(\cdot,\theta_*)}{du}+\sigma(\cdot)\equiv 2$, implying that $n\sum_{i=1}^{n-1}\Delta H_{n,j'}(i_n)\Delta H_{n,j}(i_n)\to 2\int_0^1 H_j'(u)H_{j'}'(u)du$ with prob. converging to 1. It therefore follows that

$$\bar{A}_n = [\widehat{\Xi}_nH_n(\cdot),H_n(\cdot)] \to A := 2[H'(\cdot),H'(\cdot)] \tag{A.39}$$

with prob. converging to 1. This limit result can also be related to Lemma 3 (ii.b). In Section A.1.3, we

derive the expansion

$$\sqrt{n}\Delta H_n(\cdot) = n^{-1/2}H'(\cdot) - H'(\cdot)\Delta\widetilde{g}_n(\cdot) - n^{-1/2}H''(\cdot)\widetilde{g}_n(\cdot)\Delta\widetilde{g}_n(\cdot) + o_{\mathbb{P}}(1), \tag{A.40}$$

so that Assumption 3 (ii) holds by letting $C_1(\cdot) = H'(\cdot)$, $C_2(\cdot) = -H'(\cdot)$, $C_3(\cdot) = -H''(\cdot)$, and $\widetilde{h}_n(\cdot) = \widetilde{g}_n(\cdot)$. Lemma 3 (ii.b) now leads to $\bar{A}_n \to [C_1(\cdot), C_1(\cdot)] + [\sigma(\cdot)C_2(\cdot), \sigma(\cdot)C_2(\cdot)] = [H'(\cdot), H'(\cdot)] + [H'(\cdot), H'(\cdot)] = 2[H'(\cdot), H'(\cdot)]$ by noting that $\sigma(\cdot) = \tau(\cdot) \equiv 1$ and $\Phi_{22} = 1$.

Next, we note that $D_n := \nabla'_\theta F_n(\theta_*)\widehat{\Sigma}_n^{-1}\sqrt{n}(\widehat{P}_n - F_n(\theta_*)) = [\widehat{\Xi}_n H_n(\cdot), \widetilde{g}_n(\cdot)]$, and the j-th row element of $[\widehat{\Xi}_n H_n(\cdot), \widetilde{g}_n(\cdot)]$ is obtained as

$$\begin{aligned}(\widehat{\Xi}_n H_{n,j}(\cdot), \widetilde{g}_n(\cdot)) &= n\sum_{i=1}^{n-1} \Delta H_{n,j}(i_n)\,\Delta\widetilde{g}_n(i_n) \\ &= \sum_{i=1}^{n-1} H'_j(i_n)\,\Delta\widetilde{g}_n(i_n) + \sum_{i=1}^{n-1} H''_j(i_n)\,\widetilde{g}_n(i_n)\,(\Delta\widetilde{g}_n(i_n))^2 - \sqrt{n}\sum_{i=1}^{n-1} H'_j(i_n)\,(\Delta\widetilde{g}_n(i_n))^2 + o_{\mathbb{P}}(1)\end{aligned} \tag{A.41}$$

by applying (A.6) and (A.8) in Section A.1.3 and the fact that $\widehat{d}_n(\cdot)$ converges to $(\cdot)$ uniformly on $[0,1]$. Here, we note that

$$\sum_{i=1}^{n-1} H'_j(i_n)\,\Delta\widetilde{g}_n(i_n) \Rightarrow \mathcal{Z}_j^{(1)} := \int_0^1 H'_j(u)d\mathcal{B}^0(u) \sim \mathcal{N}(0, (H_j(\cdot), H_j(\cdot))), \tag{A.42}$$

and

$$\sum_{i=1}^{n-1} H''_j(i_n)\,\widetilde{g}_n(i_n)\,(\Delta\widetilde{g}_n(i_n))^2 \Rightarrow \mathcal{Z}_j^{(2)} := \int_0^1 H''_j(u)\mathcal{B}^0(u)du, \tag{A.43}$$

using the fact that $\widetilde{g}_n(\cdot) \Rightarrow \mathcal{B}^0(\cdot)$ and $\sum_{i=1}^{n-1} H''_j(i_n)\widetilde{g}_n(i_n)(\Delta\widetilde{g}_n(i_n))^2 = n^{-1}\sum_{i=1}^{n-1} H''_j(i_n)\widetilde{g}_n(i_n) + o_{\mathbb{P}}(1)$. We also note that $\int_0^1 H'_j(u)d\mathcal{B}^0(u) + \int_0^1 H''_j(u)\mathcal{B}^0(u)du = 0$ by integration by parts, so that $\mathcal{Z}_j^{(1)} = -\mathcal{Z}_j^{(2)}$, from which it follows that $\mathcal{Z}_j^{(2)} \sim \mathcal{N}(0, (H_j(\cdot), H_j(\cdot)))$ and the sum of the first two terms on the right side of (A.41) is negligible in prob.

In addition, if we apply the dominated convergence theorem to obtain

$$\nabla_\theta \int_0^1 \frac{f(F^{-1}(u,\theta_*),\theta)}{f(F^{-1}(u,\theta_*),\theta_*)}du = \int_0^1 \frac{\nabla_\theta f(F^{-1}(u,\theta_*),\theta)}{f(F^{-1}(u,\theta_*),\theta_*)}du,$$

uniformly in θ, then

$$H'(u) = -\nabla_\theta(\partial/\partial u)F(F^{-1}(u,\theta_*),\theta)|_{\theta=\theta_*} = -\left.\frac{\nabla_\theta f(F^{-1}(u,\theta_*),\theta)}{f(F^{-1}(u,\theta_*),\theta_*)}\right|_{\theta=\theta_*},$$

so that applying the dominated convergence theorem implies that

$$\int_0^1 H'(u)du = -\int_0^1 \left.\frac{\nabla_\theta f(F^{-1}(u,\theta_*),\theta)}{f(F^{-1}(u,\theta_*),\theta_*)}\right|_{\theta=\theta_*} du = -\nabla_\theta \int_0^1 \frac{f(F^{-1}(u,\theta_*),\theta_*)}{f(F^{-1}(u,\theta_*),\theta_*)}du = 0, \tag{A.44}$$

viz., $\int_0^1 H'(u)du = 0$. By this fact, $n^{-1}\sum_{i=1}^{n-1} H'(i_n) \to \int_0^1 H'(u)du = 0$ with prob. converging to 1, so that $\sum_{i=1}^{n-1} H'(i_n) = o(n^{-1})$ by theorem 1 (c) of Chui (1971) under the given conditions for the infinite dimensional MCMD estimator. Further note that $(\Delta\widetilde{g}_n(\cdot))^2 = n(\Delta\widehat{d}_n(\cdot))^2 - 2\Delta\widehat{d}_n(\cdot) + n^{-1}$ and that each $\Delta\widehat{d}_n(i_n)$ is an increment of the order statistics constructed by IID uniform random variables, so that $(\Delta\widehat{d}_n(\frac{1}{n}), \ldots, \Delta\widehat{d}_n(1))'$ follows a Dirichlet distribution with parameter ι_n. Using this condition, Section A.3.2 shows that for each i, $\mathbb{E}[(\Delta\widetilde{g}_n(i_n)^2] = \frac{n-1}{n(n+1)}$. Hence, we can rewrite the third term of (A.41) as

$$\begin{aligned}
&\sqrt{n}\sum_{i=1}^{n-1} H_j'(i_n)\left(\Delta\widetilde{g}_n(i_n)\right)^2 = \sqrt{n}\sum_{i=1}^{n-1} H_j'(i_n)\left\{\left(\Delta\widetilde{g}_n(i_n)\right)^2 - \frac{n-1}{n(n+1)}\right\} + o_{\mathbb{P}}(1) \\
&= \sqrt{n}\sum_{i=1}^{n-1} H_j'(i_n)\left[\left(\sqrt{n}\Delta\widehat{d}_n(i_n)\right)^2 - \frac{2n}{n(n+1)}\right] - 2\sqrt{n}\sum_{i=1}^{n-1} H_j'(i_n)\left(\Delta\widehat{d}_n(i_n) - \frac{1}{n}\right) + o_{\mathbb{P}}(1).
\end{aligned}$$

Here, (A.42) implies that $\sum_{i=1}^{n-1} H_j'(i_n)\sqrt{n}\left(\Delta\widehat{d}_n(i_n) - \frac{1}{n}\right) = -\sum_{i=1}^{n-1} H_j'(i_n)\Delta\widetilde{g}_n(i_n) \Rightarrow \mathcal{Z}_j^{(1)} := -\int_0^1 H_j'(u)d\mathcal{B}^o(u)$, and we already showed that $\mathrm{var}[\sqrt{n}\sum_{i=1}^{n-1} H_j'(i_n)\{(\sqrt{n}\Delta\widehat{d}_n(i_n))^2 - \frac{2n}{n(n+1)}\}] \to 20(H_j'(\cdot), H_j'(\cdot))$ in Section A.3.1. Therefore, if we apply CLT, it follows that

$$\sqrt{n}\sum_{i=1}^{n-1} H_j'(i_n)\left(\Delta\widetilde{g}_n(i_n)\right)^2 \Rightarrow \mathcal{Z}_j^{(3)} - 2\mathcal{Z}_j^{(1)}, \tag{A.45}$$

where $\mathcal{Z}_j^{(3)} \sim \mathcal{N}(0, \upsilon_j^2)$, and $\upsilon_j^2 := 20(H_j'(\cdot), H_j'(\cdot))$. We now plug (A.42), (A.43), (A.45) into (A.41) to deduce that $(\widehat{\Xi}_n H_{n,j}(\cdot), \widetilde{g}_n(\cdot)) \Rightarrow \mathcal{Z}_j^{(3)} - 2\mathcal{Z}_j^{(1)} \sim \mathcal{N}(0, 8(H_j'(\cdot), H_j'(\cdot)))$ by noting that $\mathbb{E}[\mathcal{Z}_j^{(1)}\mathcal{Z}_j^{(3)}] = 4(H_j'(\cdot), H_j'(\cdot))$ as verified in Section A.3.3.

We now extend this result to $[\widehat{\Xi}_n H_n(\cdot), \widetilde{g}_n(\cdot)]$:

$$[\widehat{\Xi}_n H_n(\cdot), \widetilde{g}_n(\cdot)] \Rightarrow \mathcal{D} := -\mathcal{Z}^{(3)} + 2\mathcal{Z}^{(1)} \sim \mathcal{N}(0, 8[H'(\cdot), H'(\cdot)]), \tag{A.46}$$

where $\mathcal{Z}^{(1)}$ and $\mathcal{Z}^{(3)}$ are the weak limits of $\sum H'(i_n)\Delta\widetilde{g}_n(i_n)$ and $\sqrt{n}\sum H'(i_n)\{(\sqrt{n}\Delta\widehat{d}_n(i_n))^2 - \frac{2n}{n(n+1)}\}$, respectively.

The weak limit on the right side can be associated with Lemmas 3 (ii.c and ii.d). Given that $\sigma^2(\cdot) \equiv 1$, $\widetilde{g}_n(\cdot) \Rightarrow \mathcal{B}^0(\cdot)$, and $C_1(\cdot) = H'(\cdot)$, $C_2(\cdot) = -H'(\cdot)$, $C_3(\cdot) = -H''(\cdot)$, and $\widetilde{h}_n(\cdot) = \widetilde{g}_n(\cdot)$ from (A.40), we note that $[\sigma^2(\cdot), C_2(\cdot)] = 0$ by (A.44). Therefore, $[\widehat{\Xi}_n H_n(\cdot), \widetilde{g}_n(\cdot)] \Rightarrow \mathcal{Z} - [H'(\cdot), d\mathcal{B}^0(\cdot)] - [H''(\cdot), \mathcal{B}^0(\cdot)]$ by Lemmas 3 (ii.c and ii.d). Here, $[H'(\cdot), d\mathcal{B}^0(\cdot)] + [H''(\cdot), \mathcal{B}^0(\cdot)] = 0$ by the integration by parts, and this

implies that $\mathcal{Z} = \mathcal{D}$ in (A.46), so that $\Gamma = 8[H'(\cdot), H'(\cdot)]$. This result can be affirmed by deriving that $\Gamma_1(\cdot) \equiv 8$ and $\Gamma_2(\cdot, \circ) \equiv 4$ through some tedious algebra. Using this, $\int_0^1 \int_0^1 \Gamma_2(u,v) C_2(u) C_2(v)' du dv$ of Lemma 3 (ii.d) is identical to $4 \int_0^1 H'(u) du \int_0^1 H'(u)' du = 0$ by (A.44), so that $\Gamma = 8 \int_0^1 H'(u) H'(u)' du$, which is $8[H'(\cdot), H'(\cdot)]$.

Finally, using the findings above the limit distribution of the infinite dimensional MCMD estimator can be obtained as follows:

$$\sqrt{n}(\widetilde{\theta}_n - \theta_*) = -\bar{A}_n^{-1} D_n + o_{\mathbb{P}}(1) \Rightarrow -A^{-1}\mathcal{D} \sim \mathcal{N}(0, 2[H'(\cdot), H'(\cdot)]^{-1}),$$

where we combined (A.39) and (A.46) to obtain the limit.

(iv) We note that $J_n = q_n(\widetilde{\theta}_n) = q_n(\theta_*) - \frac{1}{2} \bar{D}_n' \bar{A}_n^{-1} \bar{D}_n + o_{\mathbb{P}}(1)$ by applying a second-order Taylor expansion, where $\bar{D}_n := \nabla_\theta \bar{G}_n(\theta_*) \widehat{\Sigma}_n^{-1} \bar{G}_n(\theta_*) = O_{\mathbb{P}}(n^{-1/2})$ by (A.46) and $\bar{A}_n = O_{\mathbb{P}}(1)$, so that $J_n = q_n(\theta_*) + O_{\mathbb{P}}(n^{-1})$. Furthermore, note that $q_n(\theta_*) - n = n\{\sum_{i=1}^{n-1} (\Delta \widetilde{g}_n(i_n))^2 - 1\} = n\{n \sum_{i=1}^{n-1} (\Delta \widehat{d}_n(i_n))^2 - 2\} + o_{\mathbb{P}}(n^{-1})$, where the first equality follows from (A.31) in Section A.1, and the second equality holds by the fact that $\widetilde{g}_n(\cdot) := \sqrt{n}((\cdot) - \widehat{d}_n(\cdot))$. Using the distributional condition of the elementary coverage, Section A.3.2 shows that $\mathrm{var}(\sum_{i=1}^{n-1} (\Delta \widetilde{g}_n(i_n))^2 - 1) = 4n^{-1} + o(n^{-1})$, implying that $\sqrt{n}\{\sum_{i=1}^{n-1} (\Delta \widetilde{g}_n(i_n))^2 - 1\} \overset{\mathrm{A}}{\sim} \mathcal{N}(0, 4)$, so that $(q_n(\theta_*) - n)/\sqrt{n} \overset{\mathrm{A}}{\sim} \mathcal{N}(0, 4)$. Therefore, it now follows that $(J_n - n)/\sqrt{4n} \overset{\mathrm{A}}{\sim} \mathcal{N}(0, 1)$ under $\mathcal{H}_0$. ■

A.6 Empirical Supplements

In this section, we provide supplements related to the empirical application in Section 4.

A.6.1 Functional Shapes of the Brownian Motion and Brownian Bridge Kernels

In this section, we display the functional shapes of the BM- and BB-kernels. Note that when n is finite, the BM- and BB-kernels are defined as follows:

$$\ddot{\Sigma}_n := \begin{bmatrix} \frac{1}{n} & \frac{1}{n} & \cdots & \frac{1}{n} \\ \frac{1}{n} & \frac{2}{n} & \cdots & \frac{2}{n} \\ \vdots & \vdots & \ddots & \vdots \\ \frac{1}{n} & \frac{2}{n} & \cdots & 1 \end{bmatrix} \quad \text{or} \quad \widetilde{\Sigma}_n := \begin{bmatrix} \frac{1}{n}(1 - \frac{1}{n}) & \frac{1}{n}(1 - \frac{2}{n}) & \cdots & \frac{1}{n}(1 - \frac{n-1}{n}) \\ \frac{1}{n}(1 - \frac{2}{n}) & \frac{2}{n}(1 - \frac{2}{n}) & \cdots & \frac{2}{n}(1 - \frac{2}{n}) \\ \vdots & \vdots & \ddots & \vdots \\ \frac{1}{n}(1 - \frac{n-1}{n}) & \frac{2}{n}(1 - \frac{n-1}{n}) & \cdots & \frac{n-1}{n}(1 - \frac{n-1}{n}) \end{bmatrix}.$$

For the case of $\ddot{\Sigma}_n$, $\widehat{\Sigma}_n^{(j,i)} = \min[j_n, i_n]$, and we let $\ddot{\sigma}_n(\cdot, \circ)$ denote $\widehat{\sigma}_n(\cdot, \circ)$, which converges to $\ddot{\sigma}(\cdot, \circ) := \min[\cdot, \circ]$ uniformly on $[0,1] \times [0,1]$. Figure A.4 (a) shows the functional shape of $\ddot{\Sigma}_n$ for $n = 25$, and Figure A.4 (b) shows it for $n = 100$. Although it is not continuous for finite n, the limit kernel $\ddot{\sigma}(\cdot, \circ)$

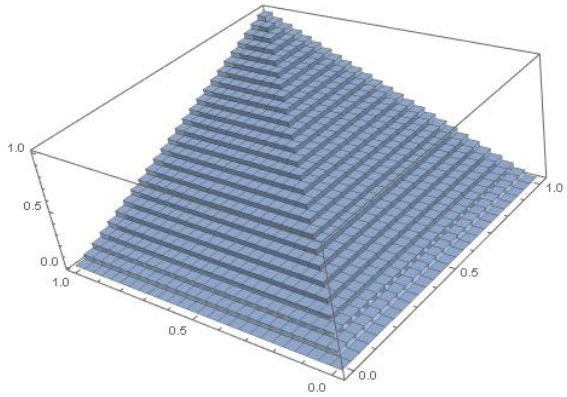

(a) Brownian motion kernel ($n = 25$)

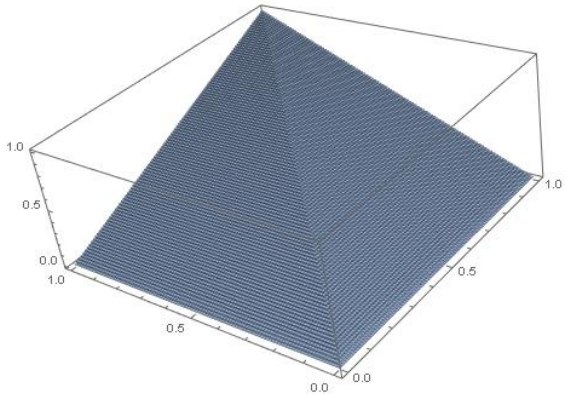

(b) Brownian motion kernel ($n = 100$)

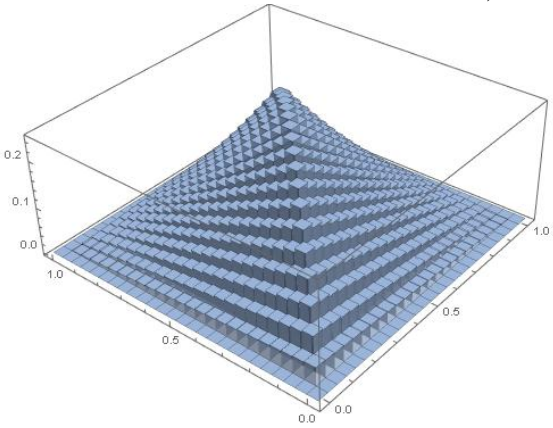

(c) Brownian bridge kernel ($n = 25$)

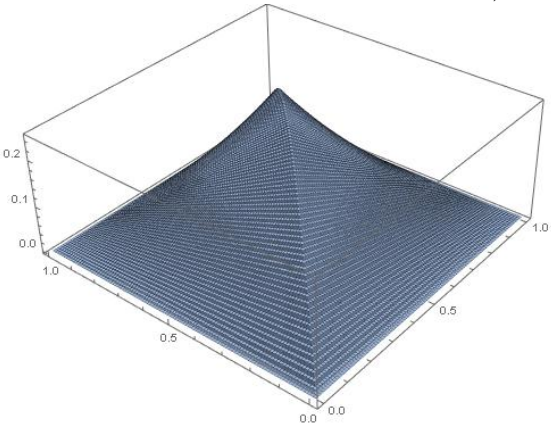

(d) Brownian bridge kernel ($n = 100$)

Figure A.4: FUNCTIONAL SHAPES OF THE BROWNIAN MOTION AND BROWNIAN BRIDGE KERNELS. For $n = 25$ and 100, each figure shows the shapes of the Brownian motion and Brownian bridge kernel functions.

is a continuous function.

For the case of $\widetilde{\Sigma}_n$, $\widehat{\Sigma}_n^{(j,i)} = \min[j_n, i_n](1 - \max[j_n, i_n])$, and we let $\widetilde{\sigma}_n(\cdot, \circ)$ denote $\widehat{\sigma}_n(\cdot, \circ)$, which converges to $\widetilde{\sigma}(\cdot, \circ) := \min[\cdot, \circ](1 - \max[\cdot, \circ])$ uniformly on $[0, 1] \times [0, 1]$. Figures A.4 (c) and (d) show the functional shapes of $\widetilde{\Sigma}_n$ for $n = 25$ and $n = 100$, respectively. Although it is not continuous for finite n, the limit kernel $\ddot{\sigma}(\cdot, \circ)$ is a continuous function.

A.6.2 Supplementary Information for the Empirical Analysis

In this section, we provide supplementary information for the empirical analysis. First, we demonstrate that if the Pareto hypothesis is supported for characterizing the upper labor income distribution, the estimated Pareto parameter provides a measure of heavy-tailedness and thereby income inequality. For this demonstration, we display the functional shapes of the Pareto PDFs and CDFs for $b_x = 1$ and $\theta_* = 1$, 2, and 3 in the upper panel of Figure A.5. Evidently the density levels of higher incomes decrease as θ_* increases,

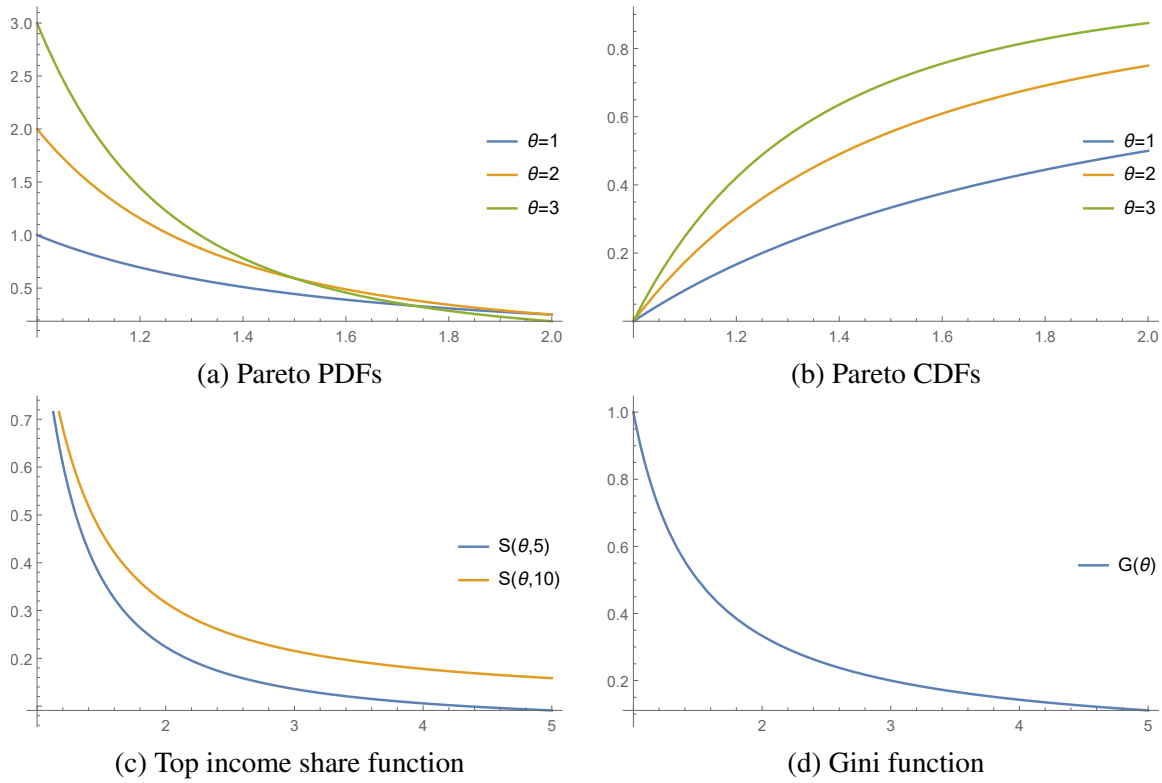

(a) Pareto PDFs

(b) Pareto CDFs

(c) Top income share function

(d) Gini function

Figure A.5: PDFs, CDFs, Top Income Share, and Gini Functions of the Pareto Random Variables. The figures in the upper panel show the shapes of the Pareto PDF and CDF for $\theta_* = 1$ 2, and 3. The top income share function shows the functional shapes of the $q\%$ top income share coefficient as a function of θ_* for $q = 5$ and 10, and the Gini function shows the functional shape of the Gini coefficient as a function of θ_*.

and heavy-tailed distributions (with fewer finite moments) occur for lower values of θ_*. Additionally, CDFs with higher θ_* uniformly dominate CDFs with lower θ_*, so that income distributions with a lower θ_* are more unequally distributed than those with higher θ_*. This relationship can be linked to traditional income inequality indices. In fact, under the Pareto distribution, the top x-percent income share $S(\theta_*, x)$ and the Gini coefficient $G(\theta_*)$ can be represented directly by functions of θ_* as follows:

$$S(\theta_*, x) := \left(\frac{x}{100}\right)^{\frac{\theta_*-1}{\theta_*}} \quad \text{and} \quad G(\theta_*) := \frac{1}{2\theta_* - 1},$$

The lower panel of Figure A.5 shows the functional shapes of $S(\cdot, x)$ and $G(\cdot)$ for $x = 5$ and 10. The functions have a negative slope, indicating that income equality indices improve as θ_* increases. We leverage this characteristic by estimating the Pareto parameter from the top 10% labor income observations. Specifically, using the results in Table A.10, we compute the top 5% income shares and Gini coefficients by $S(\widehat{\theta}_n, 5)$ and $G(\widehat{\theta}_n)$, where $\widehat{\theta}_n$ denotes the infinite dimensional MCMD estimates for the data of each cohort that do not reject the Pareto distribution condition.

Classification	1960	1961	1962	Sum
Female	2,591	2,576	2,540	7,707
Male	2,479	2,456	2,358	7,293
Sum	5,070	5,032	4,898	15,000
High School or below	1,108	1,187	1,094	3,389
BA or equivalent	2,659	2,646	2,689	7,994
MA or equivalent	535	515	487	1,537
Doctorate or equivalent	768	684	628	2,080
Sum	5,070	5,032	4,898	15,000
White or Caucasian	4,106	4,085	3,954	12,145
Black or African American	644	627	619	1,890
Asian	258	250	251	759
Etc.	62	70	74	206
Sum	5,070	5,032	4,898	15,000

Table A.9: SAMPLE SIZES OF CLASSIFIED DATA SETS. This table shows the sample sizes of the classified datasets.

Some caution is needed in using this approach as the Gini coefficient obtained in this manner should be considered an approximate value based on the upper end of the distribution. It may not be accurate to assume that the entire labor income distribution follows a Pareto distribution, as only the top 10% incomes are tested for the right tail distribution. On the contrary, the top 5% income shares can be reliably estimated through this method since they are computed from the right tail income distributions. Therefore, we focused attention on the top 5% labor income shares for the empirical application in Section 4.

Second, we discuss the inferential results of applying the U-test. Table A.9 presents the distribution of the cohorts categorized by gender, education, and race, and Table A.10 reports the inferential findings obtained by applying the U-test for each cohort using the datasets from 1980 to 2018. The table specifically provides information for each cohort, including the sample size of the top 10% labor income datasets and the number of datasets that do not reject the Pareto distribution hypothesis. For instance, for the female cohort born in 1960, there are 260 top 10% labor income observations, and out of the 39 datasets between 1980 and 2018, 27 of them do not reject the Pareto distribution hypothesis at the 1% significance level. We summarize the inferential findings as follows.

(a) The analysis shows that gender, education, and race all have an impact on inference. When individuals are categorized based on their gender, education, and race, a substantial number of datasets do not reject the Pareto hypothesis. This outcome can be compared with the bottom panel of Table A.10, where observations are not classified. Note that numbers in the upper panels are overall higher than the corresponding numbers in the bottom panel for each cohort born in 1960, 1961, and 1962. This finding indicates that it is difficult to reject the Pareto hypothesis from more homogeneous sectors of

individuals.

(b) Although detailed results are not reported here, the Pareto hypothesis is found to be appropriate at higher income levels. If b_x is increased to represent the top 5% of labor income for each cohort, the hypothesis cannot be rejected in a substantial number of datasets. This suggests that the Pareto distribution is also well-suited for capturing the right tail of the income distribution.

(c) Importantly, classifying observations into homogeneous groups or increasing b_x inevitably reduces sample size and therefore type II errors may occur in inference. For our analysis, therefore, b_x was selected to give the top 10% labor income level of each cohort data, which provides moderate sample sizes in the cohorts; and groups with sample sizes less than 25 were removed from analysis. As a result, individuals not belonging to white or Caucasian, black or African American, or Asian races were removed from the analysis. □

A.6.3 Measuring Income Inequality by Gini Coefficients

In this section we provide the estimated Gini coefficients using annual data for each year. The evolution of the Gini coefficients is shown in parallel to those in Figures 2 to 5. For the female and male cohorts, Figure A.6 shows the estimated Gini coefficients as functions of time between 1980 and 2018. Likewise, Figures A.7 and A.8 show the estimated Gini coefficients from the datasets classified by education and race, respectively. Figure A.9 shows the Gini coefficients when datasets are not classified. The implications of these figures are broadly the same as those from Figures 2 to 5.

Classification	Size \ Obs.	1960	1961	1962
Female	n	260	258	255
	1%	27	28	26
	5%	25	24	24
	10%	22	23	20
Male	n	248	246	236
	1%	33	31	32
	5%	31	26	28
	10%	27	23	27
High School or below	n	111	119	110
	1%	28	38	39
	5%	32	36	37
	10%	31	36	35
BA or equivalent	n	266	265	269
	1%	34	34	33
	5%	32	33	32
	10%	31	33	28
MA or equivalent	n	54	52	49
	1%	38	39	39
	5%	38	39	38
	10%	38	36	36
Doctorate or equivalent	n	77	69	63
	1%	34	28	34
	5%	32	27	32
	10%	29	24	32
White or Caucasian	n	411	409	396
	1%	29	33	29
	5%	28	31	24
	10%	25	28	19
Black or African American	n	65	63	62
	1%	38	37	39
	5%	37	36	38
	10%	35	36	37
Asian	n	26	26	26
	1%	36	39	37
	5%	36	38	37
	10%	36	35	36
Etc.	n	7	8	8
	1%	39	39	38
	5%	39	39	38
	10%	39	38	38
All	n	508	504	490
	1%	30	29	29
	5%	23	28	26
	10%	18	23	21

Table A.10: NUMBER OF DATA SETS NOT REJECTING THE PARETO DISTRIBUTION HYPOTHESIS. This table shows the number of the top 10% CWHS datasets between 1980 and 2018 that do not reject the Pareto distribution hypothesis by the U-test. As an example, when the females are restricted to top 10% individuals who are born in 1960 and the level of significance is 1%, 27 datasets between 1980 and 2017 do not reject the Pareto distribution hypothesis. Here, n denotes the average sample size of the top 10% individuals in the datasets.

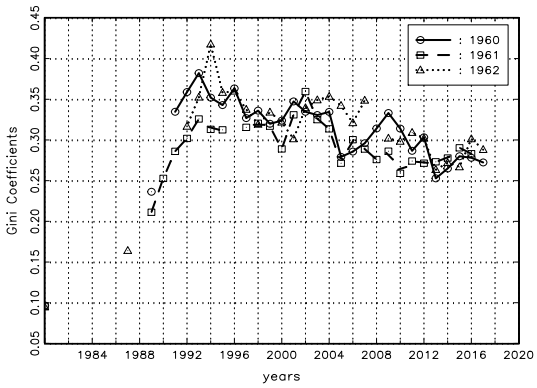

(a) Female

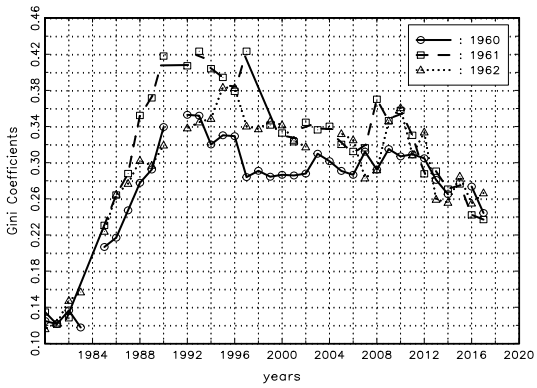

(b) Male

Figure A.6: GINI COEFFICIENTS OF GENDER COHORTS BETWEEN 1980 AND 2018. The figures show the Gini coefficients of gender cohorts estimated by imposing the Pareto distribution to the top 10% CWHS observations. Missing values signify the p-value of the U-test less than 1%.

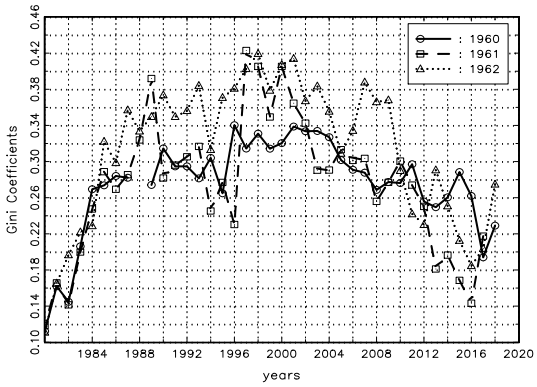

(a) High school or below

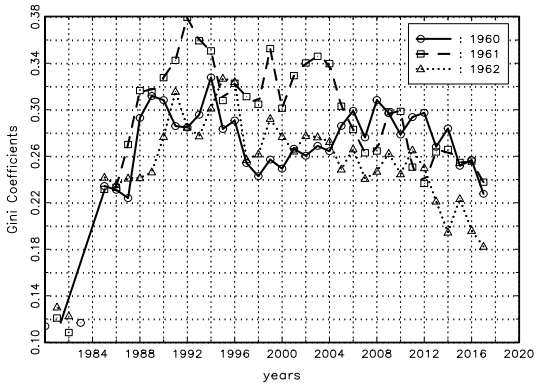

(b) BA or equivalent

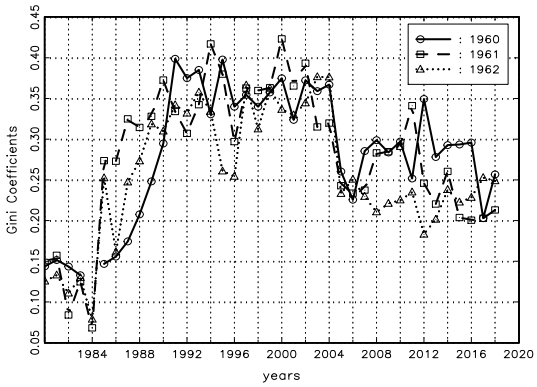

(c) MA or equivalent

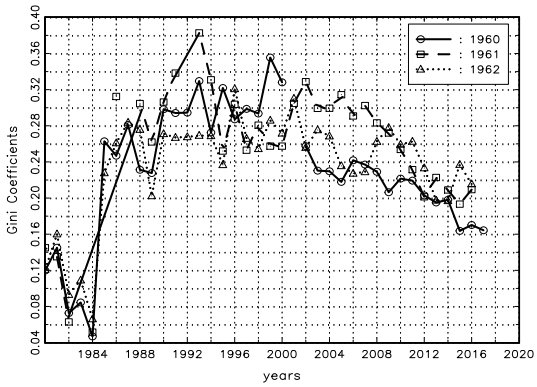

(d) Doctorate or equivalent

Figure A.7: GINI COEFFICIENTS WITHIN THE SAME EDUCATION COHORTS BETWEEN 1980 AND 2018. The figures show the Gini coefficients within the same education cohorts estimated by imposing the Pareto distribution to the top 10% CWHS observations. Missing values signify the p-value of the U-test less than 1%.

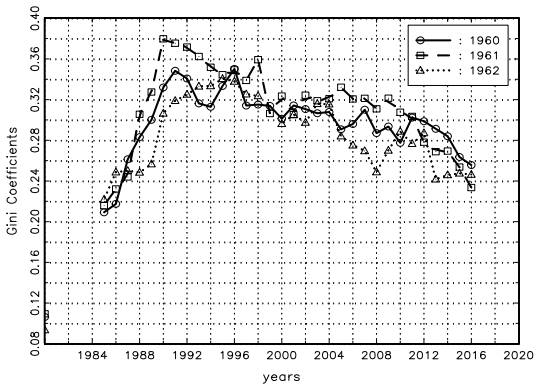

(a) White or Caucasian

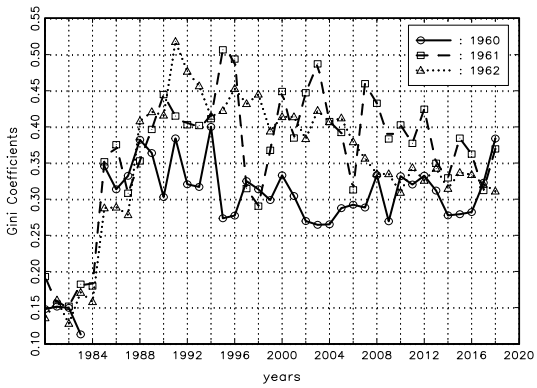

(b) Black or African American

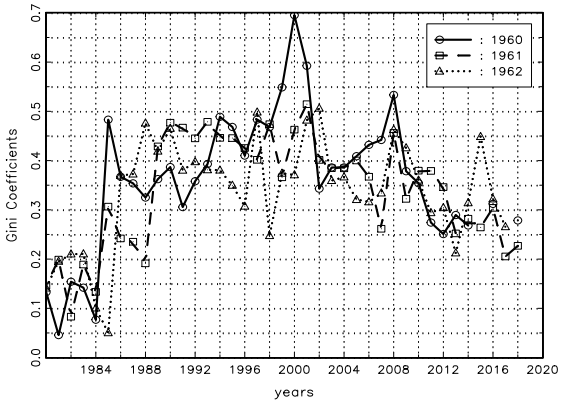

(c) Asian

Figure A.8: GINI COEFFICIENTS WITHIN THE SAME RACE COHORTS BETWEEN 1980 AND 2018. The figures show the Gini coefficients within the same race cohorts estimated by imposing the Pareto distribution to the top 10% CWHS observations. Missing values signify the p-value of the U-test less than 1%.

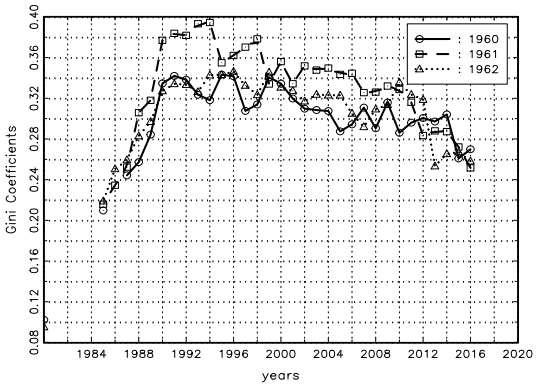

Figure A.9: GINI COEFFICIENTS USING AGGREGATED OBSERVATIONS FOR EACH YEAR BETWEEN 1980 AND 2018. The figures show the Gini coefficients of aggregated observations estimated by imposing the Pareto distribution to the top 10% CWHS observations. Missing values signify the p-value of the U-test less than 1%.